Norwegian University
of Life Sciences

Master's Thesis 2021 60 ECTS
Faculty of Environmental Sciences and Natural Resource Management

The effects of biochar on immobilizing Pb, Zn, Cu and Cd in contaminated soils from the mining sites in Kabwe (Zambia) and Folldal (Norway)

Cecilie Brandsvoll
Environment and Natural Resources

Abstract

Mining activities and resulting waste products are among the main sources of severe heavy metal pollution in the world. This study aims to examine i) the level of soil contamination, ii) mobility and ii) bioavailability of Pb, Zn, Cu and Cd in two mine-influenced areas in Kabwe in Zambia, and Folldal in Norway. Secondly, this study aims to discover the effects of pigeon pea biochar (pyrolyzed at 600ºC) on immobilizing these metals. The methods used were i) Total soil metal contents though total digestion and elemental analysis, using international threshold guidelines to determine level of contamination. ii) Equilibrium batch-titration experiment with metal speciation of equilibrium solution using WHAM VII, and iii) Diffusive gradients in thin films (DGT) to determine bioavailability. The two latter experiments were done in parallel with and without the treatment of biochar. The main findings showed that the adjacent areas to the mine (15–1580m) in Kabwe is severely polluted by Pb and Zn, and excessive levels of Cu were detected in the mine tailings in Folldal. The biochar treatment significantly ($p<0.05$) reduced the bioavailable metal levels in the most polluted sample in Kabwe by 64±8%, 68±3%, 29±17% and 63±3% for Pb, Zn, Cu and Cd, respectively, with similar effects detected for metal mobility. The Folldal samples showed diverse effects to the biochar treatment, with significantly reduced mobility of Cu by 92±1% and 13±1% detected for two different samples. The metal immobilization properties of biochar were mainly assigned to the biochar-induced increase in pH causing hydrolysis of the free metal ions and precipitation of hydroxides or carbonates, but significant ($p<0.05$) sorption also occurred. However, using biochar with higher CEC would likely increase the observed effects. The study further highlights the importance of investigating mobility and/or bioavailability of metals, as the total metal concentration alone failed to describe the true environmental risks associated with the mine tailings in Folldal.

Acknowledgement

This thesis marks the end of my 5 years at NMBU which has left me with plenty of good memories and acquired knowledge in the fields of soil and environment. For the latter I would like to thank all engaged and knowledgeable staff at the Faculty of Environmental Sciences and Natural Resource Management at NMBU.

This project in many ways started with a two-week summer school course at The University of Zambia in January/February of 2020. A fieldtrip to the Kabwe mine sparked my interest to the challenges related to trace metal pollution and land reclamation. During my stay I was fortunate to be accompanied by my supervisors; Prof. Jan Mulder, Dr. Åsgeir R. Almås and Dr. Vegard Martinsen, to whom I give my sincerest gratitude. Thank you for all your help, valuable feedback and interesting discussions!

I would also like to give a special thanks to Ikabongo Mukumbuta, whose help was invaluable. As the COVID-19 pandemic hit the world in the start of 2020, many changes to the original thesis plan had to be made, including the cancellation of the planned field trip to Zambia in the summer months of 2020. Ikabongo's offer to help collect the soil samples in Kabwe and assisting the shipment to Norway was therefore fundamental for this thesis. For his help and efforts, I am sincerely grateful.

The cancelled trip to Kabwe, paired with a desire to include field work in the thesis, made way for the field work in Folldal with Prof. Gudny Okkenhaug and Dr. Gabrielle Dublet- Adli from NGI. I would like to thank both for welcoming me along and for sharing their knowledge and expertise in the field. In addition, I would like to thank Irene E. Eriksen, Valentina Zivanovic, Pia Frostad and Oddny Gimmingsrud for assisting me with the lab work and running of analysis.

Lastly, I would like to thank my husband, Ashley, for keeping me fed and motivated during the COVID lockdown, and for showing the greatest level of support during this whole process.

Thank you!

Table of contents

1. Introduction

Mining activities and resulting waste products are among the main sources of severe heavy metal pollution. Industrial processes and poorly managed tailings can degrade the adjacent environment through pollution with trace metals to nearby soils and water sources. This master's thesis is based on laboratory experiments aimed to give a deeper understanding of the environmental fate of lead (Pb), Zinc (Zn), Copper (Cu) and Cadmium (Cd) present in soils in two different areas influenced by mining activity. The experiments further investigate the effect of biochar as a remediation measure to reduce the mobility and bioavailability of the metals in question. Soil samples were gathered along a 1500 meter long southbound transect from a tailing disposal site in Kabwe, central Zambia, in addition to mine tailing's samples from Folldal, south-eastern Norway. The disparate nature of the sites and materials gives the thesis a wider perspective of the diversity in mining sites and their representative contamination problems, in addition to a wider insight into the effects of biochar (biochar) by testing on different materials.

The demand for metals and mined minerals increases concomitantly to the global increase in population and economy. A report from USGS (Rogich & Matos, 2008) describing the global flows of metals state that from 1970 to 2004, the global demand for Cu and Zn increased by twofold, while Pb increased with 50% over the same period. In mining operations, the tailings to ore ratio is high, generally 200:1 (Kossoff et al., 2014). Consequently, the process of mining these metals, even from high grade ores, generates a vast mass of tailings and waste rock. Following a depletion of high-grade ores due to the steady increase in demand, mining of lower grade tailings becomes more and more common, which in turn produces more waste material (Wills & Napier-Munn, 2006).The environmental burden of these waste materials is largely depending on the method of disposal. Due to the widely diverse nature of mine tailings, available disposal sites and environmental regulations and enforcement, a variety of different methods are in use globally, associated with varying degrees of environmental impact (Sofrá & Boger, 2002). The assessment of disposal method is immensely site specific and will not be further explored in this thesis. This thesis aims to answer two main questions:

1) What is the mobility and bioavailability of heavy metals in mine tailings and in adjacent soils due to historic mining activities in Folldal (Norway) and Kabwe (Zambia)? Kabwe is widely known for its lead and zinc mines and associated

contamination problems, whereas the areas around the old copper mine in Folldal suffer from acid mine drainage and contamination of the local river, Folla.

2) What is the potential of biochar to stabilize heavy metals in soils, reducing their mobility and bioavailability?

Kabwe is the capital of the central province of Zambia and the country's 4th largest city by population. The mining industry in the area reached full scale production in 1906 until production ceased in 1994. In the following years the area has been dominated by artisanal mining. In its heyday, Kabwe boasted one of the largest and richest lead mines in Africa. Today it is known as one of the ten most polluted cities in the world according to a report from the blacksmith institute/Pure earth (2007), a non-profit NGO monitoring pollution in the developing world. The pollution in the area is a legacy of 90 years of unregulated lead mining and smelting operations. The most prominent pollution problems is related to the lack of measures put in place to reduce aeolian transport from the contaminated mine tailings (Tembo et al., 2006), and drainage of hazardous material from the closed mine in The Kabwe Canal (Minestry of mines, 2016). The transport of lead causes soil and water pollution, as well as direct human exposure through inhalation of dust particles. In sum this has led to severe lead exposure to the population of Kabwe.

WHO identifies lead as 1 of 10 chemical of major health concern, and a joint report from pure earth and UNICEF (2020) state that one in three of the world's children – up to 800 million globally – have blood lead levels at or above the 5µg/dL, a level associated with decreased intelligence in children, behavioral difficulties and learning problems. A recent report on the blood lead levels of people in Kabwe show devastating numbers, as the township closest to where the samples of this report were gathered, showed mean blood levels of 45.7 µg/dL. Of the total number of children sampled in the study (n = 562), 23% exceeded 45 µg/dL, the threshold required for chelation therapy (Yabe et al., 2020).

The relevance of the pollution problem in Kabwe is evident in light of the current class action lawsuit against the mining company Anglo American over alleged mass lead poisoning of children in Zambia (Carrington, 2020). The company was responsible for the Kabwe mine from 1925 to 1974, a time-period when the majority of the pollution was caused. The lawsuit alleges that the company is liable for substantial emissions of lead into the local environment

due to deficiencies in the operation of the mine and for failing to ensure the clean-up of contaminated land. The lawsuit claims that more than 100,000 people may have been poisoned by the contamination of lead from the mine, over generations. The lawsuit calls for financial compensation, medical screening of children and women, and a clean-up of the area (BBC, 2020). The latter part of this compensation demand is of special relevance to this thesis, as the remediation effect of biochar is being tested on these very soils.

A report by Ikenaka et al. (2012) issue that heavy metal pollution is one of the most important problems in Zambia generally, and also point to the steady increase in this type of pollution though mining and smelting operations. Renewed interest in the Kabwe deposits is linked to recent advances in technology and new economic potential of non-sulphide Zn. The total concentrations Pb and Zn in the mine tailings are 5612 mg/kg and 4258mg/kg respectively (Mbuki & Mbewe, 2017). It is estimated that an approximate of 1,9 Mt of mainly Zn-rich silicate resources (13,4wt% Zn and 1,5wt% Pb) remained in situ after the operating mine closed in 1994 (Kamona & Friedrich, 2007). Due to the interest of further mining activities coinciding with current active artisanal mining in the area, conventional pollution measures like covering the mine tailings for example, will not be applicable in Kabwe. Moreover, the high population density around the mine makes alternative measures such as the possibility of using biochar as a remediation measure for the affected areas around the mine, more relevant and interesting for further exploration.

Folldal is, similar to Kabwe, a town with a long history of mining. During the almost 200 years of operation from 1748 to 1968, large amounts of minerals rich in sulfur (S), Cu and Zn were extracted from ores in the area. A substantial mass of mine tailings and waste rocks from the mining activities has been deposited in the open, around and under, the area that is now the center of Folldal town (Kvennås et al., 2015). Aeriation and contact with water from the ambient environment induce the oxidation of the sulphide and sulfosalt minerals in the deposited masses and causes generation of acids, resulting in enhanced mobilization of the toxic trace metals present in the deposits. This process is known as acid mine drainage (AMD) and is the most prominent environmental problem in the area (Kvennås et al., 2015). AMD with high levels of copper, but also iron, zinc and cadmium leaches from the tailings and drains into the recipient river Folla. It is estimated that around 15-20 tonnes of Cu is annually discharged into Folla through AMD. As a direct consequence, a 12 km stretch of the river downstream from Folldal center is described as severely polluted and lacks fish and

other native aquatic organisms (Kvennås et al., 2015; Torgersen, 2015). The situation in Folldal has been described in the media as Norway's largest remaining discharge of heavy metals to fresh water (Kampestuen, 2021).

The Norwegian Environment Agency (Miljødirektoratet) has issued that amendment measures should be put in place to reduce the copper leaching by 60-90% to recover the polluted river. The Norwegian Geotechnical Institute (Norges geotekniske institutt, NGI) suggested a combination of many different measures to reach this goal based on covering the tailings with an oxygen barrier to terminate the oxidation, the main driver of AMD. However, the covering of the tailings contradicts with the interest of the Norwegian Directorate for Cultural Heritage (Riksantikvaren). They issue that the area around the mine and the associated tailings is an important cultural heritage. The characteristic red color of the tailings, caused by the precipitation of iron oxides, is regarded as a part of the cultural heritage of the site. Consequently, the directorate advises against any measures that alters the aesthetics of the area, such as the implementation of the oxygen barrier suggested by NGI (Kvennås et al., 2015). These are disputes that characterizes the current situation in Folldal and is therefore worth mentioning.

The sampling and planning of the field work in Folldal were carried out in collaboration with NGI, but this thesis is not directly linked to any ongoing projects in Folldal. The use of biochar is not a suggested measure of remediation by NGI, accordingly, this thesis is an assessment of an alternative measure to the ones suggested by NGI in “Folldal gruver - Vurdering av mulige tiltak mot avrenning fra tidligere gruvevirksomhet” (2015). The results may be viewed as a general assessment of the potential of biochar to remediate AMD generating sediments.
The remediation effect of biochar on polluted sediments has received global attention and has shown promising results (Dume et al., 2016; Fellet et al., 2011; Houben et al., 2013; Karami et al., 2011). Many different remediation methods have been tried on the soils of Kabwe. However, few studies have tested the effect of biochar on the soils, with the exception of the master’s thesis by Tina Kapandula (2020). Her column test provided inconclusive results on the effect of biochar on immobilization and bioavailability of Pb. Consequently, the current thesis follows the analytical recommendation for further studies by Kampandula (2020), with the aim to give more conclusive results about the stabilizing effects of biochar on trace metals in contaminated Kabwe soils.

Biochar has also shown to be an effective measure in reducing toxic constituents from AMD derived materials like the ones found in Folldal. A combined batch- and column study on tailings from an abandoned Cu mine in South Korea suggest that biochar can completely remove dissolved constitutes of Fe, Al, Cu, and As, and reduced the concentrations of Zn, Mn, and SO_4^{2-} by 99%, 61%, and 31%, respectively (Oh & Yoon, 2013). In addition to reducing the leaching of trace elements, another study (Yang et al., 2020) confirms that biochar can reduce chalcopyrite ($CuFeS_2$) biodissolution, which is a biogeochemical process known to play an important role in the formation AMD. Chalcopyrite is a mineral also described to be present in Folldal (Page, 1964). This thesis is the first to assess the remediation effect of biochar on the tailings in Folldal.

The laboratory work of this thesis can be divided in three parts; 1) General soil analysis, to give information about the general soil chemical and physical properties of the contaminated soils. 2) A batch-titration experiment aimed to determine the solubility and speciation of the trace metals in solution as a function of pH, and 3) A diffuse gradient in thin films (DGT) experiment used to determine the bioavailable fraction of the trace metals. The two latter experiments include parallel series with and without the addition of biochar to determine its effects on metal mobility and bioavailability.

The wider perspective of these experiments is to gain better knowledge about the fate of the trace metals, to provide a better assessment of the threats they pose to the surrounding population and environment. The standard and most advocated procedure to determine level of contamination of sediments is to measure the total metal contents, which are indicative, yet indiscriminate to quantify environmental and human health risks. To evaluate the potential risk and toxicity of trace metals, an assessment of the fraction of the total metals that are in dissolved and bioavailable form is required (Sauvé et al., 2000). The fractionation is assessed in experiments 2 and 3, respectively.

2. Theory

2.1 Trace metal pollution

There are many ways to refer to the group of pollutants that include Pb, Cu, Cd and Zn, namely: heavy metals, trace metals and potentially harmful elements. The latter reflect an important narrative, which is that Zn and Cu are micronutrients to higher plants and

deficiency of these can impair plant functions and reduce yield. However, if these elements are present in excessive amounts, they are toxic to plants and microbial communities in the soil (Alloway, 2012). Trace metals have a wide range of pathways to enter soils and can generally be divided into geogenic and anthropogenic sources; however, the potential mobility and associated risk of trace metals from anthropogenic sources are much higher compared to the geogenically contaminated soils (Palansooriya et al., 2020).

The mobility varies between the trace metals, and a study of urban soils in China (Luo et al., 2012) found that the mobility decreased in the following order Cd >Zn >Pb >Cu. The mobility of trace metals is governed by many soil geochemical properties such as sorption and desorption, precipitation, interactions with organic matter and Fe, Mn, Al and S. The mobility is therefore affected by the presence of clay minerals, metal oxides, and OM in soils which increases the CEC and provide a greater surface area for trace metal sorption (Palansooriya et al., 2020). The trace metal retention by OM is linked to properties such as ion exchange, complexation and adsorption, where functional groups like phenols, carboxyl, carboxylate and amino groups act as binding sites. Immobilizing trace metals refers to stabilizing or reducing their mobility with the aim to reduce the plant-uptake and the overall bioavailability.

The toxicity of trace metals relates to the form of species in which the metals are present in the environment and the corresponding bioavailability. The bioavailable metal fraction often corresponds to the labile metals in the dissolved metal fraction. However, it may also include the labile metal fraction on the soil solid phase made available by desorption through changes in the physiochemical environment of the soil, a soil metal fraction termed geochemically active (Almås & Singh, 2017). The availability of the latter is affected by factors like pH and solution composition. These factors are often in favor of increased availability in the rhizosphere related to plant nutrient uptake mechanisms (Degryse et al., 2009). Trace metal pollution in soils is not only limited to affect the local soil microbial communities and plants but can also affect lager segments of the environment. Transport can occur when contaminated soil disperse via wind suspended particles, and erosion, leaching or runoff can contaminate water sources. The trace metals in soils can also spread following bioaccumulation by plants, affecting food webs and posing great risks to ecological systems and human health.

pH is regarded as a master variable because it influences the mobility and bioavailability of trace metals. At elevated pH levels the net negative charge of the soil matrix increases due to deprotonation of amphoteric sites and reduced competition between the metal ions and H^+ and Al^{3+}, inducing more of the trace metals to adsorb to the solid phase. High pH can also reduce the dissolved metal species by hydrolysis and precipitation of hydroxide species (Palansooriya et al., 2020).

There are many scientific approaches to describe the extent of contamination in soils. The simplest approach is to measure total metal contents and use threshold values from the literature to determine the contamination state of the soil. This is, however, an indiscriminate method as it does not differentiate between the inert metal fraction and the geochemically active metal fraction. The latter poses the greatest environmental risk in terms of mobility and toxicity. It is therefore desirable to assess the proportion of these fractions to get a more realistic estimate of the environmental risk for the soil in question (Sauvé et al., 2000).

A simple approach to differentiate the two fractions is by measuring the partitioning between the metal bound to soil solid, and the dissolved fraction in solution at equilibrium. This approach is based on the fact that dissolved metals are more mobile and presumably more bioavailable, and that the metals bound to soil solids are strongly retained, and hence not bioavailable and immobile. Solid-solution ratios of metals are dependent on a series of physiochemical soil properties like soil texture, total metal burden, and organic matter content (Sauvé et al., 2000), as well as the concentration of organic and inorganic ligands in soil water, the free metal concentration in solution and pH. As already mentioned, pH is regarded as a master variable of soil-solution systems because it influences most of the chemical species, especially metal hydrolysis, deprotonation of organic acids and equilibria in the carbonate system (Sauvé et al., 2000). The pH also influences the competitive binding between metal ions and protons to clay minerals and oxides and dissolved ligands (Tipping et al., 2003).

The solid-solution partitioning alone fails to differentiate the metal species present in solution. Total dissolved metal (Me) concentration is made up by the sum of free metals (Me^{2+}), other inorganic metal species like $Me(OH)_2$, $Me(OH)_3^+$, $MeHCO_3^-$, $MeCO_3$, $Me(CO_3)_2^{2-}$, $MeNO_3^+$, $MeCl^-$, $MeSO_4$, as well as complexes with inorganic ligands like DOM (Sauvé et al., 2000). It is important to differentiate between these species, as the different species are associated

with different relative bioavailability and toxicity. It is therefore desirable to assess the speciation of the dissolved metal fraction to further improve our understanding of the real environmental risk associated with the contaminated soil in question.

The equilibrium-batch approach, as described here, addresses the labile metal species in solution only, which is important for the assessment of metal mobility and transport. However, the bioavailable metals present in soils additionally include the geochemically active metals in the solid phase and in dissolved complexes (Almås & Singh, 2017). A direct approach to measure bioavailability is by the use of DGT® (Diffuse Gradient in Thin Films), a passive sampler in the shape of a small plastic device that is inserted in a water-saturated soil sample. The bioavailable metal measured here is defined as the chemically labile metal fraction in pore water in addition to the geochemically active metal in the solid soil (Almås & Singh, 2017). The readily available metal ions diffuse through a filter and a diffusive layer and accumulate on a negatively charged Chelex resin in the innermost part of the DGT device. As the readily available metal ions accumulate on the resin, the immediate metal concentration in the soil adjacent to the device lowers. The decrease in the metal solute concentration in the interface of the device induces replenishment of dissolved metal ions from the solid phase. This effect is not included in conventional methods, like metal extractions with dilute salt extracts. In that way, the DGT can measure the bioavailable fraction to a greater detail.

A combination of these methods is used to assess the contamination state of the selected soils in this thesis. Experiment 1 is a batch-titration experiment aimed to determine i) the solubility of selected trace metals, and ii) their speciation in solution, by the use of WHAM speciation model. Experiment 2 is a DGT experiment aimed to measure the bioavailable fraction of the selected metals in the same soils.

2.2 Biochar

Biochar is a carbon-rich product that can be produced from a range of organic materials through the process of pyrolysis, which involves burning of organic materials at high temperatures (>350°C) under anoxic conditions (Hofstad, 2020). Biochar have been proven effective for remediation of contaminated soil and is also used as a soil enhancer for degraded agricultural soils. Because biochar can be made from most organic materials, the use of

organic waste products for making biochar make way for a sustainable way of closing the loop (Palansooriya et al., 2020).

Biochar has been shown to resist microbial degradation (Fellet et al., 2011), hence the organic carbon sequestered in biochar is highly recalcitrant as illustrated by the 1000–2000-year-old Terra Preta soils, a result of incorporated biochar in soils by ancient indigenous populations in Amazonia. The Terra Preta soils are characterized by high fertility, greater CEC and nutrient retention (Fellet et al., 2011; Mia et al., 2017). The C sequestration aspect of the biochar contributes to mitigating climate change as it is a net carbon sink that allows a stable carbon pool to build up in soils (Winsley, 2007). The use of biochar can therefore be described as a low-cost, sustainable way to improve highly degraded lands (Fellet et al., 2011).

The chemical and physical properties of biochar may vary depending on several factors, such as the type of feedstock and the charring conditions (Fellet et al., 2011). The main properties of biochar that contributes to the efficiency in immobilizing trace metals is generally related to: i) The increase in pH associated to the content of alkaline minerals in ashes from the charring process. ii) Precipitation of metals with CO_3^{2-} and/or PO_4^{3-} species, especially for Pb. iii) Net negative charge that contributes to electrostatic adsorption of cations. iv) General contribution of higher specific surface area and micropores. v) Complexation reactions with functional groups on biochar (Palansooriya et al., 2020).

As mentioned, the biochar itself degrades slowly in the natural environment, with an estimated carbon half-life of 10^2-10^7 years (Zimmerman, 2010). It should be noted that leaching of alkalinity is an aging effect that might reduce the effectiveness of metal immobilization over time (O'Connor et al., 2018; Palansooriya et al., 2020). However, when comparing the aging effect of alkaline ash to liming, the most widely adopted metal immobilizing soil treatment, a study by Ruttens et al. (2010) suggest that the immobilization effect on metals in soils remediated with cyclonic ash was more effective in withstanding the aging effect compared to liming (Fellet et al., 2011). The effect of cyclonic ash is comparable to the effect from biochar related ashes, although biochar only contributes with small quantities of ash when compared.

Dissolved organic matter (DOM) is the bioavailable and mobile fraction of organic matter in soil defined as the fraction of organic matter in solution that is smaller than 45 μm. Around

50% of DOM is dissolved organic carbon (DOC), referring to the elemental carbon content of DOM. High DOM in soil facilitates the formation of soluble metal complexes, increasing the soluble and mobile metal fraction (Palansooriya et al., 2020). Adding biochar to soils can potentially cause higher DOM solubility from the mineral phase though an increase in pH, as well as potential supply of DOM from the biochar itself. By contrast, the micropores in biochar might sorb DOM and give a subsequent increase of negatively charged functional groups on the biochar surface, which in turn can enhance the retention of metals (Egene et al., 2018; Smebye et al., 2016). It has been shown that the DOM binding effect is governed by the size of the DOM in question, where smaller aliphatic DOM molecules have larger affinity to biochar than larger aromatic ones, due to size exclusion of the micropores. Moreover, the extent of DOM binding to biochar depends on the ionic strength and pH of the solution (Smebye et al., 2016). The amount of DOC release from the biochar itself is related to pyrolysis temperature, where pyrolysis at higher temperatures is associated with lower DOC concentrations. In turn this reduces mobility of metals with high affinity to DOM, like Pb and Cu (Egene et al., 2018; Palansooriya et al., 2020).

A wide range of studies have been carried out over the last few years to evaluate the potential of using biochar as a measure to recover contaminated lands (Ali et al., 2019; Fellet et al., 2011; Houben et al., 2013; Lehmann, 2007; O'Connor et al., 2018; Yang et al., 2020). Some have shown a reduction in Pb and Zn mobility up to 100% in acidic soils amended with biochar produced at 700°C (Ahmad et al., 2017). The effect was ascribed to metal-hydroxides precipitation due to biochar-induced pH increase. Another study (Egene et al., 2018) reported a 66% and 77% reduction on pore water Cd and Zn concentrations, respectively, after a 3-year period from the addition of 4wt% holmoak wood biochar (pyrolysed at 650 °C) to soils in Campine region, situated in the north-eastern Belgium and south-eastern Netherlands. The amendment effect was ascribed to the consistently higher pH and lower concentrations of dissolved organic carbon (DOC) in the amended soils. The monitoring over 3 years additionally found that the immobilization effect remained relatively effective over time, without significant biochar aging being detected. A critical review paper (Palansooriya et al., 2020) investigating the effects reported from biochar treatment based on >60 published articles found that the median values of immobilizing efficiency of biochar for Pb was >85%, Zn was 70–77%, Cu >85% and effects on Cd was 50–60%.

However, some negative effects related to the addition of biochar have also been detected. A known problem with using biochar amendments on multi-element polluted soils is the mobilization of oxyanions like Antimony (Sb) and Arsenic (As). The effect is ascribed to the biochar -induced rise in pH, competition with phosphate and repulsive electrostatic forces between the anions and the net negatively charged biochar surface (Gu et al., 2020). Another negative effect can be unwanted elements or hazardous chemicals present in the biochar itself. For example, a paper by Fellet et al. (2011) discovered that the Cu leachability increased with increasing biochar application rate, and concluded that this was related to high Cu levels in the biochar itself, and further issue that more research is needed to look into the biochar contribution of other hazardous organic chemicals like PAH's, PCDD and others.

The potential difference in effects of biochar application at field versus lab scale is important to recognize. The effect of biochar on immobilizing trace metals in contaminated land in field scale was reviewed by O'Connor et al. (2018). The paper evaluated 29 field studies from 8 different countries and found that the most important biochar factors governing the effect included biochar properties, feedstock type, application rate, soil properties and meteorological factors. The paper concludes that biochar application can potentially reduce contaminant bioavailability also at field scale. Moreover, the review article by Palansooriya et al. (2020) concludes that soil amendments such as biochar, compost and others are recommended due to their high efficiency as soil conditioners and immobilizing agents, low cost, applicability and economic feasibility.

2.3 Acid mine drainage (AMD)

The main source of AMD is the oxidation of sulphide mineral ores (typically PbS, ZnS, CuS, FeAsS) exposed though mining operations. Of the metal sulphides, pyrite (FeS_2) is regarded as the main mineral responsible for generating AMD due to its ease of oxidation reactions when exposed to oxygen, water and microorganisms (Kefeni et al., 2017).

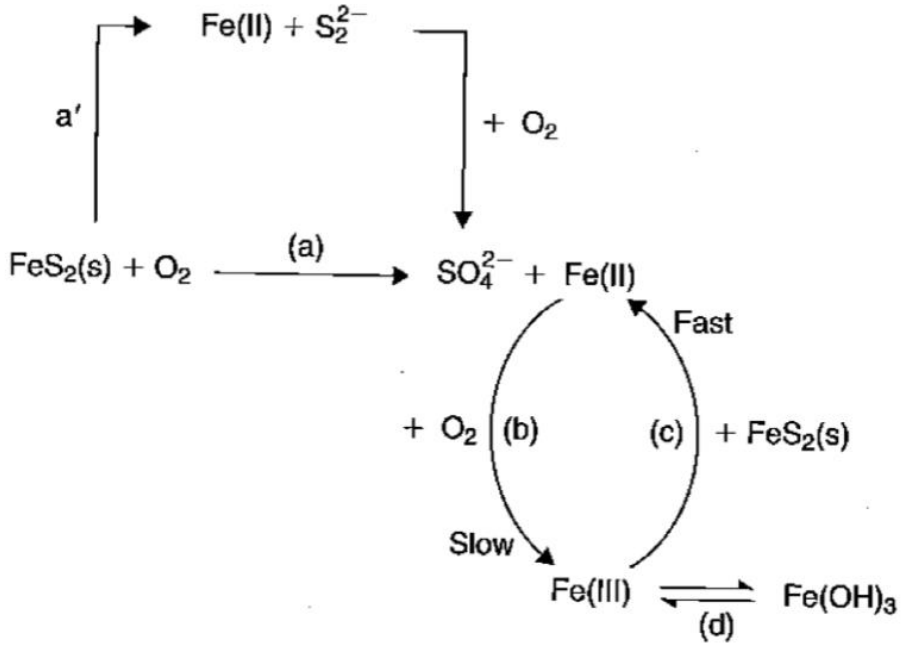

Figure 1: Acid mine drainage reactions (Stumm et al., 1996).

The AMD can pose severe problems to the local environment as it generates pollution to soils, water sources and aquatic communities. The environmental problems of AMD are associated with the low pH, high concentration of potentially toxic dissolved metals (e.g. Fe, Cu, Zn, Cd) and metalloids (e.g. arsenic and antimony).

2.4 Diffusive gradients in thin films (DGT)

The DGT is a passive sampling technique used for measuring inorganic ion concentrations in soil solution, water and sediments. The technique is useful for assessing environmentally and biologically relevant concentrations and related potential effects on living organisms (Puschenreiter, 2017). The DGT is a 2.5 cm diameter plastic device, which includes a Chelex-100 resin for cation binding. The DGT is deployed for a set period of time in soil, water or sediment, in- or ex-situ, and can give a quantitative estimate of the labile metal fraction.

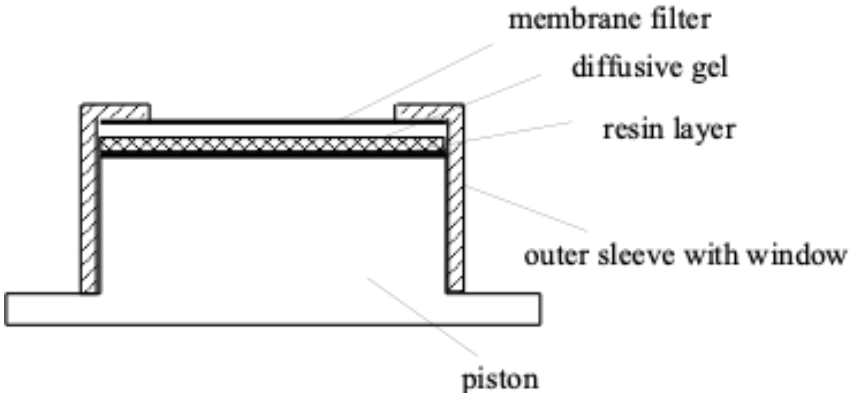

Figure 2: Illustrative cross-section of the DGT showing the main parts of the device. The size of the plastic base/piston is 2.5 cm in diameter. The device is placed with the membrane filter directly down into soil or sediment. Illustration taken from Hooda et al. (1999).

The DGT measures the sum of dissolved species and the labile metal fraction bound to the soil matrix. Metal ions in pore water, which are depleted at the DGT surface, will be replenished through desorption of the labile metal fraction from solid soil to the pore water. Both of these metal fractions will diffuse into the cation binding resin in the DGT. Thus, the accumulated mass of cations represent the sum of the labile cations in porewater plus the desorbed labile fraction from soil surfaces during time of deployment. The theory of cation quantification in the DGT's relies on the flux (mol cm-2 s-1) of cations into the Chelex-100 resin making use of Fick's first law of diffusion ($J = D\ dC/dx$, where D is the diffusion coefficient (cm2 s-1) and dC/dx (mol cm-4)) is the concentration gradient), where labile cation solutes are accumulated by one-way diffusion flux, as the chelex resin works as an ultimate sink of the metals within the set timeframe. The metals diffuse from the soil though a protective membrane filter and an inert well-defined open pored hydrogel (coined the diffusive gel), as illustrated in Figure 3. The diffusive gel also acts as a filter for metal complexes larger than the pore size of the diffusive gel. This allows only metal ions, inorganic and small organic metal complexes to pass through and be measured, in addition to the labile metals in larger complexes that can dissociate in the interface and pass though the diffusive gel layer (Gimpel et al., 2001).

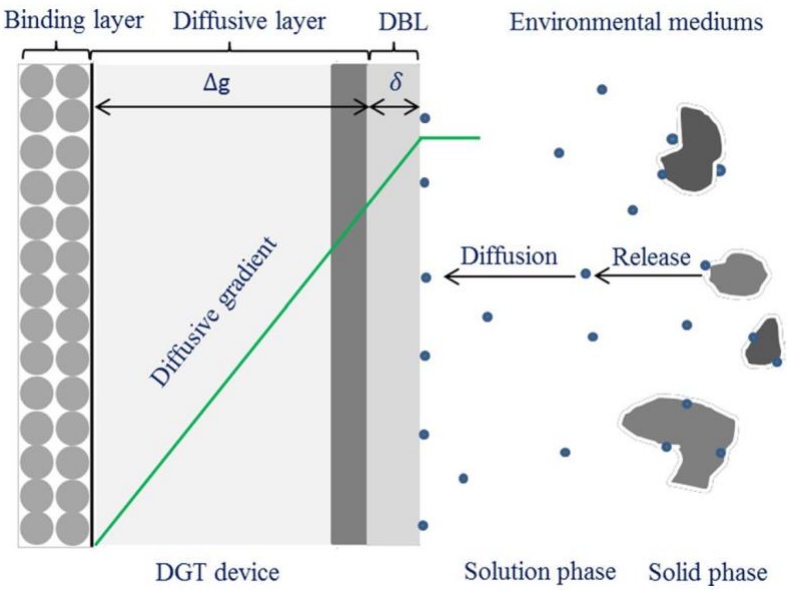

Figure 3: Illustration of the two mechanisms of release and diffusion from the soil matrix and the concentration gradient in gel layer within the DGT device. Illustration form (Li et al., 2019). The green line can be interpreted as a linear relationship between distance from soil in the diffusive layer (x-axis) and concentration (y-axis), when the metal supply is unlimited.

The mass of metals accumulated (M) can be calculated from the ICP element analysis of the Chelex-resin, given in µg/l (Ce), according to the following equation:

$$M = Ce\ (V_{HNO3} + Vgel)/fe \qquad \textit{Equation 1}$$

The concentration of metal measured by DGT (C-DGT) at the interface of the DGT in contact with soil, can be calculated using equation:

$$C\text{-}DGT = M\Delta g/DtA \qquad \textit{Equation 2}$$

Table 1: Summary of parameters for Equations 1 and 2. Content compiled from the official DGT® website: dgtreaseach.com

Equation parameters	Explanation	Unit	Value
A	Exposure area	Cm^2	3.14
t,6	Deployment time (after 6 hours)	seconds	21600
t,48	Deployment time (after 48 hours)	seconds	172800
Δg	Thickness of diffusive gel and filter membrane	cm	0.094

V_{HNO3}	Volume of HNO3 extractant added to the resin	L	1.0E-02
V_{gel}	Volume of the gel	L	1.60E-04
fe	Elution factor, assuming that the extractant is able to extract 80% of the metal bound to the resin	-	0.8
D_{Cd}	Diffusion coefficient of Cd in the gel	cm^2/s	5.61E-06
D_{Cu}	Diffusion coefficient of Cu in the gel	cm^2/s	5.74E-06
D_{Pb}	Diffusion coefficient of Pb in the gel	cm^2/s	7.40E-06
D_{Zn}	Diffusion coefficient of Zn in the gel	cm^2/s	5.60E-06

The ratio of metal mass measured in DGT at 48 hours over the mass measured in DGT at 6 hours can give an indication about the kinetics of metal resupply from the soil to the DGT. If the ratio is 8 (28/6=8), the supply of metals to the DGT is regarded as unlimited as the soil solution sustains a constant concentration in the interface of the DGT device over time. This suggest that the metal replenishment from the geochemically active soil fraction is not kinetically restricted. If the ratio is above 8, the geochemically active metal soil fraction supply more metal to the DGT device than the replenishment initiated by the equilibrium solution around the DGT device. This can be possible due to the high milliequivalent associated with the DGT resin, causing the DGT to be an ultimate sink of geochemically active metals.

3. Kabwe study site

The Kabwe mine is located at 1180 m elevation at latitude 14°27′S and longitude 28°26′E in Central Zambia, about 110 km north of the capital, Lusaka. The annual mean temperature and precipitation is 20.7°C and 919mm, with most of the rain falling between September and May (Climate-data.org).

Figure 4: Map showing the position of Kabwe and the capitol, Lusaka, in Zambia. Map Compiled from google earth pro software.

Sample Point	Distance from mine tailings (m)
Z1	15
Z2	105
Z3	203
Z4	840
Z5	1580

Figure 5: Map showing the spatial position of the sample sites in Kabwe. The main mining area is situated within the area outlined in black. The mine tailings closest to the sample area are deposited along the southernmost east-west fixed black line. The distance to each sample as presented in the table is measured from this line. Three replicate soil samples were gathered at each sample point. Map compiled from Google earth pro software.

The soil in Kabwe has developed from the weathering residue of a range of different geological bedrocks, and is influenced by different topography and moisture regimes, in addition to areas with strong anthropogenic influences (Kříbek et al., 2019). The soils in the area are dominated by Ferralsols, which represents the highest stage of parent material weathering, and have a thin humus layer. However, due to the mining activities in Kabwe, some areas also may classify as Technosols (Kříbek et al., 2019). The Pb and Zn contents in the Kabwe soils can in some areas reach 2.6 wt% and 3 wt%, respectively (Tembo et al., 2006).

Under its operating years, the Kabwe mine was Zambia's main producer of Pb and Zn with a production total of 1.8 million tonnes (t) 0.8 million t, respectively. The mine also contributed with relatively small amounts of other trace metals such as Cd (235 t), Ag (79 t), Cu (64 t), and fused vanadium (V) oxide (Kamona & Friedrich, 2007; Kříbek et al., 2019; Nakayama et al., 2011). The major ore minerals in Kabwe are mostly confined to massive dolomites and include pyrite [FeS_2], sphalerite [ZnS], and chalcopyrite [$CuFeS_2$]. The major non-sulfide ores include cerussite [$PbCO_3$], willemite [Zn_2SiO_4], smithsonite [$ZnCO_3$] and V, As, Mo and Cu minerals (Kamona & Friedrich, 2007; Kříbek et al., 2019).

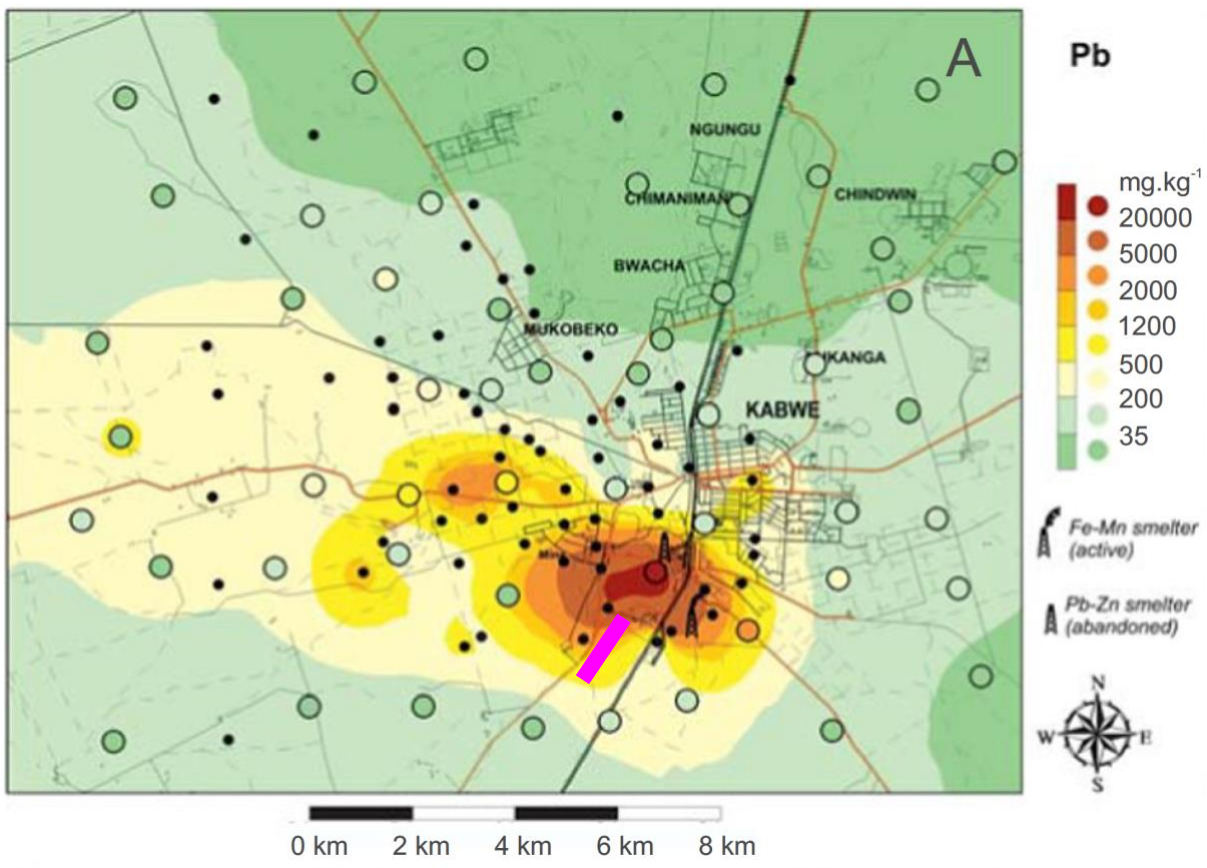

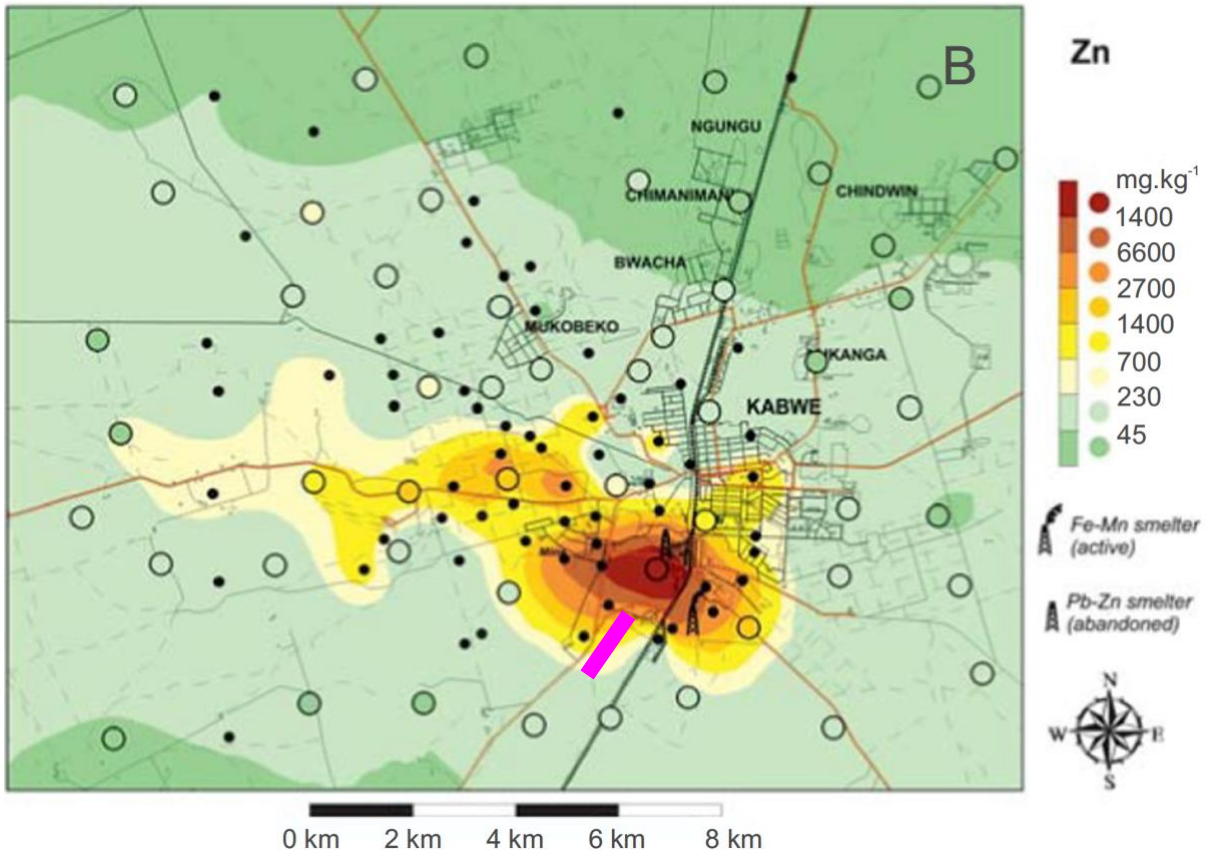

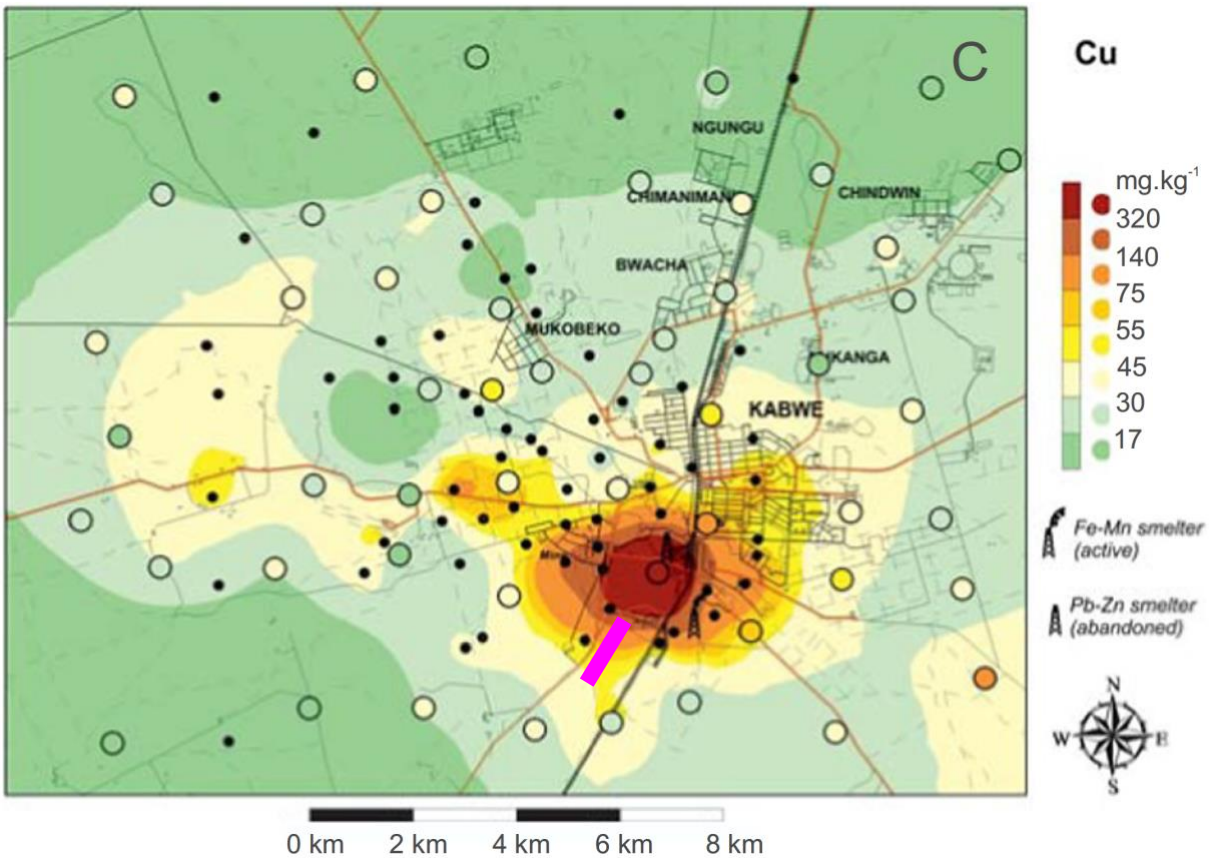

Figure 6: Distribution of Pb, Zn and Cu in soils around Kabwe. The contour map presents the concentration in the topsoil collected 0-3cm, and the color- filled circles present the concentrations in subsurface soil collected at 70-80cm depth. The

bright pink line indicates the approximate length of the sample transect from this study as presented in Figure 5. The maps are compiled from Kříbek et al. (2019).

Figure 6 shows the distribution of metals in the area around the mine, given in total soil concentrations (mg/kg). The pollution is related to a combination of dust fallout and emissions from historical Zn-Pb smelting operations, suspended dust from tailing ponds and slag deposits, in addition to emissions from an active (as of 2019) ferromanganese smelter (Kříbek et al., 2019). The dust generation is described as generally high in areas like Kabwe, due to the prolonged dry season. The spatial distribution patterns concurs with the south-easterly to easterly wind direction dominating in the area (Kříbek et al., 2019).

One of the major pathways of the trace metals to humans in Kabwe is though ingestion of soil dust, especially among children. The exposure to children in linked to outdoor play and partly also due to their short height, as it increases their exposure to dispersed particles (Kříbek et al., 2019). In addition to direct exposure though dust ingestion, it is known that vegetables grown in heavy metal contaminated soils can pose a risk to human health for the people that live close to mining areas (Kachenko & Singh, 2006). As local agriculture is oriented around the production of vegetables such as cassava, sweet potato, rape and lettuce (Kříbek et al., 2019), a part of this master project is to assess the bioavailable fraction of Pb, Zn, Cu and Cd present in the soils of Kabwe, and the effects of biochar remediation.

Many different remediation methods have been tried on the soils of Kabwe, namely phytoremediation(Leteinturier et al., 2001; Mbuki & Mbewe, 2017; Yoshii et al., 2020), bioremediation (Mwandira et al., 2019a; Mwandira et al., 2019b), detoxification of lead by coupled extraction-cementation method (Silwamba et al., 2020), humate and superphosphate amendments (Kříbek et al., 2019), and immobilization by dolomite, calcined dolomite, and magnesium oxide (Tangviroon et al., 2020).

The extensive study by Kříbek et al. (2019) on soil contamination near the Kabwe Pb-Zn smelter, provides an assessment of environmental impacts and several proposed remediation measures. The study included a plant-availability study (diethylenetriaminepentaacetic acid (DTPA) and triethanolamine (TEA) extractable fraction) of potential harmful elements, revealing that a significant proportion of the contaminants are present in a plant available form. The study states that the soil in areas used for cultivation of vegetables should be

removed to a minimum depth of 30 cm. However, the paper further issues the problem related to the cost of this measure, and recommends cheaper methods for land reclamation, with the aim of achieving a stabilized immobile forms of the Pb and Cd in highly contaminated areas. The paper looked into amendments of humate and triple superphosphate (TSP) solutions, tested separately and as a mix. Application of TSP showed that the plant availability of Pb and Cd decreased significantly. The TSP and humate mixture did not have a significant effect in reducing the bioavailability of Pb, Cd and Zn, relative to the TSP treatment alone. The plant availability of Zn was not affected by the phosphate treatment. The effect of biochar was not assessed in this study.

Another relevant study is a master's thesis by Kapandula (2020) from the University of Zambia, who carried out column experiments to assess the immobilization effect of biochar on Zn and Pb mobility in Kabwe soils. The experiment used 2% and 4% pine wood biochar amendment, in addition to a lime treatment, resulting in a soil pH similar to that of the 4% biochar treatment. The main findings showed that 4% biochar amendment helped reduce the leaching as well as the bioavailability of Zn (61% reduction, $p<0.05$), while increasing leaching and bioavailability of Pb (28% increase, $p<0.05$), with similar results for the lime treated samples. These results are contrary to many other recent publications (Dume et al., 2016; Fellet et al., 2011; Houben et al., 2013; Karami et al., 2011), whioch indicate that treatment with biochar reduces leachable Pb. In her thesis Kapandula suggests that the unexpected increased leaching of Pb maybe due the lack of appropriate filtration of the leachate so that the colloidal fraction is not excluded. Thus, further study using finer filters and speciation analysis of the leachate to prevent overestimation of dissolved Pb by including colloidal Pb as part of the dissolved fraction is warranted. The stated suggestion has been considered, hence finer filters and speciation analysis is carried out as part of my thesis.

Another master's thesis (Kabaso, 2019) presented results from a field study showing that addition of 4.5wt% biochar reduced the Pb concentrations in the mobile fraction of the soil and improved the establishment of lemongrass. The results were attributed to reduced soil acidity, increased soil carbon and generally reduced exchangeable amount of Pb in soil.

Fellet et al. (2011) studied the effects of application of biochar on mine tailings in general. The study concluded that the effects on decreased bioavailability of Cd, Pb and Zn in addition

to soil enhancement resulting in increased water and nutrient retention, are in favor of biochar applications to polluted environments.

4. Folldal study site

Folldal is located in the northern part of Innlandet county in central Norway at an altitude of 700 meters, at latitude 62°11′N and longitude 10°02′E. The Folldal town center is surrounded by pristine mountain areas, with the mountain park of Rondane in close proximity.

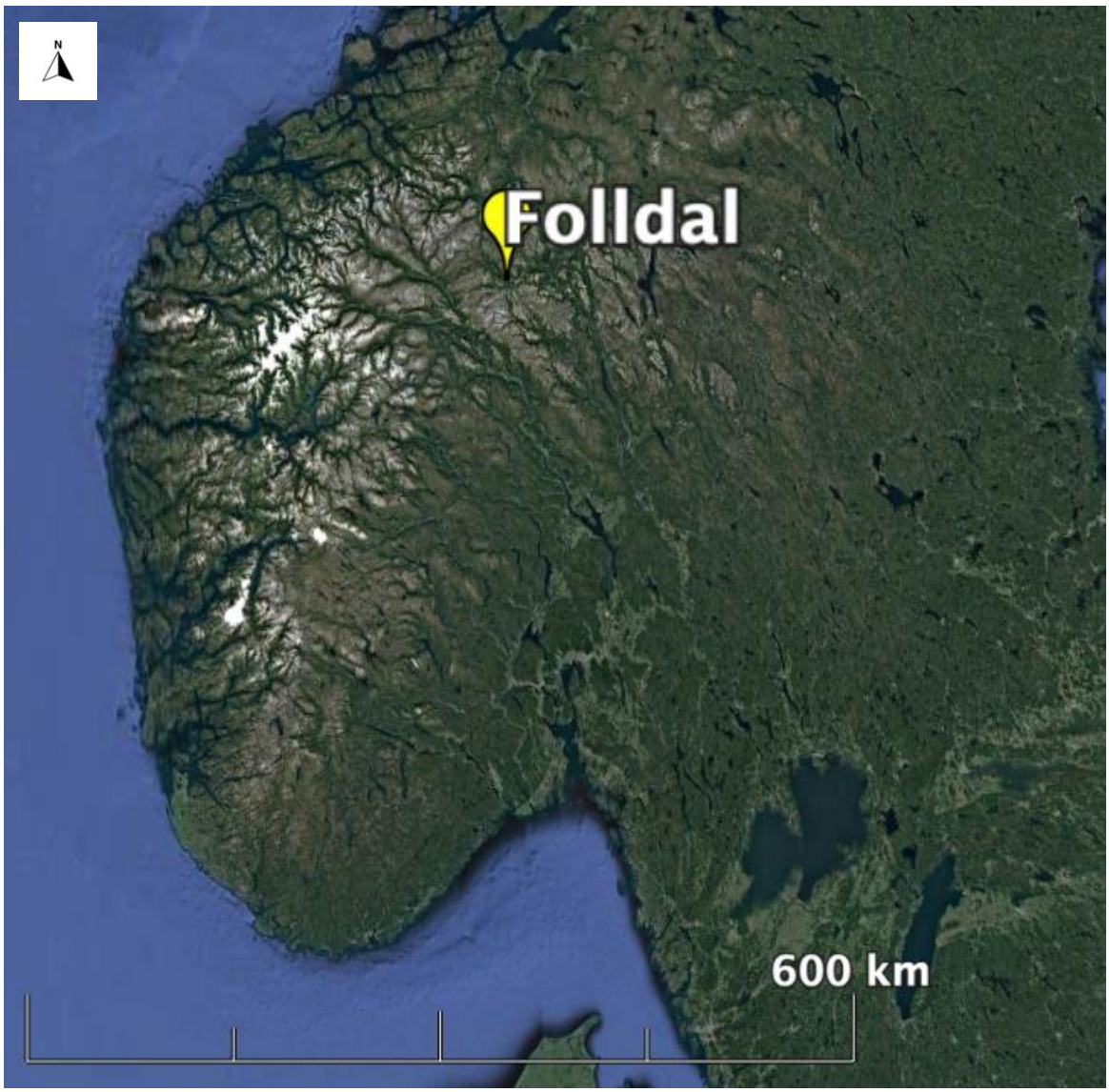

Figure 7: Map showing the position of Folldal in Norway. Map compiled from Google earth pro software.

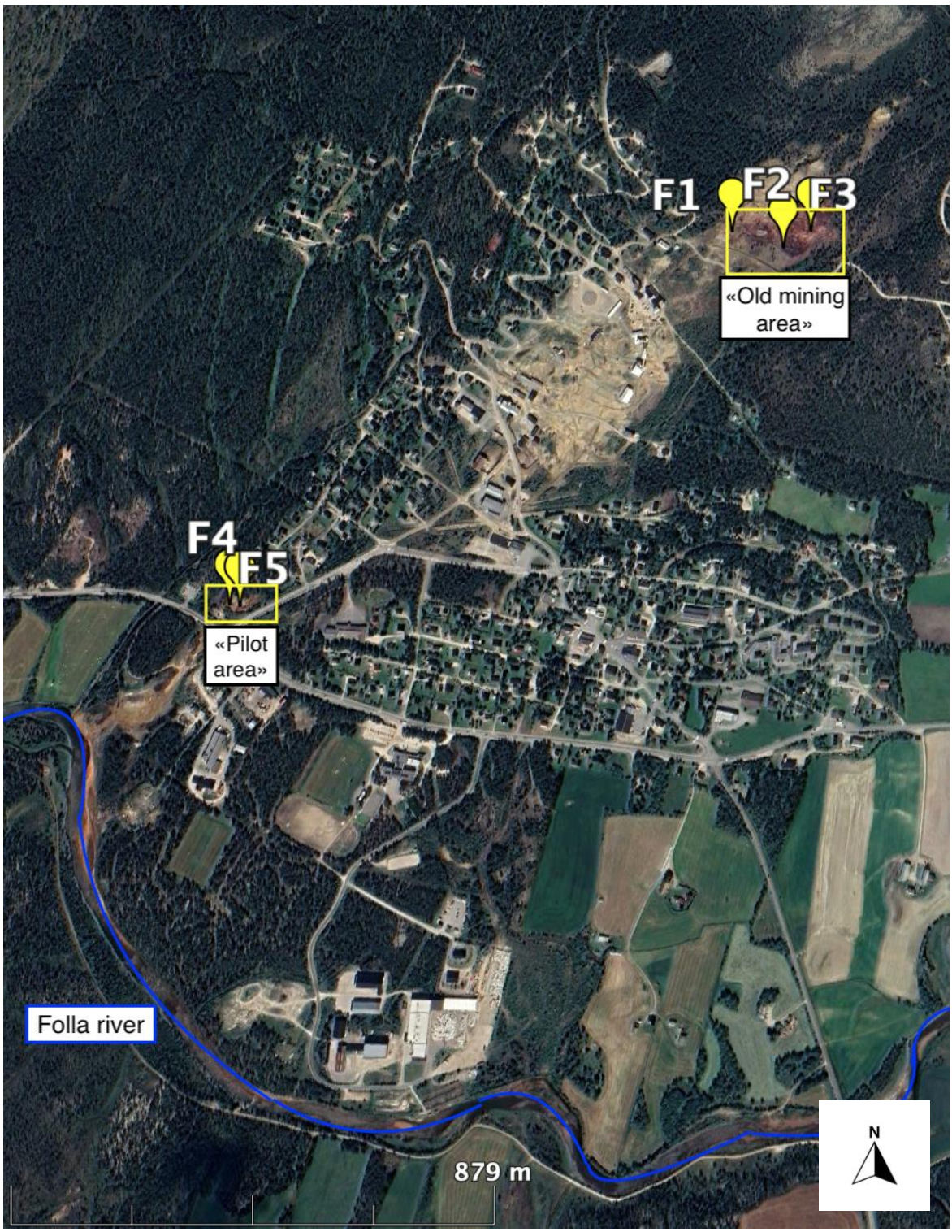

Figure 8: Location of sampling points in Folldal. The Folldal town center is situated in the center of the map. Map compiled from Google earth pro software.

The climate is characterized as dry and cold, and the region is regarded as one of the most arid in Norway, with a mean temperature of 4°C and mean annual precipitation of 360mm, generally concentrated in the summer months.

The first ores in the area were discovered by a farmer in 1745, and the production was concentrated in two periods; from 1748 to 1878, and from 1906, until the economical viable resources were depleted and the mine closed, in 1941 (Folldal gruver, 2021). The vast mass of tailings was deposited in the immediate areas around the mine. A survey carried out by NGI (Kvennås et al., 2015) detected four main areas of the deposited tailings, which are regarded as the main sources generating AMD to the River (Figure 9); Old mining area (N), Main mining area (S), Sludge pool (A), and industrial area (C). The samples in this thesis were collected from area N and A, as illustrated in Figure 8. These areas also show the highest acid generating potential, as illustrated by the legend in Figure 9. The mean annual amount of Cu leached to Folla from the area is estimated to be 15-20 t, where the high concentration episodes are linked to runoff events caused by snowmelt and rainfall, mainly concentrated between April-September (Kvennås et al., 2015).

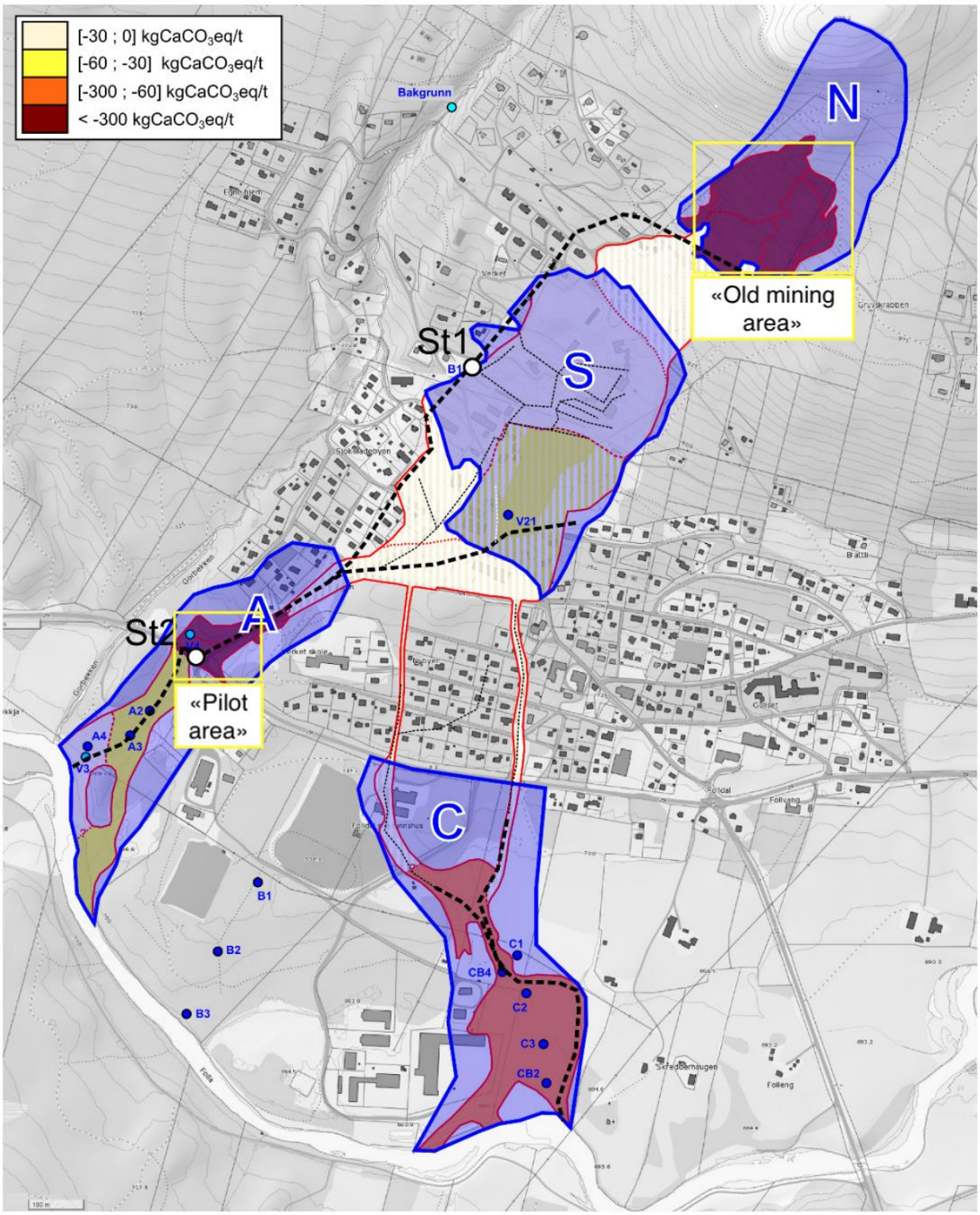

Figure 9: Main areas contributing to Cu-contamination in Folldal; Old mining area (N), Main mining area (S), sludge pool (A) and industrial area(C). Yellow outlined sample areas correspond to those in Figure 8. Broken black lines illustrates surficial drainage pathways to Folla river. Legend is related to underlying map-layer describing acid generating potential. All other map notations can be ignored for the present study. Map compiled from Kvennås et al. (2015).

5. Methodology and procedures in field and laboratory

5.1 Field work, Kabwe

A total of 15 soil samples à 1 kg were collected from 5 sample points (Z1, Z2, Z3, Z4, Z5), in triplicate, with increasing distance from the mine tailings. The sample points were collected along a 1589 meter long southbound transect from the mine tailings, as pictured in the map in Figure 5. The samples were collected from the upper 10 cm of the soil with a shovel and kept in 3L zip-lock bags. The replicates were collected with a 1-meter spatial interval at each sample point. The samples were collected the 22nd of May 2020, stored cool and dry until shipment and arrived in Norway in the end of August 2020. Sample pretreatment and lab analysis was carried out from October to December 2020.

5.2 Field work, Folldal

A total of 5 samples were collected from Folldal, 3 samples from the "old mining area" (N) area and 2 samples from the "pilot area" (A) as seen in figures 8 and 9. The tailings in Folldal are a mixture of different mine residue, hence the sediment composition and heterogeneity varies equally as much in the horizontal as in the vertical plane. To ensure that the collected samples was representative to the heterogeneity of the tailings, the sample points were chosen based on the surface coloration of the tailings. The colors varied from green, yellow, red and dark purple, as illustrated in picture of the dispersed samples in Figure 10. The samples were collected from the upper 45 cm of the tailings and homogenized in a large bucket to get a representative sample. The samples were collected the 29th and 30th of September 2020 and stored and transported in 3L plastic zip-lock bags. Pretreatment and lab-analysis was carried out from October to December 2020.

5.3 Biochar

The particular biochar batch used in this thesis has previously been extensively analyzed through the work of Munera-Echeverri et al. (2018), with the main properties presented in Table 2.

Table 2: Biochar properties. Data compiled from (Munera-Echeverri et al., 2018).

Feedstock	Pyrolysis temp.	Charring method	Pretreatment	DM of biochar	pH*	CEC**	OC	Ca	K	Na	Mg
	ºC		Sieving	%		cmol+/kg	%	g/kg	g/kg	g/kg	g/kg
Pigeon pea biochar	600	Earth-mound kiln	0.5 - 2 mm	95.5	10.4	6.5–11.5	56.1	12	15	0.30	8.3

** Measured in 1:5 ratio of deionized water and raw biochar.*

*** CEC values results from two different washing procedures, by Munera-Echeverri et al. (2018).*

The biochar feedstock used was pigeon pea *(Cajanus cajan)*. The feedstock was pyrolyzed to around 600 ºC in an earth-mound kiln in Mkushi, Zambia, and was crushed and sieved to 0.5 – 2mm biochar fractions prior to analyses and soil application.

5.4 Sample preparation and soil chemical analysis

5.4.1 Sample preparation

The 15 Kabwe samples were dried in a drying cabinet shortly after collection, before they were stored dry and shipped to Norway. Upon arrival the samples were dried again over-night in a 45°C drying cabinet. The Folldal samples were kept field moist for 1-2 days after being sampled before they were dried in a drying cabinet at 45°C during the 5 following days. After drying, all soil samples were sieved though a 2mm mesh stainless-steel with a porcelain pestle. The samples were stored dry in 3L plastic zip-lock bags. A fraction of each sample was crushed with an agat mortar machine prior to analysis of total composition and total carbon (C) and nitrogen (N) content.

5.4.2 Soil organic matter (SOM) and pH

pH

For pH measurement, 10 ml of soil sample and 25 ml water was added to a plastic beaker and shaken by hand until the soil was dispersed in water. The samples were allowed to settle overnight and was re-suspended the next day and left to settle for 15 minutes before pH was measured with MeterLab™PHM210 standard pH meter. The pH meter was calibrated using pH 4 and pH 7 standards.

Soil organic matter (SOM)

Loss on ignition (LOI) and dry matter (DM) was measured gravimetrically by heating the samples in an oven at 105°C overnight to measure the dry matter content (DM). this was followed by LOI determination by heating the samples in a muffle oven at 550°C for more than 3 hours. For most soils, the LOI value gives a good estimate of SOM. However, to prevent overestimation of SOM in mineral soils due to weight loss caused by evaporation of crystalline water associated with clays at high temperatures, a correction figure related to clay content was applied (see appendix table A 1).

The high sulphur (S) content for the Folldal samples interfered with the LOI value (see result section). Hence, the SOM value for these samples were estimated by multiplying the organic (total) carbon value with a conversion factor of 2. This is based on the assumption that total carbon is a measure for soil organic carbon (SOC) due to low inorganic carbon content, and that around 50% of the elements in SOM is carbon, as described by Pribyl (2010).

5.4.3 Cation exchange capacity (CEC)

3.00 g soil was suspended in 50mL 1M NH4CH3CO2 (100 mL Erlenmeyer flasks) overnight. The suspension was then passed through a Whatman™ blue ribbon filter paper into a 250mL volumetric flask, followed by a dilution to 250mL by NH4CH3CO2. The concentrations of Ca, Mg, Na and K was determined by the ICP analyzer, whereas exchangeable acidity was determined by titration (1N NaOH) to pH 7.00. The exchangeable acidity (expressed as H+) and base cations was corrected for dilution, valence, atomic-and soil mass to present the results in units cmol(c+)/kg. The CEC was calculated as the sum of exchangeable acidity and Na, K, Mg, Ca in cmol(c+)/kg. Base saturation (BS) was calculated as the percentage of base cations (Na, K, Mg, Ca) in the total CEC.

5.4.4 Total carbon (C) and nitrogen (N)

After weighing in 150 mg crushed soil sample was washed with 2M HCl and filtered using a Whatman GF/F glassfiber filter for removal of soil carbonates. The samples were washed with deionized water to remove excessive chlorine, followed by drying at 70ºC in a drying cabinet. The dry samples were added Iron Chip and Copper Metal Accelerator to stimulate combustion of the sample in the analyzer instrument; Leco 628 Series (Elemental Analysis by Combustion). The method of dry combustion method was carried out as described in Nelson and Sommers (1996). The main principle of the carbon analysis is based on combustion of the

sample at 1050 ºC, where all emitted CO_2 is quantitively measured in an infrared cell, giving a measurement of total carbon (sum of organic and inorganic C) in the sample.

Total N was measured by the *Dumas* method described in Bremner and Mulvaney (1982). The principle is similar to that of total C. The sample is fully combusted, and NO_x gases are further reduced by copper to N_2, which is measured by a thermal conductivity cell in the Leco CHN628 instrument.

5.4.5 Particle size distribution

The unsorted nature of the Folldal samples made it problematic to get a representative sample to the analysis chamber of the laser diffraction analysis instrument; Bechman coulter LS13 320 Laser Diffraction Particle Analyzer. Additional complications were related to the magnetic properties of particles in the Folldal samples, resulting in excessive sedimentation in the metallic sample chamber. As a result, the pipette method was used to analyze the particle size distribution, as the method proved to experience less interference with the properties of the Folldal samples. The pipette method was carried out for10 samples, one replicate from each of the following sample points: Z1, Z2, Z3, Z4, Z5, F1, F2. F3, F4 and F5 (Figures 5 and 8). The same replicate samples included here were used in further experiments (DGT and Batch).

The pipette method is divided into 4 steps*:*

1. Pre-treatment: Removal of SOM and amorphous compounds (cementing agents) and dispersion of particles in solution.
2. Pipette method: To measure silt and clay fractions by fractionation of the particle sizes according to the sedimentation rate of a spherical particle falls in water with a given density, based on the principles of Stoke's law.
3. Sieving: to measure the sand fraction
4. Drying: to establish a weight percentage of all the particle size fractions.

For the pretreatment, 10g soil sample was added to an 800ml glass beaker, followed by 20ml water and 10 mL of 35% H_2O_2 to oxidize organic matter. Upon completion of the reaction, additional 10 mL of 35% H_2O_2 was added. During the secondary reaction, the beakers were moved to a heated plate at 120°C to boost the reaction. To evaporate any excessive H_2O_2, the beakers were filled with water and left to evaporate on the heated plate until 90ml solution

remained. The beakers were then re-filled with distilled water and added 10 mL of 2M HCl was added to dissolve the amorphous compounds (e.g. carbonates, oxides) that may cement individual particles. In addition, 3 drops of 1M $MgCl_2$ were added to increase the sedimentation velocity. The samples were then left to settle overnight. The following washing procedure was carried out two times over; water was removed from the beakers with a suction hose and the beaker was refilled with water and to which 3 drops of $MgCl_2$ were added.

A strong exothermic reaction occurred when the Folldal samples were added H_2O_2 in the pretreatment process, probably due to an oxidation reaction of the reduced compounds (e.g. sulfides) in the mineral phase. To prevent the reaction from altering the particle size of the samples, the Folldal samples were excluded from the pretreatment with H_2O_2 prior to analyzing by the pipette method. The main aim of the pretreatment is to remove any organic and amorphous matter from the samples. Folldal samples contain minor quantities of organic matter, and although some amorphous materials may be present, the exclusion of this step was not regarded as a major inaccuracy. The rest of the procedure of the pipette method follow the description of Campbell et al. (1986); Elonen (1971), with the setup as pictured in Figure 10. The soil texture was classified according to the soil texture guideline (Jahn et al., 2006).

Figure 10: Picture of the pipette and dispersed samples. From left: Z1, Z2, Z3, Z4, Z5, F1, F2, F3, F4 and F5 (see figures 5 and 8).

5.4.6 Total chemical composition of soils - element analysis

A total of 20 soil samples;15 from Zambia and 5 from Folldal, were analyzed with respect to the total concentration of Al, Ca, Fe, K, Mg, Na, S, Zn, Cu, Cd, Pb. The decomposition of the samples were done by ultra pure (UP) concentrated acid making use of an in UltraCLAVE microwave digestion system from Milestone in teflon test tubes at 260ºC. A mixture of UP-HNO3 and UP-HF was used for the extraction of K, Na, Cu, Pb, whereas UP- HNO3 was used for the extraction of Al, Ca, Fe, Mg, S, Zn and Cd. The element concentrations in the final extracts were determined by either an ICP-OES, or and ICP-MS. Reference material (NCS DC 73325) and blanks were included for quality assessment.

5.5 Diffuse gradient in thin film (DGT) experiment

The experiment included three samples from Kabwe, and two from Folldal; soil sample Z1, Z3, Z5, F2 and F4. The experiment was conducted with and without the addition of biochar. The experiment had two time intervals of DGT deployment time of 6 and 48 hours. Each soil sample with treatments (BC=biochar) and time interval (6 and 48 h) had DGT measurements in triplicates, as illustrated in Figure 11.

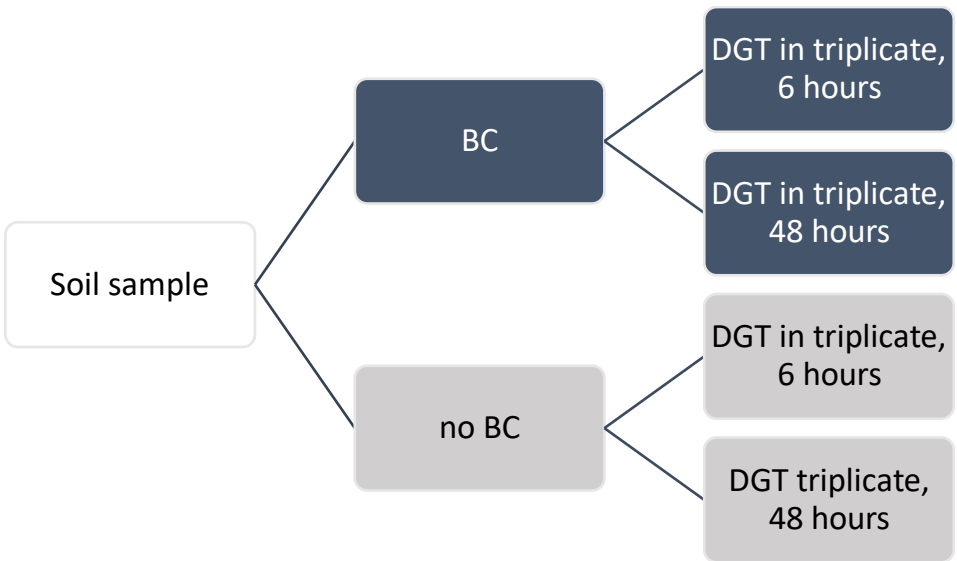

Figure 11: Schematic figure of the experimental setup. This was carried out for 5 soil samples. With biochar (BC) and 5 soil samples without biochar (no BC). DGT devices were set up in triplicate in each sample for both exposure times.

The DGT devices were kept in the refrigerator prior to use, as recommended by the producer. The five soil samples in two parallel series (one with and one without biochar) were added to ten 15x20 cm plastic boxes with a soil depth of minimum 2 cm. The series with biochar consisted of 4wt% and 2wt% biochar for the Kabwe and Folldal samples, respectively. All samples were saturated with distilled water to 100% of the water holding capacity and left to equilibrate overnight. Six DGT's were added to each box the following day, where 3 replicates were left for 6 hours, and 3 replicates left for 48 hours. The boxes were kept with lids on during this time to ensure constant soil saturation. Immediately after removal, excessive soil was rinsed off the device with distilled water to stop diffusion. After rinsing, the device was disassembled and the Chelex resin was carefully separated from the device and placed in individual 15mL plastic test tubes containing 10 mL 10% ultra clean HNO_3 for conservation. The samples were kept in the refrigerator prior to element analysis. Due to considerable variations in element concentrations between the samples, both ICP-OES and ICP-MS instruments, which have different elemental detection limits, were used to analyze the eluates. The experiment also included four DGT blanks kept in original packaging during the experiment. They were conserved and stored in the same manner as the rest of the samples after experiment completion. Four blank samples of the UP-10% HNO_3 used for preservation were also included.

5.6 Batch titration experiment

This experiment was based on the same five soil samples as included in the DGT experiment: Sample Z1, Z3, Z5, F2 and F4. The aim of this experiment was to measure the equilibrium concentration of dissolved metal species in solution of 0.01M KCl background electrolyte and to assess how pH, as a master variable, influences the solubility and solution speciation of Pb, Zn, Cu and Cd in these five soils. In addition, in a parallel series the effect of biochar addition on the metal solubility is investigated. The biochar used in this study had been produced from pigeon pea biomass (see section 5.3).

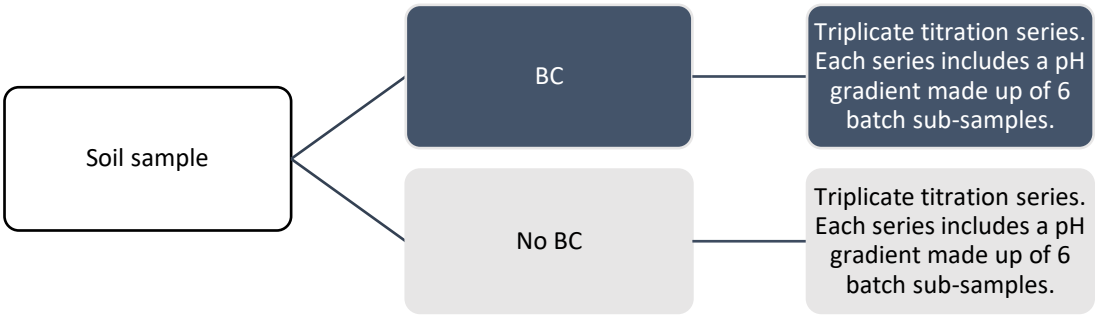

Figure 12: Illustrative setup of the batch titration experiment. This was carried out for 5 soil samples with biochar (BC) and 5 soil samples without biochar (BC). A titration series of one soil sample consisted of 6 individual batches in which the pH had been manipulated through the addition of 0.01 M HCl (Kabwe soil samples) or 0.01 M KOH (Folldal soil samples). All batches had as background electrolyte 0.01 M KCl.

The batch suspensions were made by adding 1.00-4.00g soil (see Table 3) to 50mL plastic test tubes with a background electrolyte solution of 40mL, containing 0.01M KCl and varying concentrations of either 0.01M HCl (Kabwe soils) or 0.01M KOH (Folldal soils; see Table 3). An electrolyte background solution of 0.01M KCl was chosen to ensure reasonably uniform ionic strength in all suspensions. The solid:solution (g/ml) ratio was 1:10 for the Kabwe samples, and 1:40 for Folldal. The low ratio of the latter was required due to the high exchangeable acidity present in the mine tailings, (see map in Figure 9). The pigeon pea biochar addition was set to 4wt% for the Kabwe samples, and 2wt% for the Folldal samples. With background electrolyte (0.01 M KCl) alone the equilibrium pH of the soil samples from Kabwe was about 6, while for the Folldal samples this about 2. To create a similar pH range for the suspensions of both soils, dilute strong acid (HCl) was added to Kabwe samples and dilute strong base (KOH) to Folldal samples. The titration series for each soil consisted of 6 batch samples with an increasing amount of added HCl (Kabwe) or KOH (Folldal), creating a pH range covering a minimum of 2 pH units.

Table 3: Summery of the batch titration experiment. The full experiment included triplicates of all titration series described in the table and was carried out in parallel; with and without addition of biochar. Three blanks from each batch of KOH, HCl and KCl used were also included.

Soil Sample	Titration series	Soil (g)	Biochar wt%	0.01M KOH (mL)	0.01M HCl (mL)	0.01M KCl (mL)
Z1	**a**	**4.00**	**4.00**	**-**	**0.0**	**40.0**
Z1	b	4.00	4.00	-	4.0	36.0
Z1	c	4.00	4.00	-	8.0	32.0
Z1	d	4.00	4.00	-	16.0	24.0
Z1	e	4.00	4.00	-	19.0	21.0

Z1	f	4.00	4.00	-	22.0	18.0
Z3	**a**	**4.00**	**4.00**	**-**	**0.0**	**40.0**
Z3	b	4.00	4.00	-	9.0	31.0
Z3	c	4.00	4.00	-	15.0	25.0
Z3	d	4.00	4.00	-	20.0	20.0
Z3	e	4.00	4.00	-	25.0	15.0
Z3	f	4.00	4.00	-	30.0	10.0
Z5	**a**	**4.00**	**4.00**	**-**	**0.0**	**40.0**
Z5	b	4.00	4.00	-	2.0	38.0
Z5	c	4.00	4.00	-	4.0	36.0
Z5	d	4.00	4.00	-	6.0	34.0
Z5	e	4.00	4.00	-	8.0	32.0
Z5	f	4.00	4.00	-	10.0	30.0
F2	**a**	**1.00**	**2.00**	**0.0**	**-**	**40.0**
F2	b	1.00	2.00	1.0	-	39.0
F2	c	1.00	2.00	1.5	-	38.5
F2	d	1.00	2.00	2.0	-	38.0
F2	e	1.00	2.00	2.5	-	37.5
F2	f	1.00	2.00	3.0	-	37.0
F4	**a**	**1.00**	**2.00**	**0.0**	**-**	**40.0**
F4	b	1.00	2.00	4.0	-	36.0
F4	c	1.00	2.00	6.0	-	34.0
F4	d	1.00	2.00	7.0	-	33.0
F4	e	1.00	2.00	8.0	-	32.0
F4	f	1.00	2.00	9.0	-	31.0

Triplicate suspension series were made of each of the five selected soil samples (both with and without BC), where soil and biochar were weighted to two decimal accuracy and the added volume of respective solutions as shown in Table 3, were added by pipette. Initial lab tests indicated that changes in pH following acid or base addition declined rapidly and little change was observed after more than 4 days equilibration. Therefore, an equilibration time of 7 days was deemed to be sufficient. The batch suspensions were shaken by hand once every day to disperse the sediment in solution. After 7 days the suspensions were centrifuged at 4500 rotations per minute for 20 minutes prior to filtration though 0.45µm millipore filter. The equilibrium pH was measured in sub samples the same day, while the remainder was stored in the refrigerator until analysis of DOC within a few days. To a second sub-sample was was added 10% UP HNO_3 for preservation upon ICP analysis to ensure sample quality. Four blanks for each of the respective 0.01M solutions were used; KCl, HCl, KOH and 10%

UP HNO_3 were included in the ICP analysis, in addition to a reference solution sample (1643H) to detect analytical drift and ensure analytical accuracy.

Preliminary trials

A preliminary experiment was required to establish the amount of HCl and KOH needed to create a pH range of about 2 units for each sample. This was done by trial-and-error through making test-batches with a range of added concentrations of acid or base; also these suspensions were shaken daily over a week before equilibrium pH was measured. This process was carried out for several series before the appropriate amount of titrant was established.

5.6.1 Dissolved organic carbon (DOC)

Shimadzu TOC-V CPN Total organic carbon analyzer was used to determine the DOC concentrations.

5.7 Solution speciation modeling (WHAM)

For speciation of the soil solution, the Windermere Humic Aqueous Model (WHAM) VII was used. WHAM is designed to calculate equilibrium chemical speciation in surface and ground waters, sediments, and soils (Tipping, 1994). The model is a combination of several submodels accounting for binding of ions to humic surfaces, surface complexation to oxides (Fe, Al, Mn, and Si- oxides), inorganic solution chemistry speciation, and cation exchange on mineral clays. In the thesis, only speciation of elements in solution was considered.

The input data in WHAM was compiled from the titration batch titration experiment and included the total dissolved concentration of all the major cations: Ca, Mg, Mn, Na, Fe(III), Al, Zn, Cu, Pb, Cd, and the dominant anions: SO_4^{2-} and Cl^-, as detected in solution by ICP-analysis (table A 4 in Appendix) and their corresponding pH and DOC values. Additional settings included temperature set to 20ºC and the partial pressure of CO_2, pCO_2, set to $3.5e^{-4}$ atm. The output data included all relevant species in solution, including those bound by DOM. To assess the binding of ions to DOM it was assumed that DOM had the properties of fulvic acid (FA), and that 50% of the acid groups were active in proton/metal binding (Almås et al., 2006). The model was specifically set up to not include precipitation of any species even in case of over-saturation.

5.8 Data quality control and statistical analysis

For the ICP-analysis, the level of detection (LOD) and level of quantification (LOQ) was set at 3x and 10x the standard deviation of the four blanks, respectively. Samples with readings less than the LOD and LOQ was given a numerical value by dividing the LOD or LOQ value for the representative element by two. This approach only provides rough estimates but gives the benefit of a completer and more useful dataset. For rejecting outliers in datasets with small number of observations (n=3) for the analysis of the DGT and Batch experiment, a simple Q-test with 90% confidence was carried out as described by Dean and Dixon (1951).

The following statistical analysis was carried out on the dataset.

i) F-test on linear regression analysis in excel using a 95% confidence level was used for establishing the significance of the linear fit of Tot.C vs. LOI (A), Tot.C vs. SOM (B) and LOI vs. [S] (C) in Figure 13.

ii) The logarithmic relationship of total soil metal concentrations with distance from the mine in Kabwe and error bars of each sample point (n=3) was found using excel graph functions (Figure 14).

iii) The linear regression for mass uptake in DGT over the time interval of 6 and 48 hours in figures 15-18 was found using excel graph functions.

iv) The difference in DOC concentration for "field condition" samples with and without biochar (viz. triangle symbols in Figure 25) was tested using one way ANOVA in excel at a 95% confidence level. The parabolic best fit model displayed in the scatterplot graph in Figure 25 was found by using Excel graph functions.

v) Test for significant difference ($p<0.05$) in slope and intercept of the two linear models for BC and no BC in pM^{2+}–pH graphs in Figure 26–Figure 29 was established in R studio with simultaneous tests for general linear hypotheses. The two regression models (BC and no BC) were tested for linear hypothesis of i) difference in slope and intercept, ii) difference in intercept with same slope, and iii) no difference in slope and intercept (the two treatments explained by the same regression model). The models with the best fit are displayed in Figure 26–Figure 29. The presented graphs were made in excel and may therefore differ some to the statistical analysis done in R, although the same dataset was used.

vi) Significant difference in dissolved metals in the "field condition" batches with and without biochar and difference in DGT_BC and DGT_nBC at 6 hours deployment (results in percent presented in Table 8) for all soil samples was tested with one-way ANOVA in excel at 95% confidence level. Excel functions were used to find mean and SD of the percentage-based results presented.

All samples detected under LOD or LOQ were not included with a numerical value in the datasets used for statistical analysis.

6. Results

6.1 Soil chemical analysis

The results presented in this section are related to the methods described in section 5.4.2 – 5.4.5.

Table 4: Soil chemical analysis for all soil samples. Z=Kabwe samples, F=Folldal. The samples from Kabwe were collected in triplicates (see section 5.1), whereas the Folldal samples were collected from a larger homogenized sample (see section 5.2).

** Samples that were further used in DGT and batch-titration experiment.*

*** For the Kabwe samples, SOM was calculated from LOI results corrected for clay content (see table A 1 in appendix) while the Folldal samples were calculated by dividing Tot C% by a factor of 0.5.*

Location	pH	CEC (cmol (c+)/kg)	BS%	Tot. C %	Tot. N %	LOI%	SOM%**	Texture
Z1*	**5.7**	**9**	**58**	**2.02**	**0.12**	**4.6**	**3.6**	
Z 1	6.2	14	67	3.13	0.17	6.0	5.0	Sandy loam
Z 1	5.6	9	49	1.30	0.11	3.6	2.6	
Z 2	5.7	11	41	2.06	0.13	4.6	3.6	
Z 2	5.7	10	38	1.60	0.11	3.8	2.8	Sandy loam
Z 2	5.7	12	27	2.31	0.15	5.1	4.1	
Z 3*	**6.5**	**22**	**73**	**2.86**	**0.16**	**6.6**	**4.6**	
Z 3	6.4	21	66	1.93	0.12	4.9	2.9	Sandy loam
Z 3	6.4	19	68	2.64	0.16	6.1	4.1	

Z 4	5.7	17	34	1.56	0.11	4.7	2.7	
Z 4	5.6	16	40	1.73	0.14	5.2	3.2	Loam/Sandy loam
Z 4	5.8	14	40	1.42	0.12	4.4	2.4	
Z 5*	**6.0**	**12**	**30**	**1.75**	**0.13**	**5.2**	**1.4**	
Z 5	6.0	13	28	1.71	0.13	5.2	2.1	Sandy loam clay
Z 5	6.0	12	39	1.66	0.13	5.3	1.5	
F 1	2.1	32	8	0.40	0.03	7.0	0.8	Loamy sand
F 2*	**2.8**	**11**	**2**	**0.07**	**0.01**	**0.9**	**0.1**	Loamy sand
F 3	2.1	32	7	0.20	0.01	11.9	0.4	Loamy sand
F 4*	**2.1**	**20**	**4**	**0.69**	**0.05**	**4.8**	**1.4**	Loamy sand
F 5	1.8	58	12	0.48	0.03	14.1	1.0	Sand

As presented in Table 4, the soil pH in the samples from Kabwe were slightly acidic within a range of pH 5.6 – 6.5. The pH measurements follow no apparent spatial trend with distance from the mine. The pH readings from the tailings in Folldal is noticeably acidic with pH values ranging from pH 2.1 – 2.8. The CEC for Zambian soils were within normal range given the soil texture. Some of the Folldal samples showed surprisingly elevated CEC values, but only 3-4% clay content and generally low organic carbon content. The CEC for the Folldal samples, measured in ammonium acetate buffered at pH 7, is predominantly made up of exchangeable acidity (H^+ and Al^{3+}), while base cations accounted for only 2-12% of the exchangeable cations. The CEC value for the Folldal samples can therefore be considered a measure of exchangeable acidity, rather than cation exchange capacity.

There is noticeably more total carbon in the samples from Zambia compared to the samples from Folldal. The LOI values for Folldal was unexpectedly high, however, likely unrelated to high organic matter content. Some of the LOI could be accounted for by evaporation of crystalline water in clay, but as the clay content was only around 3-4% for all samples, it did not provide sufficient explanation for the high LOI values alone.

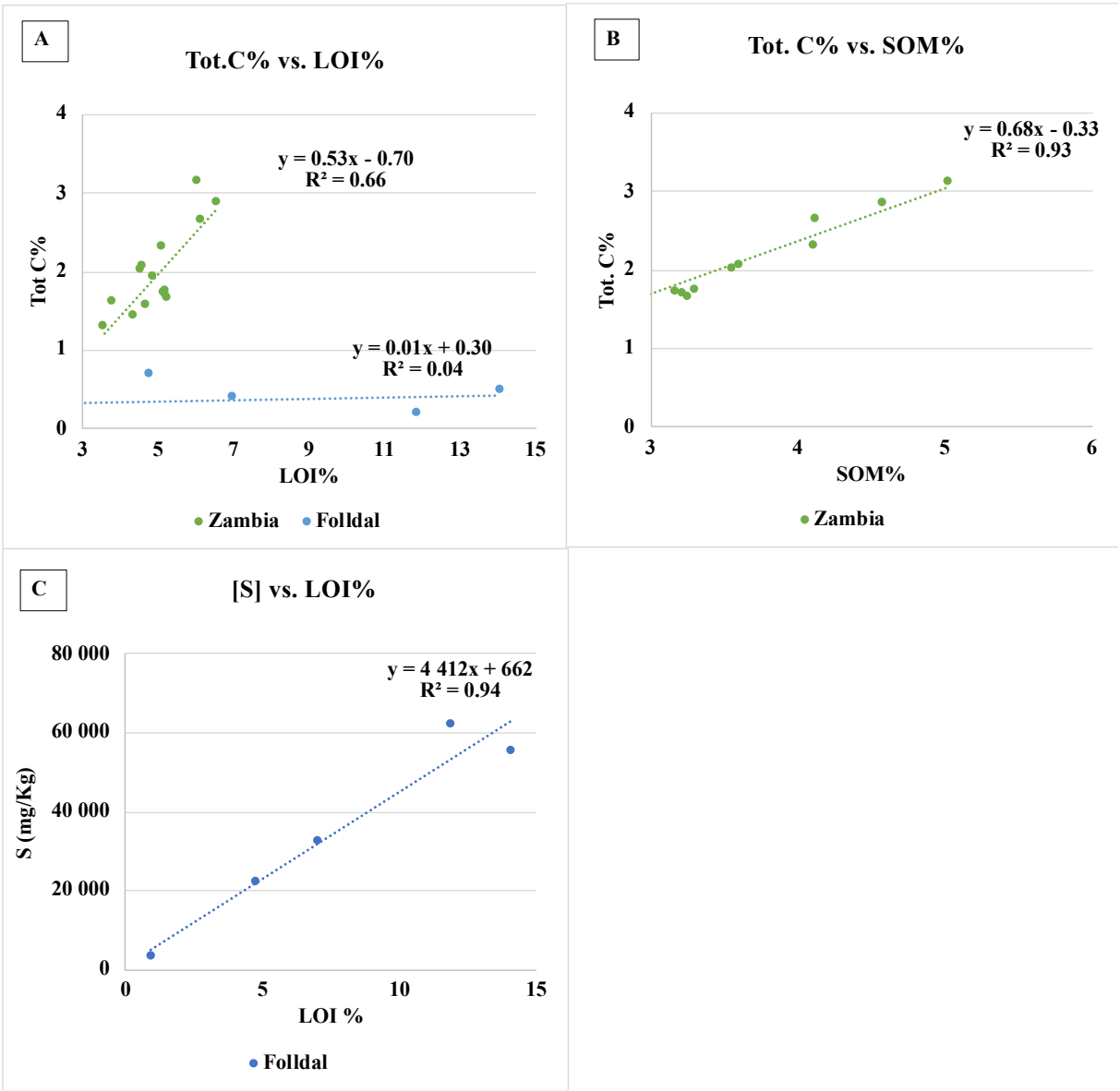

Figure 13: Simple linear regression of different variables relating to the LO results I and SOM. A) Tot.C% and LOI%, B) Tot. C% and SOM%. C) [S] in mg/kg and LOI%. The SOM% data in figure 13.B is the LOI% value corrected for clay content (see table A 1 in appendix). All regression lines presented are significant ($p<0.05$), apart from the LOI%-Tot.C% relationship for the Folldal samples (figure 13.A).

As presented in figure 13.A, the model fit of total C content and LOI in the Kabwe samples (Zambia) was good and significant ($R^2=0.66$, $p<0.05$). The model fit was further improved in figure 13.B where the LOI% data from Kabwe was corrected for crystalline water in clay ($R^2=0.93$, $p<0.05$). No significant relationship between Tot. C% and LOI% was found for the Folldal samples ($R^2=0.04$, $p>0.05$) (Figure 13.A). However, when running a simple linear regression analysis on LOI and total soil S content (13.C) a remarkably good and significant correlation was found ($R^2=0.94$, $p<0.05$).

6.2 Total metal concentrations

The results presented in this section are related to the methodology described in section 5.4.6.

Table 5: Total metal concentrations in soils from Kabwe (Z) and Folldal (F). The colors codes for different classification classes for contaminated soils according to the Norwegian soil guideline presented in

*Table 6. * Samples used in DGT and titration experiment.*

Sample	Pb	Zn	Cu	Cd
	mg/kg	mg/kg	mg/kg	mg/kg
Z 1*	**5.8E+03**	**1.7E+03**	**9.7E+01**	**3.9E+00**
Z 1	1.2E+04	3.7E+03	2.60E+02	1.1E+01
Z 1	1.4E+03	9.5E+02	1.30E+02	1.8E+00
Z 2	5.3E+03	1.5E+03	8.2E+01	6.7E+00
Z 2	4.1E+03	1.4E+03	7.7E+01	4.8E+00
Z 2	5.7E+03	1.5E+03	8.0E+01	7.2E+00
Z 3*	**3.5E+03**	**1.3E+03**	**5.5E+01**	**4.5E+00**
Z 3	1.4E+03	9.7E+02	3.5E+01	3.4E+00
Z 3	2.5E+03	1.3E+03	7.2E+01	4.2E+00
Z 4	7.4E+02	3.8E+02	3.0E+01	1.3E+00
Z 4	7.4E+02	4.3E+02	3.8E+01	1.4E+00
Z 4	8.2E+02	4.1E+02	3.0E+01	1.2E+00
Z 5*	**3.5E+02**	**2.4E+02**	**1.8E+01**	**8.9E-01**
Z 5	3.2E+02	2.6E+02	2.0E+01	8.3E-01
Z 5	3.4E+02	2.8E+02	2.1E+01	9.7E-01
F 1	6.9E+01	2.4E+02	3.40E+02	1.4E-01
F 2*	**8.7E+01**	**1.7E+03**	**2.000E+03**	**1.6E+00**
F 3	1.6E+02	1.5E+02	7.000E+03	2.5E-01
F 4*	**2.7E+01**	**3.0E+01**	**3.60E+02**	**7.3E-02**
F 5	1.5E+02	3.6E+02	1.500E+03	5.1E-01

*Table 6: Color codes for contaminated soil classes according to the Norwegian classification system (Hansen & Danielsberg, 2009). Units in mg/kg. *Class 6 is not included in the original Norwegian guideline as the highest contamination class described is class 5. It is however stated that concentrations over class 5 are considered special waste (Hansen & Danielsberg, 2009).*

	1	2	3	4	5	6

	Very good	Good	Moderate	Bad	Very bad	Special waste*
Pb	<60	60-100	100-300	300-700	700-2500	>2500
Zn	<200	200-500	500-1000	1000-5000	5000-25000	>25000
Cu	<100	100-200	200-1000	1000-8500	8500-25000	>25000
Cd	<1.5	1.5-10	10-15	15-30	30-1000	>1000

Table 7: Summery of different threshold values for contaminated soils compiled from international guidelines (mg/kg).
a: Guideline values from Norwegian Environment Agency (miljødirektoratet). The presented values are according to the classification system in Table 6, and show the threshold values of class 3, moderate. (Hansen & Danielsberg, 2009)
b: Threshold values compiled from Tóth et al. (2016)
c: Selected guideline values for "agriculture and residential areas" compiled from the Canadian Council of Ministers of the Environment (CCME, 2001).

	Pb	**Zn**	**Cu**	**Cd**
Norwegian guideline threshold (moderate) [a]	100-300	500-1000	200-1000	10-15
EU guideline threshold [b]	60	200	100	1
Canadian guideline threshold [c]	70-140	200	63	1.4-10

The metal concentrations as presented in Table 5 bring light to the difference between the two sites of Kabwe and Folldal in terms of contamination level. Alarmingly high concentrations of Pb were detected in Kabwe with levels corresponding to contamination category "very bad" to "special waste" according to the Norwegian guidelines. The levels of Zn in Kabwe were measured to category 4 "bad". the highest Cu levels were measured in Folldal, also reaching category 4. The results show considerable variations in metal concentrations between the sample points at each site, especially between the samples in Folldal. The heterogenous nature of the Folldal tailings is well illustrated by the total Zn levels at sample point F2 and F3, that were measured to contamination level 1 (very good) to level 4 (bad), over a relatively short distance (Figure 8).

The Norwegian soil contamination classes presented in
Table 6 can be considered as more liberal than other international soil quality guidelines (Table 7). The Canadian and EU guidelines are more restrictive in comparison as the

threshold values for all four metals in the two international guidelines are within what is considered contamination class “very good” and “good” in the Norwegian guideline.

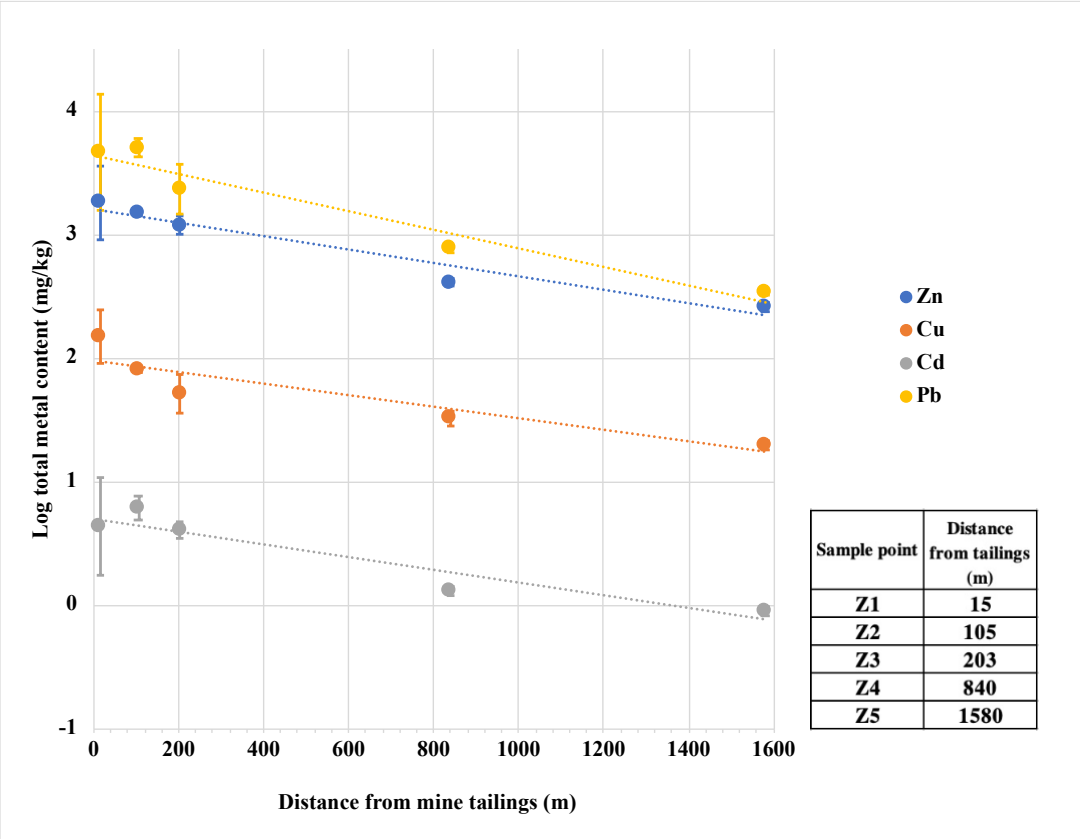

Sample point	Distance from tailings (m)
Z1	15
Z2	105
Z3	203
Z4	840
Z5	1580

Figure 14: Total soil metal concentration relative to the distance from the mine tailings. The distance from the mine tailings for each sample point is described in the table included in the figure (for map see Figure 5). The error bars relate to the standard deviation of three replicate samples taken at each sample point. The error bars for sample points Z4 (840m) and Z5 (1580m) are included but are not visible as they are smaller than the symbols. Note the logarithmic y-axis.

As presented in Figure 14 the total soil concentrations for all the metals in Kabwe follow a negative trend with distance from the mine.

6.3 Bioavailability (DGT)

The following results are related to the DGT experiment described in section 5.5.

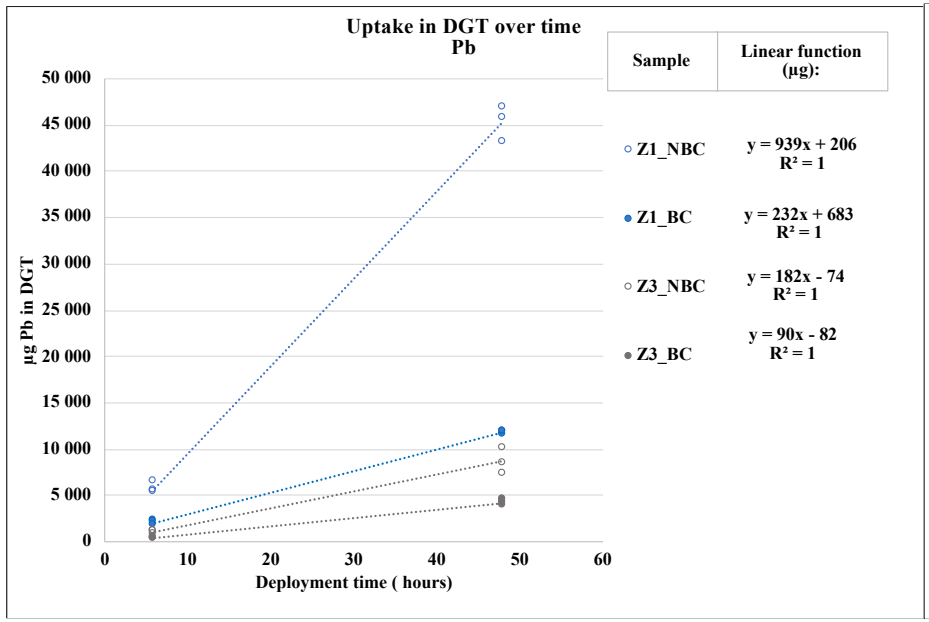

Figure 15: Pb mass (µg) diffused into the DGT resin after 6- and 48-hours deployment time for each soil sample, with the addition of biochar (BC, filled symbols) and without the addition of biochar (NBC, open symbols). Sample Z5, F2 and F4 was excluded due to overrepresentation of LOD and LOQ values. The broken lines represent regression lines for the time-window of 6-48 hours deployment. (n=6).

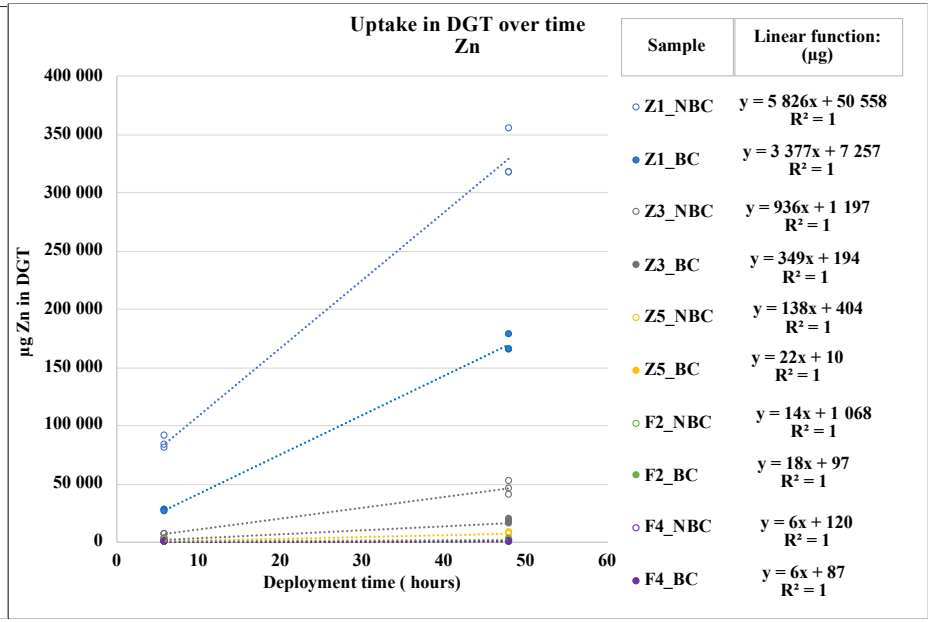

Figure 16: Zn mass (µg) diffused into the DGT resin after 6- and 48-hours deployment time for each soil sample, with the addition of biochar (BC, filled symbols) and without the addition of biochar (NBC, open symbols). The broken lines represent regression lines for the time-window of 6-48 hours deployment. (n=6).

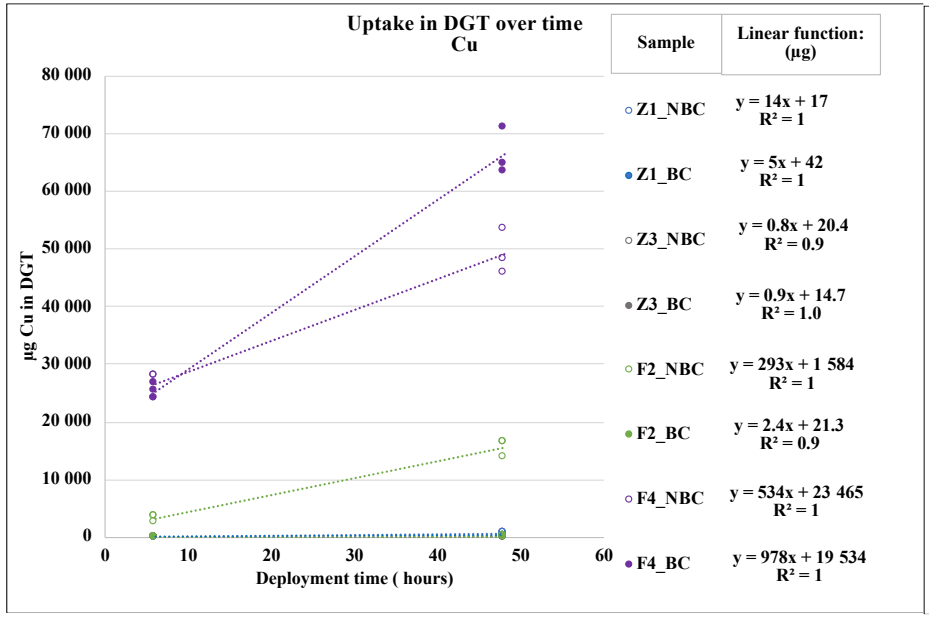

Figure 18: Cu mass (µg) diffused into the DGT resin after 6- and 48-hours deployment time in each soil sample with the addition of biochar (BC, filled symbols) and without the addition of biochar (NBC, open symbols). Sample Z5 was excluded due to overrepresentation of LOD and LOQ values. The broken lines represent regression lines for the time-window of 6-48 hours deployment. (n=6).

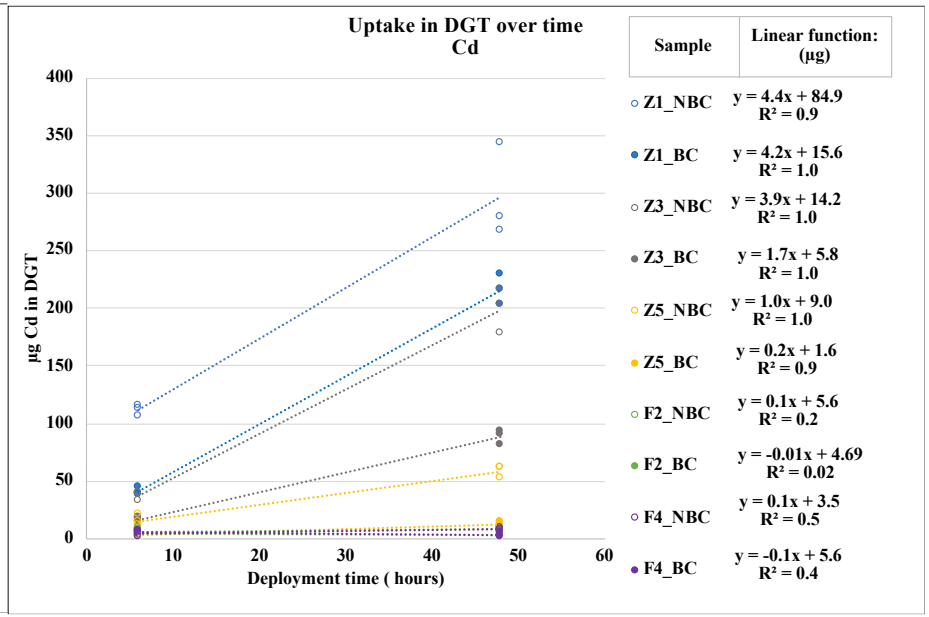

Figure 17: Cd mass (µg) diffused into the DGT resin after 6- and 48-hours deployment time in each soil sample with the addition of biochar (BC, filled symbols) and without the addition of biochar (NBC, open symbols). The broken lines represent regression lines for the time-window of 6-48 hours deployment. (n=6).

Figures 15-18 show a general trend of decreased bioavailable concentrations for all metals in samples treated with biochar (filled symbols), compared to untreated (open symbol). Figures 15-18 include regression lines for the temporal interval of 6- and 48- hour DGT deployment time. The slope of the regression line included in the figures expresses the uptake rate in µg per hour. The biochar treated samples generally showed reduced rates compared to the untreated samples, however, the addition of biochar to sample F4 increased uptake rates of DGT-available Cu over the time interval.

The apparent steady increase in mass uptake with time in figures 15-18 indicates that the DGT is a sink of all metals. The 48h/6h uptake mass ratio was 8 or above for Pb in Kabwe samples Z1 and Z3, and Zn in sample Z5 (see table A 3 in appendix).

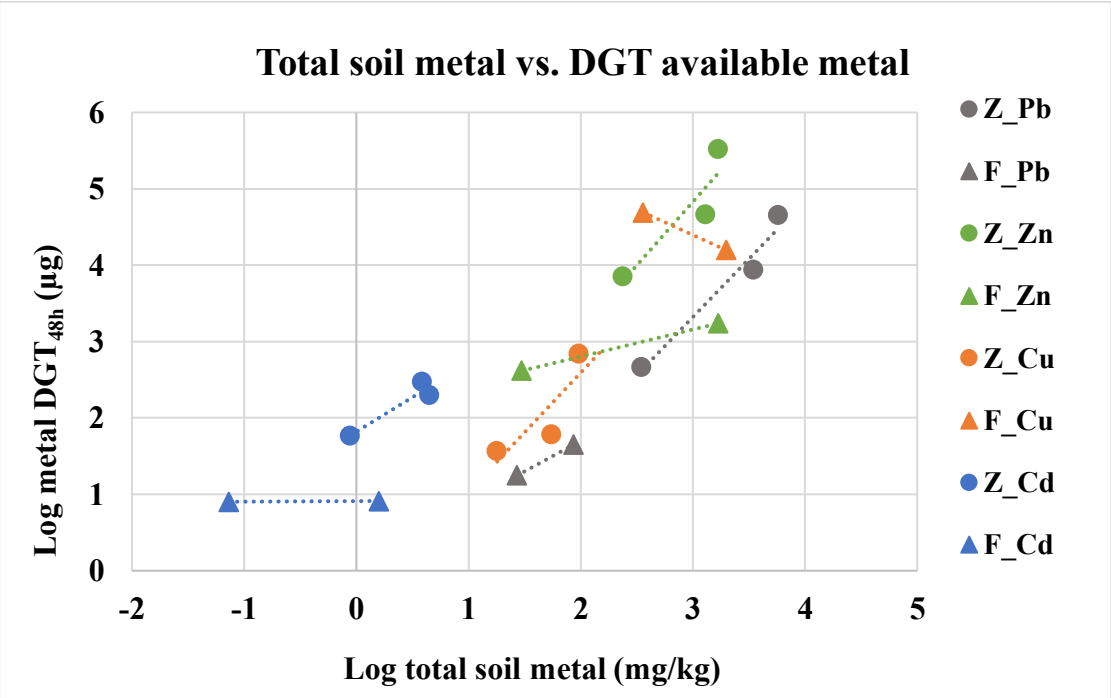

Figure 19 : Correlation between total soil metal concentrations and mass uptake in DGT after 48 hours deployment for Pb, Zn, Cu and Cd. Round symbols represent Kabwe samples (Z), and the triangular represent Folldal samples (F).

As illustrated in Figure 19, there is a general positive correlation between total soil metal concentrations and DGT mass uptake for all metals from Kabwe (round symbols) and Folldal (triangular symbols). The only clear exception to this is Cu in the Folldal samples F2 and F4, showing an apparent negatively correlated relationship.

6.4 Batch titration experiment

The following results relate to the batch titration experiment described in section 5.6. Each soil sample has six batch sub-samples (marked a-f), where “a” is in equilibrium with 0.01M KCl, referred to as “field condition”, and the additional five (b-f) are titrated with increasing levels of HCl for Kabwe and KOH for Folldal (see Table 3). The results include the total dissolved (<45µm) metal concentration and the speciation of these, with and without the addition of biochar.

6.4.1 Total dissolved metals in equilibrium solution

This section focuses on the total concentration in solution illustrated in graph 20-23 as the full height of the respective stack bars representing the sum of all major metal species in solution. However, it should be noted that this concentration (height of stackbars) is lower than the actual measured metal concentration in solution (See table A 4 in the appendix). This is because the speciation output from WHAM is given in activities in mol/L. In figure 20-23 the molar activity of each species has been converted to activities in µg/L. Due to the reasonably high ionic strength of the solution (0.01M), the total sum of activities of all species is lower than the measured concentration in solution (WHAM input data found in table A4)

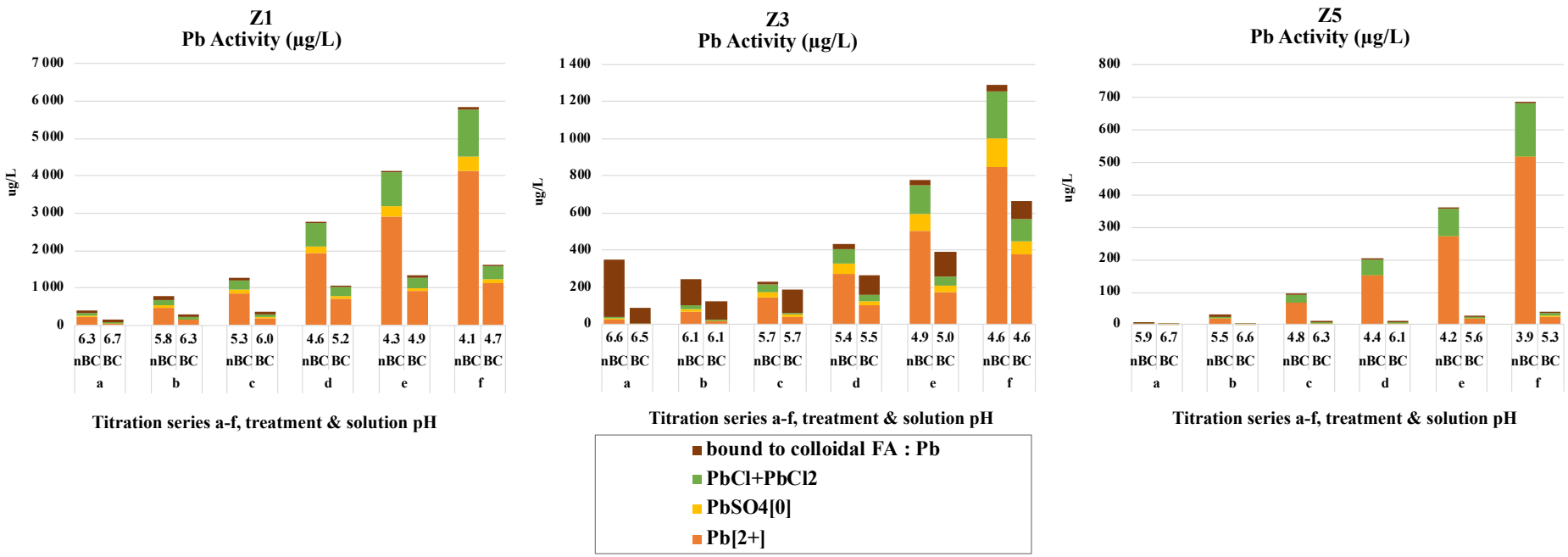

Figure 20 : Total concentration (activities in µg/L) and speciation of dissolved Pb after 6 days equilibration in the titration series (a - f), with (BC) and without (nBC) the addition of biochar. Titration series a-f represent increasing amount of 0.01 M HCl, in a background of 0.01 M KCl, added to the sample as presented in Table 3. Sample "a" for each sample represents "field condition" at equilibrium with 0.01M KCl. Sample F2 and F4 are not included in the figure as the total concentration of Pb in solution generally was below LOD. Note the difference in y-axis between the graphs. The presented results are mean values of three replicates.

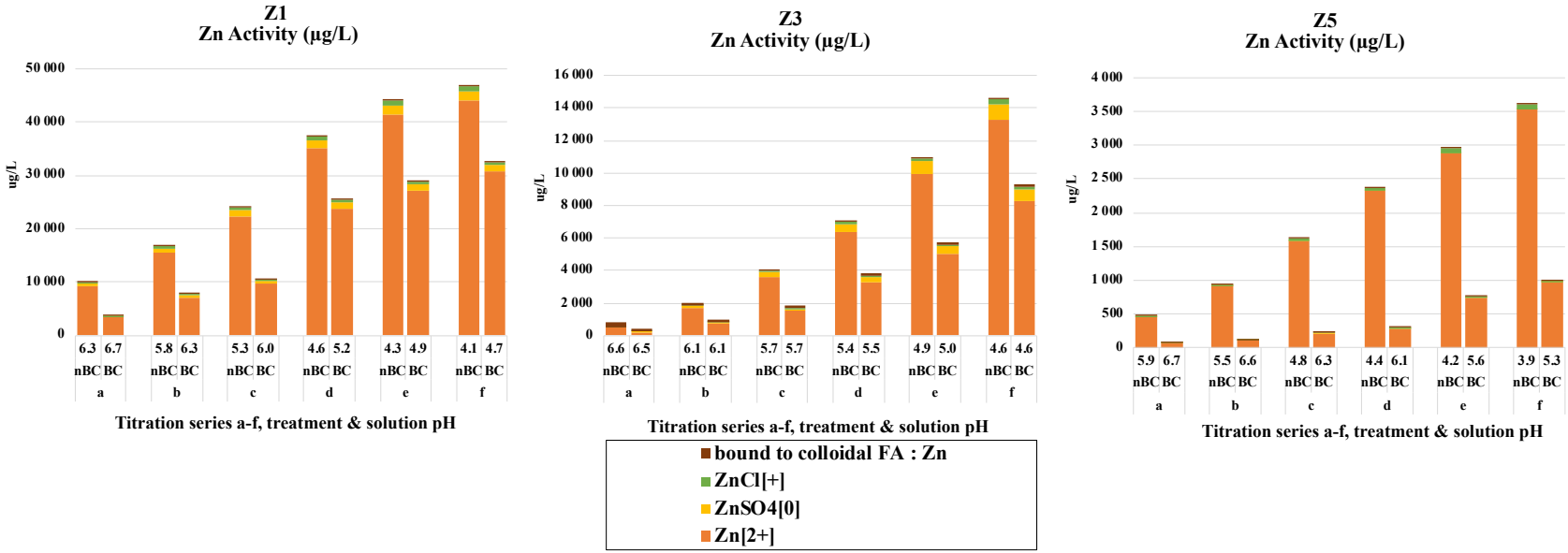

Figure 21: Total concentration (activities in µg/L) and speciation of dissolved Zn after 6 days equilibration in the titration series (a - f), with (BC) and without (nBC) the addition of biochar. Titration series a-f represent increasing amount of 0.01 M HCl, in a background of 0.01 M KCl, added to the sample as presented in Table 3. Sample "a" for each sample represents "field condition" at equilibrium with 0.01M KCl. Sample F2 and F4 are not included in the figure as the total concentration of Zn in solution generally was below LOD. Note the difference in y-axis between the graphs. The presented results are mean values of three replicates.

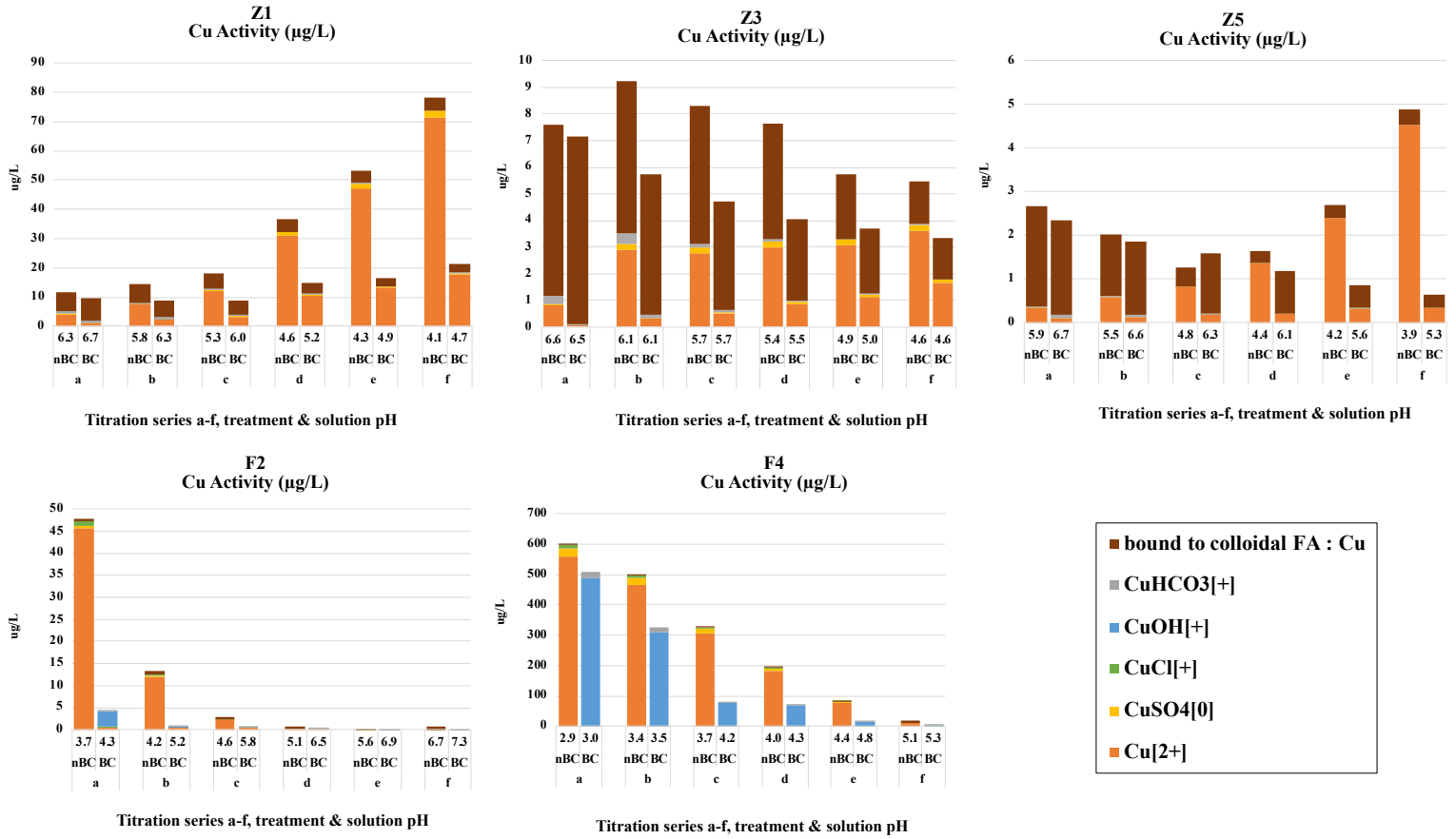

Figure 22 Total concentration (activities in µg/L) and speciation of dissolved Cu after 6 days equilibration in the titration series (a - f), with (BC) and without (nBC) the addition of biochar. Titration series a-f represent increasing amount of HCl (for Kabwe samples) and KOH (for Folldal samples) added to the sample as presented in Table 3. Sample "a" for each sample represents "field condition" at equilibrium with 0.01M KCl. Note the difference in y-axis between the graphs. The presented results are mean values of three replicates.

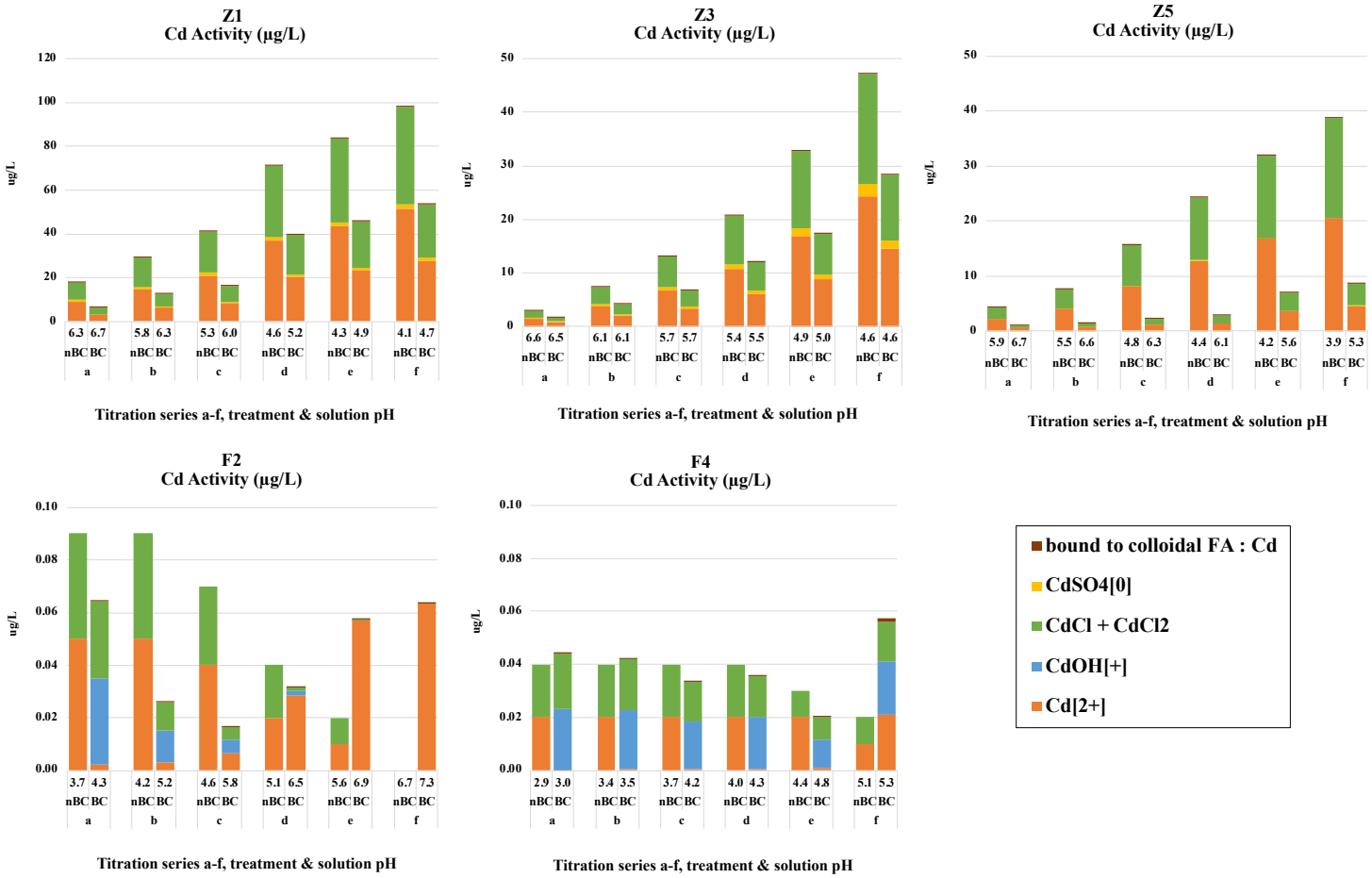

Figure 23: Total concentration (activities in µg/L) and speciation of dissolved Cd after 6 days equilibration in the titration series (a - f), with (BC) and without (nBC) the addition of biochar. Titration series a-f represent increasing amount of HCl (for Kabwe samples, Z) and KOH (for Folldal samples, F) added to the sample as presented in Table 3. Sample "a" for each sample represents "field condition" at equilibrium with 0.01M KCl. Note the difference in y-axis between the graphs. The presented results are mean values of three replicates. The readings for dissolved Cd in solution for the biochar treated F2 samples is partly represented by LOQ/LOD values and is therefore associated with more uncertainty than the other datasets.

The added amount of 0.1M HCl to the Kabwe samples and 0.01M KOH to the Folldal samples (Table 3) established form the preliminary trial, showed successful in making a pH gradient covering 2 pH units for all samples without biochar. The addition of biochar gave a general increase in pH for all samples, but the magnitude of pH increase varied over the soil samples and titration series. The addition of biochar increased the pH for all "field condition" samples (marked with "a" in figure 20-23) with a mean increase for sample Z1, Z3, Z5, F2 and F4 of 0.3, 0.4, 0.9, 0.6 and 0.1 pH units, respectively.

The general trend shows increasing total metal concentration at decreasing pH. The only clear exception of this is the total dissolved Cu concentrations decreasing with decreasing pH in samples Z3 and Z5, as long as the solution pH > 4.4 (Figure 22). This will be discussed in more detailed in the section about metal speciation. For Cd there is no clear trend in total concentration with decreasing pH in samples F2 and F4 (Figure 23). Some of the titration samples of F2 showed Cd levels under LOD and LOQ, presented in Figure 23 as half of the representative LOD or LOQ value (see section 5.8), which add additional uncertainties for interpretation of the trend.

The highest dissolved total metal activities (in µg/L) of Pb, Zn, Cu and Cd in the Kabwe samples were detected in sample Z1 (note difference in y-axis in figures 20-23) and decreased in the order Z1>Z3>Z5, concurring with the total metal concentrations (Table 5) and distance from the mine (map in Figure 5). In the Folldal samples, the apparent elevated levels of dissolved Cu in equilibrium solution for sample F4 relative to F2 in Figure 22 were unexpected, as F2 had greater total Cu concentration in the soil sample compared to F4 (Table 5).

The effect of biochar is evident as there is a clear overall reduction of total metals in solution for the treated samples (BC) compared to the untreated samples (nBC) over the titration series. The lack of a clear reducing effect of biochar on total metal concentration in solution for sample F2 and F4 (Figure 23) can also likely be attributed to solution concentrations close to the LOD and associated uncertainties.

6.4.2 Solid solution partitioning

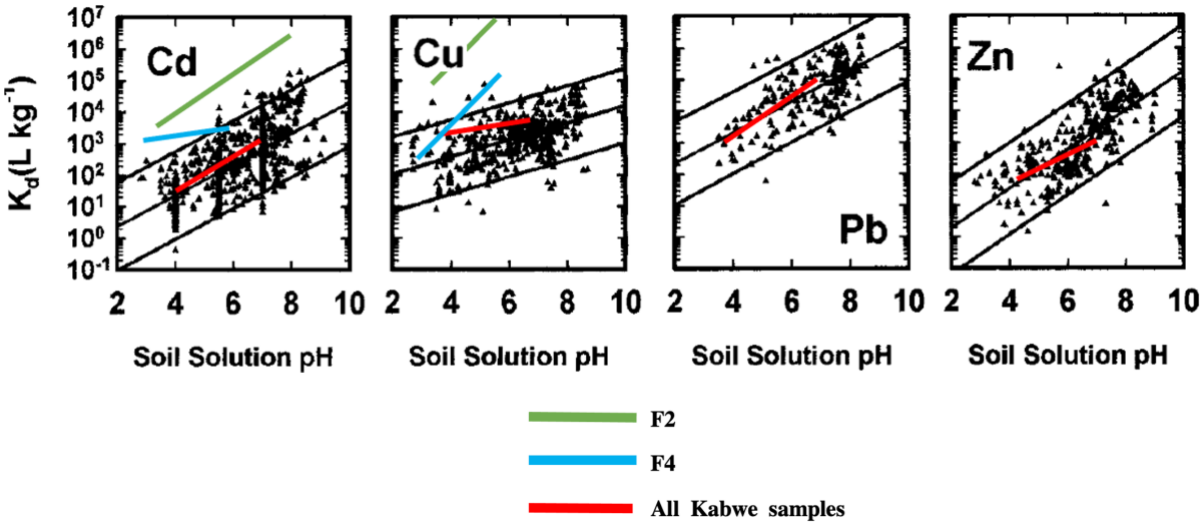

Figure 24: Simple linear regressions explaining the Kd response to changes in pH. The red line represents the linear regression for all batch samples from Kabwe, with and without addition of biochar (n=36). The green line represents the regression line of sample F2 (n=18), and the blue line for sample F4 (n=18). The Kd values are calculated from the ratio of total soil metal concentrations (Table 5) and total metal concentrations in equilibrium solution (appendix table A 4). The original data for Folldal and Kabwe, on which the regression lines are based, can be found in appendix figure A 5. The regression lines are superimposed on data from the review paper by Sauvé et al. (2000), where the upper and lower lines represent the 95% confidence interval of Kd-pH relationships from 70 different studies. The total dissolved Pb and Zn concentrations in the Folldal samples (F2 and F4) were not included in the analysis, due to low concentrations and therefore high uncertainty in the data.

As presented in Figure 24, the linear relationship of the datapoints from Kabwe (red line) fit within the 95% confidence interval of the review paper by Sauvé et al. (2000). The data in the study from Sauvé et al (2000) are comprised from 70 different studies assessing the Kd relationship with pH, covering a wide range of soils. However, the tailings from Folldal (green and blue line) generally fall outside the confidence interval. This is explained by the fact that Sauvé et al. compiled studies done on soils exclusively and did not include mine tailings or similar sediments in their dataset. The generally higher Kd values for the tailings indicate that Cu and Cd-containing phases in the Folldal tailings are less soluble than those in the contaminated soils in Kabwe.

6.4.3 DOC

The DOC was analyzed in equilibrium solutions from the batch-titration experiment, as described in section 5.6.

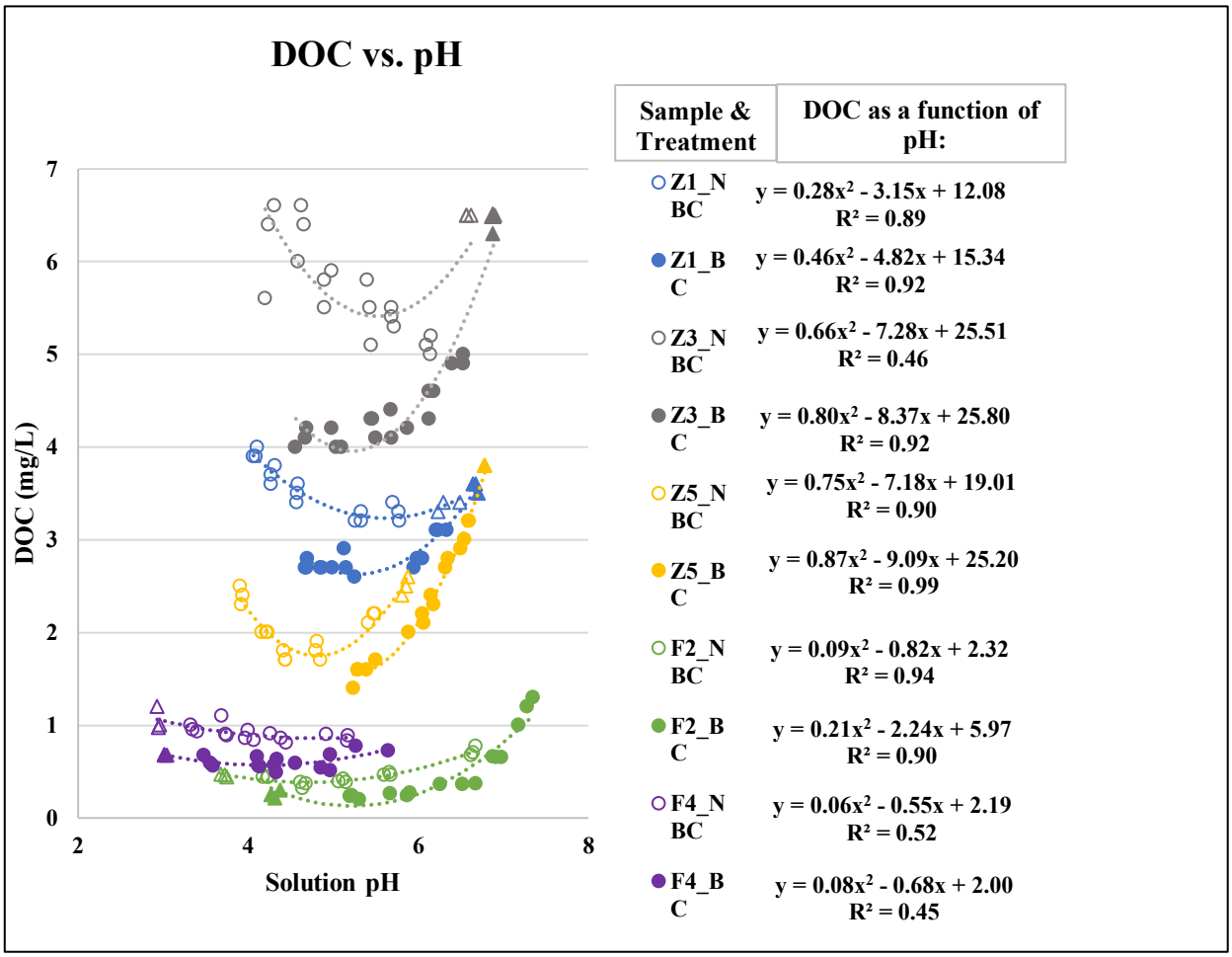

Figure 25: Best fit model for DOC as a function of solution pH for all soils, with all replicates included (n=18). Biochar treated samples (BC) are represented with filled symbols and untreated (NBC) with open symbols. The triangular symbols represent the un-titrated "field condition" batches (soil at equilibrium with 0.01M KCl) for each soil sample and treatment.

As presented in Figure 25 the DOC concentrations are lowest at around pH 5 for all samples and generally increases at lower and higher pH values, creating the apparent parabolic relationship between DOC and pH. Another prominent effect is that the biochar treated samples (filled symbols) generally show lower DOC concentrations than the untreated samples (open symbols), over the same pH range. This effect seems to be most prominent in the lower pH-range, and when comparing the "field condition"-batches for the two treatments (triangular symbols in Figure 25), the effect is less profound. In fact, there was a significant ($p<0.05$) increase of DOC in the biochar treated "field condition" batch for sample Z1 and Z5, whereas no significant change was found for sample Z3. In contrast, the biochar treatment resulted in a significant reduction ($p<0.05$) of DOC in the "field condition" batches of Folldal sample F2 and F4.

6.4.4 Metal speciation of equilibrium solutions

This section relates to the speciation of the equilibrium solutions from the batch experiment as presented in figure 20-23.

6.4.4.1 Metal speciation in 0.01 M KCl background ("field condition")

The "field-condition" for each sample referred to here is marked as nBC for sub-sample «a» in the titration series in figure 20-23. The speciation of this field condition reveals that:

i) Dissolved Pb levels in Kabwe are high and a relatively large fraction is present as Pb^{2+}. Only in Z3, where the DOC concentration is highest (Figure 25), the FA-bound fraction of dissolved Pb is of importance. Dissolved Pb in mine tailings of Folldal are low.

ii) Dissolved Zn in Kabwe soils is largely present as Zn^{2+} in all three samples. Dissolved Zn in mine tailings of Folldal are low.

iii) Dissolved Cu in Kabwe soils has a relatively important FA-bound fraction and some Cu^{2+}. In Folldal dissolved Cu is significantly higher than in Kabwe and Cu^{2+} is the main species.

iv) Dissolved Cd in Kabwe and Folldal is present as equal parts of $Cu^{2+}$and Cd-Cl species.

The metal speciation implies that many of the species are readily available in soil solution, and that DOC is an important ligand for the Pb and Cu mobility in Kabwe.

The biochar effect measured at "field condition" reveal that the net overall reduction in dissolved metals is largely attributed to the reduction in free ion activity of all metals in all sites. For Pb, the reduction in FA-bound species was additionally contributing to the total reduction in dissolved concentration. By contrast, the speciation also revealed an increase in certain species in solution in response to biochar addition, namely $CuOH^+$ and $CdOH^+$ in Folldal samples F2 and F4. As a consequence, the increase of the latter species due to biochar addition resulted in an unsignificant ($p>0.05$) net increase of dissolved Cd in sample F4 as presented in Figure 23.

6.4.4.2 Metal speciation over titration series

The solution speciation of the untreated samples (nBC) of the titration series as a whole, reveals that all five soil samples have a substantial fraction of labile metals able to be

mobilized with a reduction in solution pH (geochemically active). Other relevant species that increase in activity with a reduction in pH are Pb-Cl species in Kabwe and Cd-Cl species in both Kabwe and Folldal. Contrary, the activity of FA-bound Cu in sample Z3 and Z5 decrease with decreasing pH. This explains the divergent trend of total dissolved Cu over pH for samples Z3 and Z5 for solution pH > 4.4, as commented in section 6.4.1.

The solution speciation of the biochar treated samples (BC) over the titration series reveals that all species increases with decreased solution pH. Exceptions to this general observation is related to an increase in FA-bound species due to the mechanisms of DOC dissolution caused by changes in pH as shown in Figure 25. When comparing the speciation of all the biochar treated titration samples (BC) to the corresponding untreated titration samples(nBC), it is evident that there is a general reduction in all species in the biochar treated samples, with an especially strong reduction in free metal ions. However, the biochar addition causes an increase of $CuOH^+$ species over the titration series in the biochar treated Folldal sample F4 (Figure 22).

6.4.5 Free ion activity and pH

The following graphs show the negative logarithm of free ion activity (in mol/L) over pH. The free ion activity in figure 26-29 relates to the orange fractions of the stack bars in figure 20-23. However, note that the y-axis in figure 20-23 was converted to activities in µg/L, and that the y-axis in figure 26-29 is based on the negative logarithm of activities in mol/L. For interpretation of figure 26-29, note that the graph is double (negative) logarithmic, hence slight shifts in the figures may be of significance.

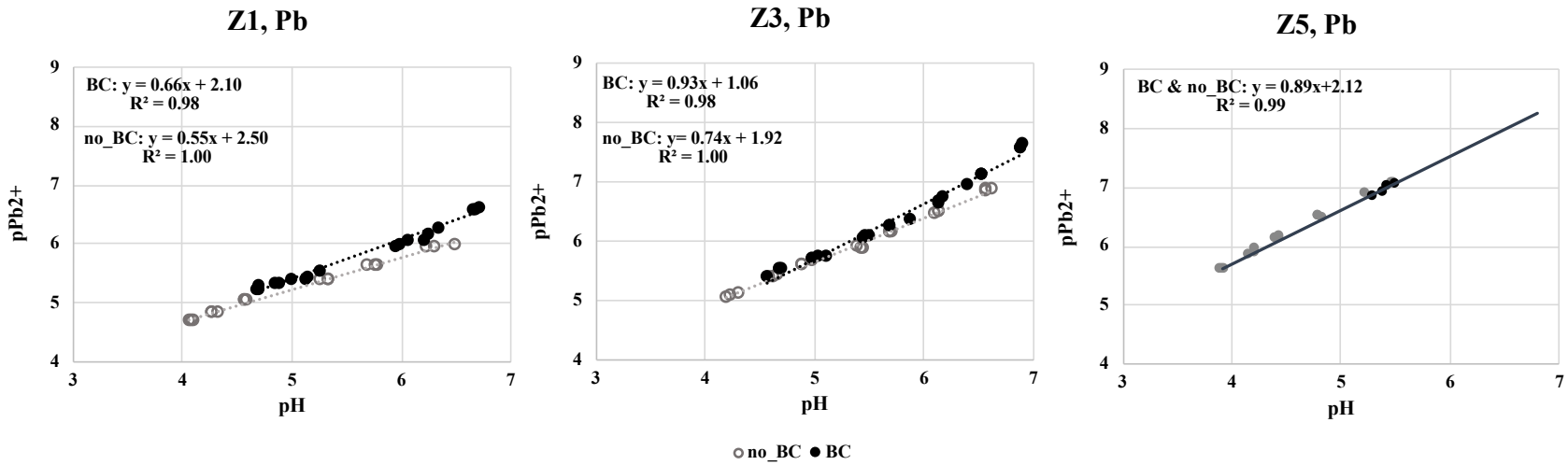

Figure 26: Negative logarithm of free ion activity of Pb (pPb^{2+}) as a function of pH for Kabwe samples Z1, Z3 and Z5. The Folldal samples are not included because the elemental concentrations of dissolved Pb were below LOD (Only readings above LOD and LOQ is included in the figure). Data from biochar treated samples are represented with filled symbols and untreated with open symbols. The regression equation in the left corner from the top is for biochar treated samples, over the expression for the untreated samples. The total variation is presented as all replicates are included in the figure. Slope and intercept of the two linear models (BC and no_BC) was statistically different ($p<0.05$) for Z1 and Z3, but not for Z5. Hence, one regression model explains the relationship of the two treatments in Z5.

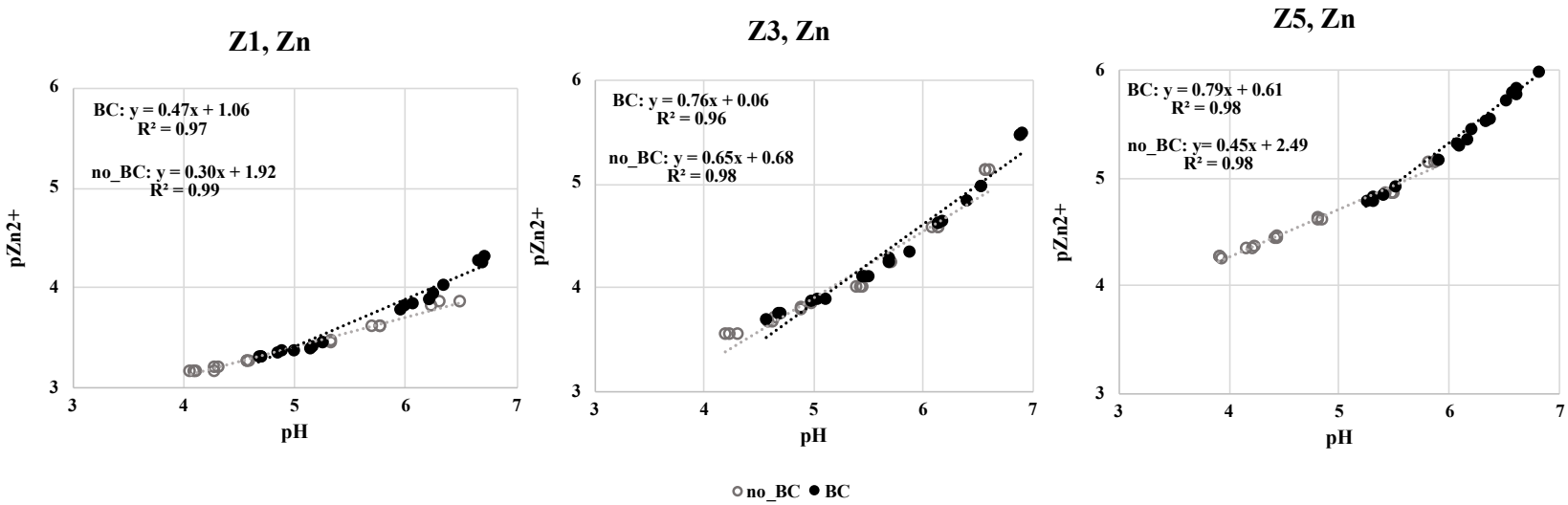

Figure 27: Negative logarithm of free ion activity (M) of Zn (pZn^{2+}) as a function of pH for Kabwe samples Z1, Z3 and Z5. The Folldal samples are not included because the elemental concentrations of dissolved Pb were below LOD (only readings above LOD and LOQ are included). Data from biochar treated samples are represented with filled symbols, and untreated with open symbols. The regression equation in the left corner from the top is for biochar treated samples, over the expression of the untreated samples. The total variation is presented as all replicates are included in the figure. Slope and intercept of the two linear models (BC and no_BC) was statistically different ($p<0.05$) for Z1, Z3 and Z5.

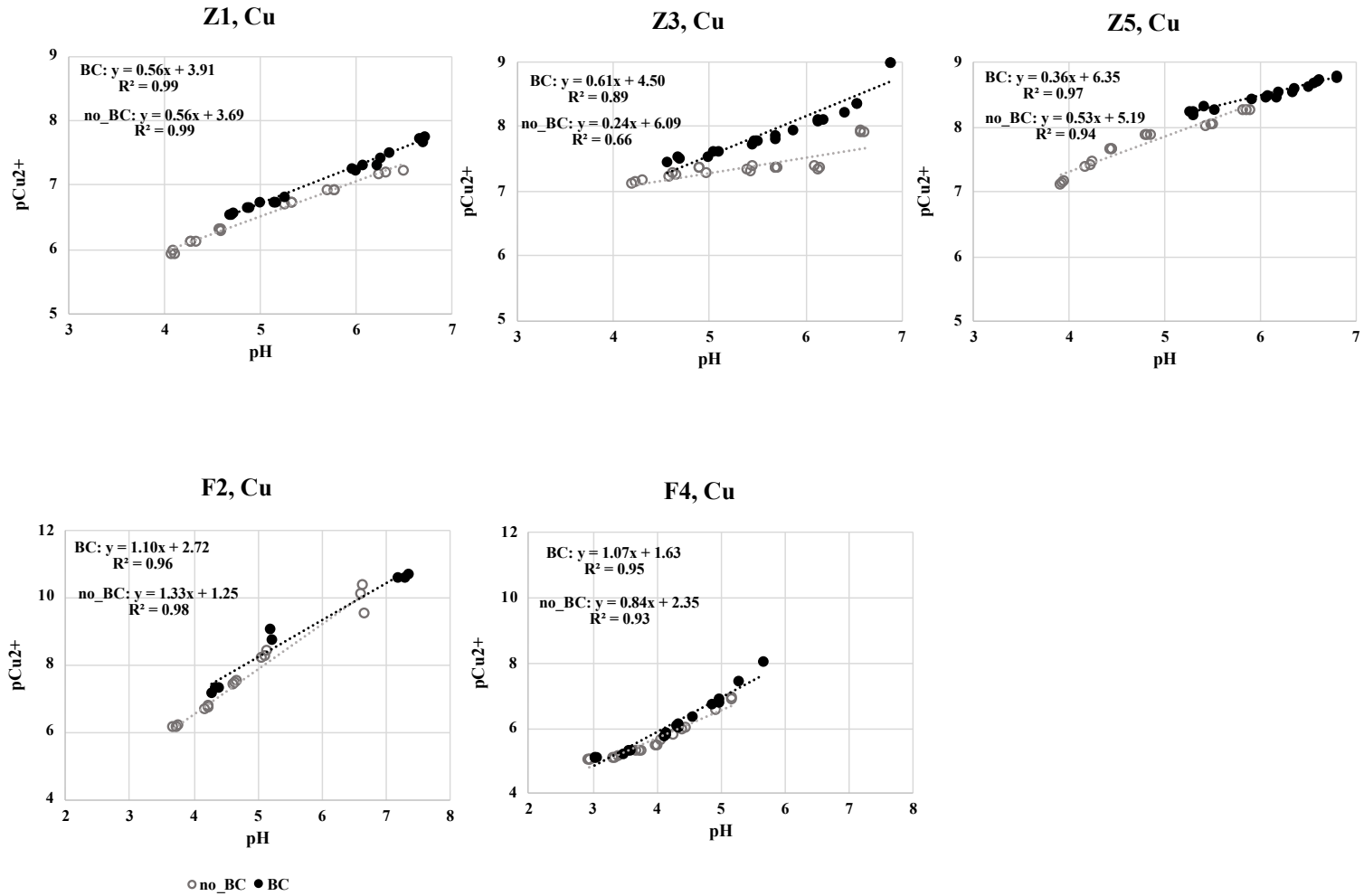

Figure 28: Negative logarithm of free ion activity(M) of Cu (pCu^{2+}) as a function of pH for sample Z1, Z3 and Z5 from Kabwe, and F2 and F4 from Folldal. Data from biochar treated samples are represented with filled symbols, and untreated with open symbols. Note that the y-axis in the coordination systems is different between the Kabwe and Folldal samples. The regression equations in the left corner from the top relates to biochaar treated samples, over the expression of the untreated samples. The total variation is presented as all replicates were included in the figure (only readings above LOD and LOQ). Slope and intercept of the two linear models (BC and no_BC) were statistically different ($p<0.05$) for sample Z3, Z5, F2 and F4. For Z1, only the intercept was statistically different.

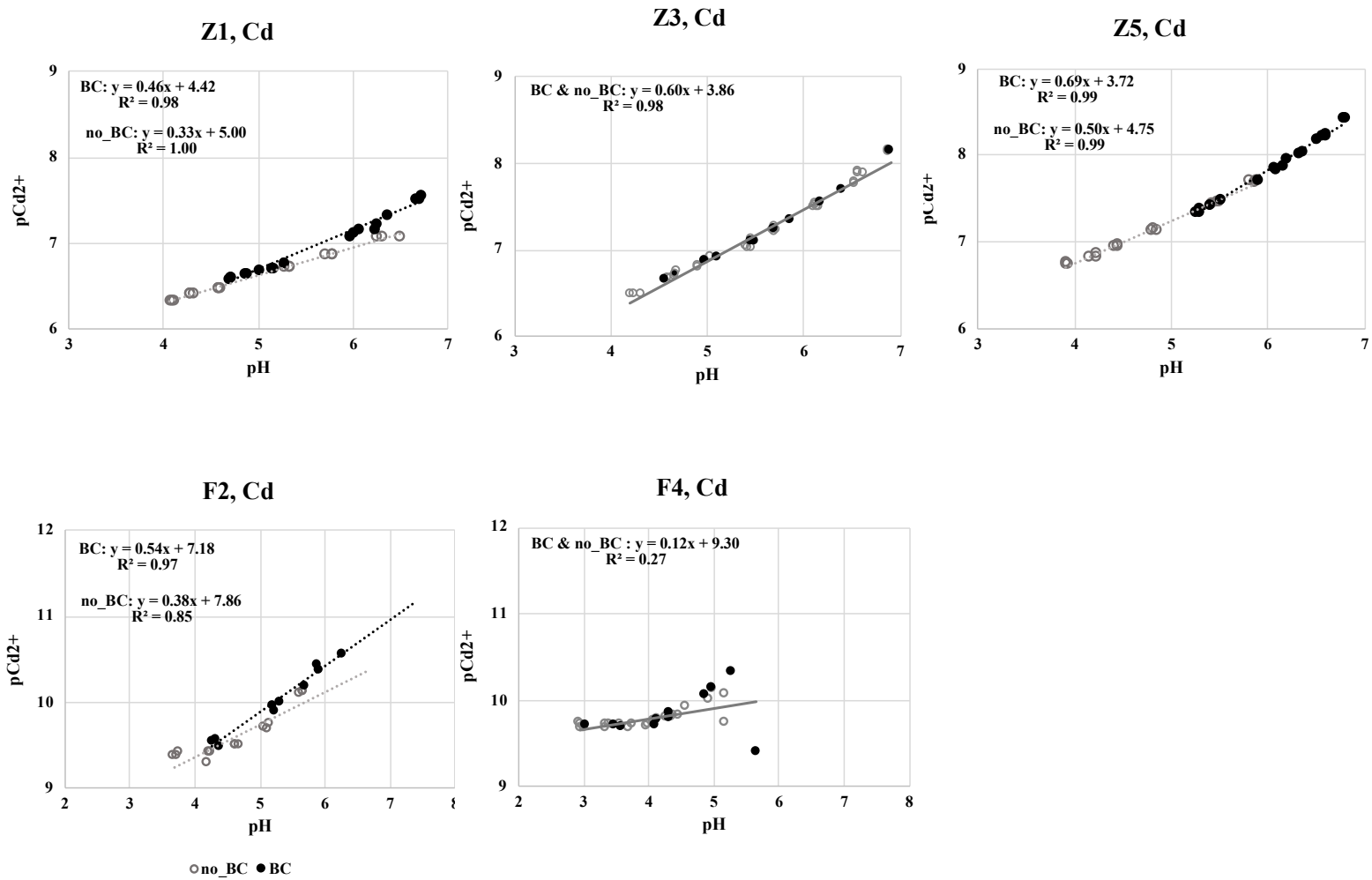

Figure 29: Negative logarithm of free ion activity (M) of Cd (pCd^{2+}) as a function of pH for sample Z1, Z3 and Z5 from Kabwe, and F2 and F4 from Folldal. Data from biochar treated samples are represented with filled symbols, and untreated with open symbols. Note that the y-axis in the coordination systems are different between the Kabwe and Folldal samples. The linear expression from the top is for biochar treated samples (BC), over the expression of the untreated sample (no_BC). The total variation is presented as all replicates are included in the figure (Only readings above LOD and LOQ). Slope and intercept of the two linear models (BC and no_BC) were statistically different ($p<0.05$) for sample Z1, Z5 and F2. The single regressions included in Z3 and F4 explains the relationship for both treatments.

There is a general good fit of all linear regression models presented in figures 26-29, with R^2 values ranging from 0.66 to 1.00 (excluding the model for Cd in sample F4). This indicates that pH is an important variable for the dissolution of all metals for all samples, with and without the treatment of biochar.

The good pPb^{2+} to pH correlation for sample Z1, Z2 and Z3 is evident by R^2 values ranging from 0.98 to 1.00 for the series with and without biochar. This implies that pH is an important variable for dissolution of free Pb ions. However, the linear pPb^{2+}-pH regression models for the samples with and without biochar are statistically ($p<0.05$) different from each other for sample Z1 and Z3. The difference is related to a difference in Pb^{2+} dissolution in response to changes in pH (slope), but also to an upwards shift of the biochar treated sample line along the y-axis (intercept). This implies that the Pb^{2+} activity in Z1 and Z3 significantly reduces when adding biochar to the samples, at any given solution pH (tested for the pH range of around 4-7). The increased slope for the same biochar treated samples further implies that immobilization of free Pb ions is significantly enhanced compared to the untreated sample when pH increases. These significant differences in slope and intercept between the two treatments for Z1 and Z3 is therefore not explained by pH as the only variable but further implies that other biochar-initiated immobilization mechanisms, like sorption, also contributes to reducing the free ion concentration in solution. In contrast, the measured effect on reduced Pb^{2+} ions in sample Z5 can be assigned to the isolated effect of the biochar induced increase in pH (no difference in slope or intercept).

The linear pZn^{2+}–pH regressions for Kabwe samples Z1, Z3 and Z5, with and without the addition of biochar are significantly ($p<0.05$) different in slope and intercept. This implies that significant biochar sorption of Zn^{2+} occurs in all Kabwe soil samples.

Significant sorption of Cu^{2+} also occurs for all biochar treated samples in Kabwe and Folldal in Figure 28. Although, for sample Z1, the Cu^{2+} response to changes in pH are the same for the two treatments (the two regression lines have the same slope). In contrast, the slope for no biochar treatment for sample F2 showed significant increased slope compared to the biochar treatment. However, this was the only observation of this apparent opposite trend.

Significant sorption of Cd^{2+} occurs for all biochar treated samples in Kabwe and Folldal, except for sample Z3 and F4 (Figure 29). The linear regressions model in sample Z3 show a good fit (R^2= 0.98), which implies that pH explains the dissolution of Cd^{2+} well for both treatments, and that insignificant ($p>0.05$) sorption occurs. The Cd regression model for sample F4 show a poor fit (R^2= 0.27) linked to the apparent scatter in the response variable pCd^{2+} at high pH.

6.5 Effect of biochar treatment on bioavailability and mobility

This section presents the immobilization effect of Pb, Zn, Cu and Cd related to the biochar treatment on both the mobility and bioavailability. The biochar effect on mobility was measured for the un-titrated samples (marked as "a") in the batch experiment (presented in appendix table A4), and the biochar effect on bioavailability was measured for DGT's at 6 hours deployment time. The biochar effects on metal mass in DGT after 6 hours deployment was used here because this reflects the effect on the most labile and mobile metal species.

*Table 8: Percentage reduction in metal concentration of the mobile and bioavailable fraction due to the addition of biochar. The % BC effect is calculated as the %difference in concentration of biochar treated samples relative to the untreated samples(([noBC]-[BC])/[noBC])*100). Values presented as DGT is data compiled from the DGT experiment at 6h deployment time (data in appendix table A 2). Biochar effects on mobility is based on the total dissolved equilibrium elemental concentration (in µg/L) for the samples in 0.01 M KCl background without addition of HCl or KOH (viz. sample "a" in speciation graphs in figure 20-23). The mean values are calculated as the mean % reduction for the triplicates with and without biochar. The SD is the standard deviation.*

	Pb				Zn				Cu				Cd			
	%BC effect, DGT_{6h}		%BC effect, mobility		%BC effect, DGT_{6h}		%BC effect, mobility		%BC effect, DGT_{6h}		%BC effect, mobility		%BC effect, DGT_{6h}		%BC effect, mobility	
	Mean	SD	Mean	SD	Mean	SD	Mean	SD	Mean	SD	Mean	SD	Mean	SD	Mean	SD
Z1	64*	8	65*	1	68*	3	63*	1	29*	17	27*	5	63*	3	65*	2
Z3	55*	6	42*	20	66*	2	40*	11	22	12	39*	18	57*	2	40*	6
Z5	LOD/LOQ	-	70*	0	77	26	83*	6	LOD/LOQ	-	14	6	78*	23	78*	7
F2	LOD/LOQ	-	LOD/LOQ	-	82*	2	LOD/LOQ	-	99*	0	92*	1	14	79	27*	12
F4	LOD/LOQ	-	LOD/LOQ	-	21*	11	LOD/LOQ	-	5	5	13*	1	-19	64	-3	2

Significant effects ($p<0.05$) on reduced bioavailability of Pb, Zn, Cu and Cd from the 4wt% biochar treatment were detected in Kabwe. In Folldal, significant effects on reduced bioavailability from the 2wt% biochar treatment were only detected for Zn and Cu. The significant effects on reduced bioavailability of the metals in Kabwe show similar effects across the sample points (Z1, Z3 and Z5), whereas the effects differ greatly among the Folldal samples. The biochar treatment was more effective in reducing bioavailable Zn and Cu for sample F2 than F4, likely related to the low pH (pH_{H2O}=2.1, Table 4) in sample F4. Biochar application was reasonably successful in reducing the bioavailability of Pb, Zn and Cd in Kabwe, with effects in the 50-70% range, whereas the measured effects of Cu were substantially lower (29±17%). The most polluted sample, Z1, Showed the most significant immobilization effects across the sample points, whereas the least polluted sample, Z5, only showed significant effects for bioavailable Cd.

The biochar treatment was significantly effective ($p<0.05$) in reducing the mobility of Pb, Zn, Cu and Cd in Kabwe for all sample points, except for Cu at sample Z5. In the Folldal tailings,

biochar significantly reduced the metal mobility of Cu in sample F2 and F4, and Cd in sample F2. As presented din Table 8, it is a clear overall concurrence between the biochar effect on bioavailability and mobility for all metals.

7. Discussion

7.1 Analysis of SOM and particle size distribution in mine tailings

The overestimation of SOM when based on LOI values in pyritic and acid sulphate soils has been described earlier in the literature as being associated with decomposition of pyrite at high temperatures (Willett & Beech, 1987). Pyrite undergoes endothermic reaction at 450-560°C (Shamsuddin et al., 1994), and as these samples were burned at 550°C, this could account for mass loss resulting in high LOI values, related to a phase transition by oxidation of sulphur from solid to gaseous state, likely thorough SO_2 emissions. Willett and Beech (1987) suggested to reduce the temperature of the LOI analysis of pyrite-containing soil samples to 375°C. However, Shamsuddin et al. (1994) issues that even this temperature overestimates the SOM due to dehydroxylation of minerals in the soil when heated to 375°C. Due to these effects, the SOM values for the Folldal samples presented in Table 4 was calculated from the total carbon content, by dividing with a factor of 0.5, based on a well-established assumption that about half of SOM is made up of organic carbon (Nelson & Sommers, 1996; Pribyl, 2010). This is further based on the assumption that most of the total carbon in the sample from Folldal was organic carbon, as few inorganic carbon constituents were expected to be present in the acidic tailings.

The nature of the Folldal tailings interfered with the method of particle distribution analysis by laser diffraction, where the observed magnetic properties interfered with the accuracy and reproducibility of the results by the Bechman coulter LS13 320 Laser Diffraction Particle Analyzer. As a result of this, the pipette method was used to determine the soil texture of the samples.

7.2 Metal contamination in Kabwe and Folldal

As discussed by Kříbek et al. (2019), The Republic of Zambia offers no official criteria for the assessment of soil contamination. Here, I use the Norwegian, EU and Canadian guideline values for soil contamination by Pb, Zn, Cu and Cd. As none of these guidelines are specified

for Zambian soils, they should be applied with appropriate caution. However, there is a consensus across all three guidelines that the levels of Pb and Zn are excessive for up to at least 1500 meters from the nearest mine waste disposal area. The distribution of metal concentration is relative to distance from the mine of Z1>Z3>Z5 (Figure 14). The trend is in line with literature suggesting that the mine is the main source of pollution in the area (Kříbek et al., 2019; Nakayama et al., 2011; Tembo et al., 2006), as illustrated in the map collection in Figure 6., the total soil Pb concentrations in sample point Z1, Z2 and Z3, covering a 200 meters distance from the mine, correspond to the levels in class 5 (Table 5). According to the Norwegian guideline (Hansen & Danielsberg, 2009) soils with greater total metal concentrations than those defined as class 5 (
Table 6) are classified as special waste and should not remain in the environment.

According to the Norwegian guideline, the contamination level of the Folldal tailings is moderate to bad with respect to the total Cu content (Table 5 and Table 6). The results also show considerable variations in metal concentrations between the sample points. This is well illustrated by the total Zn levels at sample point F2 and F3, which varied from contamination level 1 (very good) to level 4 (bad) according to the Norwegian guideline, over a relatively short distance (see map in Figure 8). This demonstrates the heterogeneous nature of the mine tailings in Folldal.

The Canadian and EU guidelines are overall more restrictive compared to the Norwegian guideline as the threshold values for all four metals (Pb, Zn, Cu and Cd) in the two international guidelines correspond to contamination class “very good” and “good” in the Norwegian guideline (Table 6 and Table 7). In light of this, it is alarming that even the most liberal guideline was added an additional class (class 5–special waste, Table 6) to categorize the extreme total soil Pb values detected in the soils of Kabwe (Table 5).

7.3 Bioavailability (DGT)

As reported by Gimpel et al. (2001), the Chelex-100 resin in the DGT can be less effective in binding metal ions in solutions with low pH due to the competition of hydrogen ions. The user manual of DGT Chelex-100 resin (Bio-Rad, 2000) indicates that metal binding effectiveness to the resin decreases in the following order in low pH solutions:

Hg > Cu > Pb ≫ Ni > Zn > Cd. The study by Gimpel et al. (2001) further confirms that Cu binds particularly strong and can be measured quantitatively down to pH 2.0, and Zn down to pH 3.5. By contrast Cd has a relatively low affinity to the Chelex resin at pH < 5 and is consequently inaccurate for quantitative measurements in solutions more acidic than this. The pH was not measured in the DGT experiment specifically, but the pH_{H2O} (measured at a 0.4 solid:solution ratio, measured after 24 hours) and pH_{KCl} (measure at 0.025 solid:solution ratio with 0.01M KCl, measured the same day) was carried out for the samples. For sample F2, pH_{H2O}= 2.8 and pH_{KCl}=3.4, and for sample F4 the pH_{H2O}= 2.1 and pH_{KCl}=2.6. Based on this, an estimate of pH~3 for sample F2, and pH~2.4 for F4 is likely indicative of the pH in soil solution of the DGT experiment. In light of this, the Cu results from the DGT experiment are considered accurate for quantitative interpretation, but the Zn and Cd results are considered less reliable. All Kabwe samples showed pH > 5 (Table 4), which allow for quantitively interpretations for DGT availability for all four metals.

The DGT graphs in figure 15–18 show a linear regression of DGT mass uptake between 6 and 48 hours deployment time. The uptake rate to the DGT is high at first, shown as the steeper rise in the initial first 6 hours (not shown), as the readily available free metal ions diffuse into the device. The uptake flattens out over time as the supply around the DGT device gets depleted and slower processes start dominating, like the supply of the labile metal fraction from the solid phase. The uptake over time is therefore not linear. However, when interpreting the ratio of diffused metals over time (6 to 48 hours) in the DGT, it is possible to assess the kinetics of the replenishment of metals from the geochemically active fraction. If the ratio is 1:1, meaning that the DGT concentration after 48 hours deployment time is more than 8 times the concentration at 6 hours (as 48/6=8), the metal supply can be regarded as unlimited. This state is comparable to the practical example of the DGT device being placed in a beaker with a magnetic stirrer in a solution with unlimited supply of the given metal. This condition of unlimited supply was found for Pb in Kabwe sample Z1, Z3 and Z5 (see table A 3 in appendix), which adds to the overall severity of the Pb pollution in Kabwe. The results from the DGT experiment support the findings of Kříbek et al. (2019) concluding that a large portion of the contaminants in Kabwe are present in the plant available fraction. The study on trace metal contamination in Kabwe by Kříbek et al. (2019) showed that the median percentage of plant-available metals (extracted with a solution of diethylentriaminopentanacetic acid (DTPA; 0.5 M) and triethanolamine (TEA; 0.1 M))

relative to the total soil metal concentrations, were 39% of Pb, 18% of Zn, 45% of Cu and 60% of Cd.

The samples with the highest bioavailable metal concentrations for Pb, Zn and Cd was found in Kabwe, and the highest bioavailable Cu concertation was found in Folldal sample F4 (figure 15-18). The correlation between the bioavailable metals (DGT metals measured at 48 hour deployment time) and total metal contents are presented in Figure 19. The positive correlation for all Kabwe samples indicates that the bioavailable metals show the same spatial distribution as found for total metal concentrations, with decreasing concentrations of sample points Z1>Z3>Z5 relative to the distance from the mine (map, Figure 5). The negative correlation for Cu in Folldal (Figure 19), however, is explained by the fact that sample F2 showed total soil metal Cu concentrations of 2000mg/kg, which was considerably higher than the concentration measured in sample F4 of 360 mg/kg (Table 5). Contrary, F4 showed considerably higher bioavailable Cu concentration compared to F2 (table A 2 in appendix). This illustrates the limitations of using total soil metal concentrations as an isolated measure for environmental risk related to bioavailability. Sample F4 has a lower pH_{H2O} than F2 (Table 4), this could be a reason why bioavailable Cu is greater in F4 than in F2, as pH is a master variable and plays an important role for both bioavailability and mobility. However, as presented in Figure 24, the Kd value for Cu is higher for sample F2 (green line) compared to F4 (blue line) over the same pH range. This implies that the difference in bioavailability (and mobility) between the two samples is not only limited to the pH effect, but additionally that a substantial proportion of Cu in F2 is not geochemically active, likely attributed to the kinetically constrained dissolution of mineral-associated Cu in mineral structures in sample F2.

The biochar treatment of 4wt% pigeon pea biochar produced at 600ºC, reduced the level of bioavailable concentration (measured in DGT at 6 hour deployment time) of Pb, Zn, Cu and Cd in the most contaminated sample point (Z1) in Kabwe significantly ($p<0.05$) by 64±8%, 68±3%, 29±17% and 63±3%, respectively, with similar biochar effects measured on metal mobility (Table 8). The biochar treatment also reduced uptake rates (µg/h) in the time interval from 6 to 48 hours after deployment following treatment of biochar for all metals, interpreted as the difference in slope in the linear regressions in figures 15-18. These results imply that the treatment of biochar can be an effective measure to reduce the bioavailability of the metals present in the soils of Kabwe, by reducing both the most labile metal species (DGT_{6h})

and by reducing the metal replenishment effect (reduced slope). The effects of biochar in this study are comparable to those presented in the review paper by Palansooriya et al. (2020) for Pb (>85%), Zn (70–77%), Cu (>80%) and Cd (55–60%). The results by Palansooriya et al. (2020) are compiled from > 60 published articles where the given results are the average biochar effects on trace metal immobilization (immobilization is defined in the article as a compilation of studies on reduced metal bio-accessibility, exchangeable fraction, labile fraction, leaching, phytoavailability, and water-soluble fraction.) The biochar used in this thesis did not perform as good for Pb and Cu immobilization compared to the reported effects in the review article. This could be due to the differences methods used, application rate, or biochar properties related to feedstock type or pyrolysis temperature, but also the contamination level and other physiochemical properties of the soils tested.

In Folldal the treatment of 2wt% pigeon pea biochar produced at 600ºC, reduced the level of Cu bioavailability by 99±0% for sample F2, but with insignificant reductions for sample F4 (Table 8). The uptake rate (µg/h) of Cu in Folldal (interpreted as the difference in slope in the linear regressions in figures 15-18) showed divergent results from the biochar treatment. The uptake rate (µg/h) of Cu for F2 decreased following biochar treatment with 99% (reducing the uptake from 293 µg/h to 2.4 µg/h.) F4, on the other hand, showed an increase in uptake rate (µg/h) of Cu following biochar addition by about 45% (increase in the uptake rate from 534 µg/h to 978 µg/h). Hence, for Folldal the biochar application significantly reduced the total amount of bioavailable Cu as well as the DGT uptake rate over 6-48 hour deployment time for sample F2. In contrast, the total reduction of bioavailable Cu for the most polluted sample in respect to bioavailable Cu, F4, was insignificant.

The biochar mechanisms responsible for the apparent reduced bioavailability of Pb, Zn, Cu and Cd in Kabwe samples Z1, Z3, Z5 and for Cu at F2 may be due to adsorption to of metals to the biochar sorption sites, or a result of biochar induced alkalinity causing metal hydrolysis and precipitation, or both. Which of these mechanisms that dominates cannot be concluded from the DGT experiment, but will be further discussed in the next section related to the batch titration experiment.

7.4 Metal solubility

At “field condition”, the total metal solubility of Pb, Zn, Cu and Cd in Kabwe follows the same spatial pattern with distance from the mine as for total metal content and bioavailability, with the decreasing order Z1>Z3>Z5 (viz. differences in y-axis for the samples in figures 20-23). For the Folldal samples, the solubility of Cu at “field condition” for F4 is higher than F2 (viz. differences in y-axis for the sample F2 and F4 in Figure 22), although the opposite relationship was found for total metal content between the two samples (Table 5), further implying that total metal content is a poor estimator for the risks associated with both the bioavailable and mobile metal fraction. The elevated total soluble Cu in F4 is attributed to the lower soil pH and subsequent increased solubility compared to sample F2, as well as the apparent lowered Kd over pH compared to F2 (Figure 24).

The Kd distribution relative to pH for Cd, Cu, Pb and Zn in the Kabwe samples correlated well with referenced literature, as the lines were within the 95% confidence interval based on the 70 soils compiled in the study by Sauvé et al. (2000) in Figure 24. The elevated Kd values of the two samples in Folldal may be ascribed to a the kinetically constrained dissolution of mineral-associated Cu and Cd in the tailings. Additionally, the Folldal samples were coarser grained compared to the finer grained Kabwe samples, and likely also coarser than the 70 compiled soils in the study by Sauvé et al. (2000). As the particle size increases, the surface area decreases, making less of the mineral-associated metals prone to dissolution.

DOC as a function of pH presented in Figure 25 show two clear trends; that the dissolution of organic carbon is parabolic with the lowest DOC levels detected at around pH 5, and that the biochar treated samples are associated with lower DOC levels over the titration series. The parabolic relationship of DOC as a function of pH confirms other studies, e.g. Almås et al. (2007). The increased DOC concentration in solution at higher pH ranges (pH > 6) has been ascribed to the increased hydrophilic character of DOC linked to gradual deprotonation and concomitant increase in net negative charge (Z_{FA}) with increase in pH. The apparent increase in DOC at lower pH values has been ascribed to dissolution of SOM bound to amorphous Al oxides, which dissolve at pH < 5 (Almås et al., 2007; Lofts et al., 2001). Both of these DOC dissolution mechanisms at both ends of the pH scale result in the apparent parabolic relationship portrayed in
Figure 25. The biochar treated samples (filled symbols) generally show lower DOC concentrations than the untreated samples (open symbols), over the lower pH range. This is likely attributed to sorption of DOC to micropores on biochar (Kasozi et al., 2010; Smebye et

al., 2016). However, a minor yet significant increase in DOC was found in the biochar treated samples Z1 and Z5 at "field condition" (viz. triangular symbols in Figure 25). The significant increase in DOC from biochar addition can be ascribed to the biochar induced increase in pH, causing mobilization of DOC from the mineral sites, and/or dissolution of DOC native to the biochar itself (Smebye et al., 2016).

The total dissolved metals in solution for the Kabwe samples are largely dominated by free ion species, although some of the dissolved Cd is also present as Cl-species. Additionally, Cu and Pb is partly dominated by FA-related species as Pb and Cu are known to make strong complexes with fulvic acids (Saar & Weber, 1980). Kabwe sample Z3 show the highest levels of SOM (Table 4) and DOC (Figure 25), as well at the highest concentrations of FA-related species of Pb and Cu. The influence of the parabolic relationship between DOC and pH on metal mobilization by complexation with FA is well illustrated in the Cu speciation of the batch titration in Figure 22. The dissolution of DOC at high pH causes a clear increase in FA-Cu species in solution for pH > 4.4. The same effect can be seen for sample Z5.

The pigeon pea biochar used in this experiment has been well described though the work of Munera-Echeverri et al. (2018), where the biochar was compared to cacao shell, corncob and rice husk derived biochars. The pigeon pea biochar showed the highest pH (10.4±0.03), but the CEC (6.5–11.5 $cmol_{(+)}\ Kg^{-1}$) was reasonably low compared to the Cacao shell biochar with CEC values close to 60 $cmol_{(+)}\ Kg^{-1}$.

There is a general good fit of all linear regression models presented in figures 26-29, with R^2 values ranging from 0.66 to 1.00 (excluding the model for Cd in sample F4). This indicates that pH is an important variable for the solubility of all metals for all samples, also for the biochar treated samples. The apparent immobilization of all metals with increased pH is ascribed to the hydrolysis of the free metal ions and precipitation of hydroxides or carbonates. There is a significant ($p<0.05$) difference in both slope and intercept of the linear pM^{2+}-pH regression lines for the two treatments (BC and no_BC) for most samples and metals. This implies that also some metal sorption by biochar contribute to the immobilization of Pb, Zn, Cu and Cd, despite of the fact that the CEC of the biochar used is generally low.

In Table 8 it is apparent that the biochar effect on metal mobility and bioavailability are closely related. As presented in figure 20-23, it is evident that the biochar effect in the batch

experiment is mainly ascribed to the reduction in free metal ions species. Moreover, only the most readily available metal species, such as the free metal ions, will diffuse into the DGT resin after 6-hour deployment time. Hence, the biochar effect measured on bioavailability and mobility presented in Table 8 are both primarily attributed to the immobilization of free metal ions. This is also supported by the fact that the biochar effect measured in DGT's at 48-hour deployment time was less comparable to the biochar effect on the mobility.

The pH in F2 were higher (pH_{H2O}=2.8) than for F4 (pH_{H2O}=2.1), which is a contributing factor to the poor biochar effect on reducing bioavailable and mobile Cu concentrations in sample F4. As interpreted from figure 26-29, the main biochar effect is ascribed to the immobilization effect caused by the biochar -induced increase in pH. Consequently, biochar addition to sample F2 resulted in a greater pH increase and therefore a greater decrease in Cu concentration in solution, compared to F4. Additionally, the difference in buffer capacity (exchangeable acidity) between the two samples is illustrated by the difference in KOH needed to increase the pH in the batch experiment (Table 3), showing that 3x more KOH was needed to increase the pH by 2 pH units for sample F4 compared to F2. This also explains the poor effects detected for sample F4, as most of the biochar -induced alkalinity will likely be buffered. Another factor assigned to the limited immobilization of the biochar treatment is the increase in $CuOH^+$ and $CdOH^+$ species in solution in biochar treated samples, as revealed by the solution speciation in Figure 22 and Figure 23.

The immediate need for remediation measures of the polluted soils of Kabwe is evident by the recent class action lawsuit (Carrington, 2020). As mentioned earlier in the discussion, the total metal concentrations of Pb in Kabwe sample Z1, Z2 and Z3, covering 200 meters from the closest mine, correspond to the levels of special waste and should not remain in the environment. The guideline (Hansen & Danielsberg, 2009) further state that particular caution should be applied to areas where humans are exposed to the contaminated sediments though soil ingestion, inhalation of particles, skin contact or ingestion of food likely affected by the contamination. Several of these exposure routes apply to the residents of Kabwe, and the most contaminated soils should therefore be removed from the site. However, it is important to issue that land reclamation methods are site specific and should take all situation-based considerations into account. Removal of the sediments is not necessarily the most applicable measure considering the circumstances in Kabwe, and a recent remediation measures proposal for Kabwe by Kříbek et al. (2019) recommend less costly in-situ land reclamation methods

over removal. Although the use of biochar is not explored in the proposal, the principle of using biochar compares with the recommended use of phosphate amendments for immobilization of plant available metals in the soils of Kabwe. Remediation measures like the use of biochar and phosphate amendments to the Kabwe soils will likely reduce the mobile and bioavailable metal fraction, hence reduce the leaching of trace metals to water sources and uptake in crops. However, the main exposure of these trace metals for the population in Kabwe is related to the ingestion of contaminated soil particles (dust), especially among children (Yabe et al., 2020). Phytostabilization, a measure based on establishing vegetation cover to reduce the dust generation, is another a measure for Kabwe proposed by Kříbek et al. (2019). A study by Fellet et al. (2011) concluded that biochar amendment properties like increased pH, nutrient retention, CEC and water holding capacity was in favor of vegetation cover establishment in the mine tailings in Cave del Predil (NE, Italy) in a phytostabilization process. When comparing the remediation methods of biochar and phosphate amendments, the most obvious argument in the favor of biochar is that it can be produced from waste products with applicable low-cost techniques in situ, e.g. by using the Kon- Tiki flame curtain method (Pandit et al., 2017), whereas phosphate treatments are more expensive and produced from a valuable plant nutrient. The effect of C sequestration by biochar treatment and the indirect effect of alleviating climate change (Winsley, 2007), further supports the use of biochar over phosphate amendments. Based on the findings in this study showing that biochar was effective in immobilizing mobile and bioavailable fractions of Pb, Zn, Cu and Cd in the soils of Kabwe, the use of biochar as an amendment is recommended remediation measure in Kabwe.

The biochar effects of reducing the dissolved metal concentrations were mainly attributed to the biochar alkalinity, causing hydrolysis of the free metal ions and precipitation of hydroxides or carbonates, but significant sorption was also observed (figures 26-29). The CEC of the biochar was generally low, hence, the use of a biochar with higher CEC would likely further improve the immobilization effects.

Folldal

As the main problem in Folldal is related to leaching and drainage of mainly Cu to the river Folla, the biochar effects on mobility if Cu are of most practical importance. The biochar application showed divergent effects on mobility of Cu with 92±1% effects measured for F2, and 13±1 for F4. The difference of effect is ascribed to the difference in soil pH, where the

the biochar induced alkalinity in low-pH sample F4 was efficiently buffered, resulting in poor metal immobilization effects. Using a biochar with higher CEC would likely also improve the effects in Folldal.

8. Conclusions and recommendations

The first objective this thesis aims to answer is: "*What is the mobility and bioavailability of heavy metals in mine tailings and in adjacent soils due to historic mining activities in Folldal (Norway) and Kabwe (Zambia)?"*

For the soils of Kabwe, the total soil metal analysis showed that the samples were highly contaminated by Pb and Zn (Table 5). According to Norwegian-, EU- and Canadian threshold guidelines (
Table 7) the soils at a 200 meter distance to the mine was classified as special waste with respect to the Pb content, and represent an immediate health risk to the local population, especially though ingestion of contaminated dust particles. The total metal concentration, bioavailable concentration (DGT) and total dissolved concentration of all metals for the Kabwe samples decrease with increasing distance from the mine (Z1>Z3>Z5). Furthermore, the DGT experiment revealed that the bioavailable Pb increased with a 1:1 relationship with time until at least 48 hours, indicating that the bioavailable replenishment of Pb for bioavailable uptake was not kinetically restricted in any of the Kabwe sample points. This indicates that a substantial part of the Pb in the solid phase is labile and available for supply to biota. The batch experiment showed that most of the species in solution are present as free metal ions for Pb, Zn, Cu and Cd (Figure 20-23), and that DOC is an important ligand for Pb and Cu in solution. Both experiments support the conclusion that the soils in Kabwe are highly contaminated, and that a substantial fraction of the metals present in these soils are both mobile and bioavailable.

For the Folldal tailings, the total soil metal concentrations of Cu are classified as moderate to bad according to the Norwegian guideline for contaminated sediments (Table 6), implying that remediation measures are needed also Folldal. Sample F2 showed the highest total concentration of 2000 mg Cu/kg, compared to the 360 mg Cu/kg found for sample F4. In contrast, the highest mobile and bioavailable Cu concentrations were found in sample F4. The difference is assigned to difference in pH, and that more of the Cu present in the contaminated

sample F2 is found in inert mineral phases. This illustrates the weakness of risk assessment based solely on total concentrations, and the importance of solubility and bioavailability experiments to reveal the true environmental risk of the sediment in question.

The second objective this thesis aims to answer is: *What is the potential of biochar to stabilize heavy metals in soils, reducing their mobility and bioavailability?*

In the soils of Kabwe, significant stabilizing effects of the biochar treatment were found for Pb, Zn, Cu and Cd for the most contaminated sample (Z1) both in reducing bioavailability and mobility. The significant ($p<0.05$) reduction in bioavailability for sample Z1 for Pb, Zn, Cu and Cd was 64±8%, 68±3%, 29±17% and 63±3%, respectively, with comparable results for reduction in mobility. The biochar immobilization effect was mainly attributed to the biochar-induced rise in pH, but significant sorption also occurred (Figure 26-29).

In the mine tailings of Folldal, the immobilizing effects of biochar showed striking differences. Strong effects on reduced bioavailability and mobility of Cu were found in sample F2 with 99±0% and 92±1% reduction, respectively. Whereas insignificant reduction in bioavailable Cu, and 13±1% reduction on Cu mobility was measured in F4. The pH was established as the master variable for controlling the free ion activity in all samples for the biochar treatments (figures 26-29), hence the main reason for the low effects detected in sample F4 is ascribed to the low sample pH that buffers the biochar derived alkalinity This is evident as the pH increased by 0.6 pH units for sample F2, but only with 0.1 units for sample F4 from the biochar addition.

<u>Recommendations</u>

LOI measurement used to estimate SOM in S-containing mine residue does not give true results due to a likely overestimation SOM caused by oxidation of the mineral Sulphur phase at high temperatures. Instead, estimating the SOM from the total C content by dividing with a factor of 0.5 gives a far better estimate. The magnetic nature of the mine tailings of Folldal also notably interfered with the particle size distribution analysis by laser diffraction, hence the use of the pipette method is recommended. Appropriate caution should also be taken when interpreting the quantification of bioavailable metals measured with the DGT technique in very acidic mine tailings, due to the metal binding limitations of the Chelex-100 resin in low pH solutions.

The study found that bioavailability and dissolution experiments provide better predictions of the true environmental risks associated with mine sediments compared to the risk estimate found using total metal analysis and guideline threshold values. However, in Kabwe the total metal content is of significance due to the transport and human exposure from ingestion of dust particles.

This findings in this study supports the recommendation of using biochar in Pb, Zn, Cu and Cd contaminated mine associated sediments. The pigeon pea biochar used in this study mainly contributed with a pH effect. Hence, better effects would be expected by using a biochar with higher associated CEC, as both sorption and pH related mechanisms would contribute to further the immobilization of the metals.

References

Ahmad, M., Lee, S. S., Lee, S. E., Al-Wabel, M. I., Tsang, D. C. W. & Ok, Y. S. (2017). Biochar-induced changes in soil properties affected immobilization/mobilization of metals/metalloids in contaminated soils. *Journal of Soils and Sediments*, 17 (3): 717-730. doi: 10.1007/s11368-015-1339-4.

Ali, A., Guo, D., Jeyasundar, P. G. S. A., Li, Y., Xiao, R., Du, J., Li, R. & Zhang, Z. (2019). Application of wood biochar in polluted soils stabilized the toxic metals and enhanced wheat (Triticum aestivum) growth and soil enzymatic activity. *Ecotoxicology and environmental safety*, 184: 109635.

Alloway, B. J. (2012). *Heavy metals in soils: trace metals and metalloids in soils and their bioavailability*, vol. 22: Springer Science & Business Media.

Almås, Å., Lofts, S., Mulder, J. & Tipping, E. (2007). Solubility of major cations and Cu, Zn and Cd in soil extracts of some contaminated agricultural soils near a zinc smelter in Norway: modelling with a multisurface extension of WHAM. *European Journal of Soil Science*, 58 (5): 1074-1086.

Almås, Å. R., Lombnæs, P., Sogn, T. A. & Mulder, J. (2006). Speciation of Cd and Zn in contaminated soils assessed by DGT-DIFS, and WHAM/Model VI in relation to uptake by spinach and ryegrass. *Chemosphere*, 62 (10): 1647-1655.

Almås, Å. R. & Singh, B. R. (2017). Trace Metal Contamination. In *Encyclopedia of Soil Science*, pp. 2364-2368: CRC Press.

BBC. (2020, 21.10.2020). Zambia: Anglo American sued for 'mass lead poisoning'. *BBC NEWS*. Available at: https://www.bbc.com/news/world-africa-54634511 (accessed: 23.02.2021).

Bio-Rad, L. (2000). Chelex®-100 and Chelex®-20 Chelating Ion Exchange Resin Instruction Manual. *Bio-Rad Laboratories*.

Blacksmith Institute & Green Cross Switzerland. (2007). *The world's worst polluted places, the top ten of the dirty thirty*. https://www.worstpolluted.org/.

Bremner, J. M. & Mulvaney, C. S. (1982). *Methods of Soil Analysis, Part 2; Agronomy* 2ed., vol. Nitrogen-total, chapter. 31: American Society of Agronomy, Inc., Madison, Wisconsin, USA.

Campbell, G. S., Klute, A. & Soil Science Society of, A. (1986). *Methods of soil analysis : Pt. 1 : Physical and mineralogical methods*. Agronomy. Madison, Wis: American Society of Agronomy : Soil Science Society of America. p. 383-412.

Carrington, D. (2020). Anglo American sued over alleged mass lead poisoning of children in Zambia. *The Guardian* Available at: https://www.theguardian.com/environment/2020/oct/21/anglo-american-sued-over-alleged-mass-lead-poisoning-of-children-in-zambia (accessed: 22.02.2021).

CCME. (2001). *Canadian soil quality guidelines for the protection of environmental and human health: Summary tables*. Canadian Council of Ministers of the Environment: Canadian Council of Ministers of the Environment, Winnipeg.
Climate-data.org. (accessed: 28.04).
Dean, R. B. & Dixon, W. J. (1951). Simplified statistics for small numbers of observations. *Analytical chemistry*, 23 (4): 636-638.
Degryse, F., Smolders, E., Zhang, H. & Davison, W. (2009). Predicting availability of mineral elements to plants with the DGT technique: a review of experimental data and interpretation by modelling. *Environmental Chemistry*, 6 (3): 198. doi: 10.1071/en09010.
Dume, B., Mosissa, T. & Nebiyu, A. (2016). Effect of biochar on soil properties and lead (Pb) availability in a military camp in South West Ethiopia. *African Journal of Environmental Science and Technology*, 10 (3): 77-85.
Egene, C. E., Van Poucke, R., Ok, Y. S., Meers, E. & Tack, F. M. G. (2018). Impact of organic amendments (biochar, compost and peat) on Cd and Zn mobility and solubility in contaminated soil of the Campine region after three years. *Science of The Total Environment*, 626: 195-202. doi: 10.1016/j.scitotenv.2018.01.054.
Ekström, G. (1926). Klassifikation av svenska åkerjordar.(Classification of Swedish soil types on farmland). Sveriges Geologiska Undersökning. Serie C. Avhandlingar och Uppsatser, 345. *Årsbok*, 20: 161.
Elonen, P. (1971). Particle-size analysis of soil. Soumen maataloustieteellisen seuran julkasuja. *Acta Agralia fennica*, 122: 112.
Fellet, G., Marchiol, L., Delle Vedove, G. & Peressotti, A. (2011). Application of biochar on mine tailings: effects and perspectives for land reclamation. *Chemosphere*, 83 (9): 1262-1267.
Folldal gruver. (2021). https://folldalgruver.no/historie (accessed: 29.04.2021).
Gimpel, J., Zhang, H., Hutchinson, W. & Davison, W. (2001). Effect of solution composition, flow and deployment time on the measurement of trace metals by the diffusive gradient in thin films technique. *Analytica Chimica Acta*, 448 (1-2): 93-103. doi: 10.1016/s0003-2670(01)01323-x.
Gu, J., Yao, J., Jordan, G., Roha, B., Min, N., Li, H. & Lu, C. (2020). Arundo donax L. stem-derived biochar increases As and Sb toxicities from nonferrous metal mine tailings. *Environmental Science and Pollution Research*, 27 (3): 2433-2443. doi: 10.1007/s11356-018-2780-x.
Hansen, H. & Danielsberg, A. (2009). Helsebaserte tilstandsklasser for forurenset grunn. *Statens forurensningstilsyn, Oslo*.
Hofstad, K. (2020). *Biokull*. Store norske leksikon. snl.no (Accessed: 09.05.2021).
Hooda, P. S., Zhang, H., Davison, W. & Edwards, A. C. (1999). Measuring bioavailable trace metals by diffusive gradients in thin films (DGT): soil moisture effects on its performance in soils. *European Journal of Soil Science*, 50 (2): 285-294. doi: 10.1046/j.1365-2389.1999.00226.x.
Houben, D., Evrard, L. & Sonnet, P. (2013). Mobility, bioavailability and pH-dependent leaching of cadmium, zinc and lead in a contaminated soil amended with biochar. *Chemosphere*, 92 (11): 1450-1457.
Ikenaka, Y., Nakayama, S. M. M., Muroya, T., Yabe, J., Konnai, S., Darwish, W. S., Muzandu, K., Choongo, K., Mainda, G., Teraoka, H., et al. (2012). Effects of Environmental Lead Contamination on Cattle in a Lead/Zinc Mining Area: Changes in Cattle Immune

Systems on Exposure to Lead in Vivo and in Vitro. *Environmental Toxicology and Chemistry*, 31 (10): 2300-2305. doi: 10.1002/etc.1951.
Jahn, R., Blume, H., Asio, V., Spaargaren, O. & Schad, P. (2006). *Guidelines for soil description*: FAO.
Kabaso, R. (2019). *The effects of biochar on chemical fractionation of lead and uptake by lemon grass in heavy metal polluted soils of Kabwe*: The University of Zambia, Department of Soil Sciences. Bachelor Of Science, Lusaka.
Kachenko, A. G. & Singh, B. (2006). Heavy metals contamination in vegetables grown in urban and metal smelter contaminated sites in Australia. *Water, air, and soil pollution*, 169 (1): 101-123.
Kamona, A. F. & Friedrich, G. H. (2007). Geology, mineralogy and stable isotope geochemistry of the Kabwe carbonate-hosted Pb–Zn deposit, Central Zambia. *Ore geology reviews*, 30 (3): 217-243. doi: 10.1016/j.oregeorev.2006.02.003.
Kampestuen, Å., K. (2021, 24.03.2021). Tonnevis med gift renner fortsatt ut etter gruvedrift. *Norsk rikskringkasting, NRK,* . Available at: https://www.nrk.no/innlandet/tildekking-av-gruveanlegget-i-folldal-ikke-nok-for-a-lose-omfattende-forurensning-1.15424392 (accessed: 21.04.21).
Kapandula, T. (2020). *Master's thesis: Effects of Biochar and lime on leaching of lead and zinc in heavy metal contaminated soils of Kabwe, Zambia*: Department Of Soil Science, The University Of Zambia.
Karami, N., Clemente, R., Moreno-Jiménez, E., Lepp, N. W. & Beesley, L. (2011). Efficiency of green waste compost and biochar soil amendments for reducing lead and copper mobility and uptake to ryegrass. *Journal of hazardous materials*, 191 (1-3): 41-48.
Kasozi, G. N., Zimmerman, A. R., Nkedi-Kizza, P. & Gao, B. (2010). Catechol and Humic Acid Sorption onto a Range of Laboratory-Produced Black Carbons (Biochars). *Environmental Science & Technology*, 44 (16): 6189-6195. doi: 10.1021/es1014423.
Kefeni, K. K., Msagati, T. A. M. & Mamba, B. B. (2017). Acid mine drainage: Prevention, treatment options, and resource recovery: A review. *Journal of Cleaner Production*, 151: 475-493. doi: https://doi.org/10.1016/j.jclepro.2017.03.082.
Kossoff, D., Dubbin, W. E., Alfredsson, M., Edwards, S. J., Macklin, M. G. & Hudson-Edwards, K. A. (2014). Mine tailings dams: Characteristics, failure, environmental impacts, and remediation. *Applied Geochemistry*, 51: 229-245. doi: 10.1016/j.apgeochem.2014.09.010.
Kříbek, B., Nyambe, I., Majer, V., Knésl, I., Mihaljevič, M., Ettler, V., Vaněk, A., Penížek, V. & Sracek, O. (2019). Soil contamination near the Kabwe Pb-Zn smelter in Zambia: Environmental impacts and remediation measures proposal. *Journal of Geochemical Exploration*, 197: 159-173.
Kvennås, M., Okkenhaug, G., Breedveld, G. & Lundgren, T. (2015). *Folldal gruver - Vurdering av mulige tiltak mot avrenning fra tidligere gruvevirksomhet* The Directorate of Mining with the Commissioner of Mines at Svalbard: Norwegian Geotechnical Institute (NGI).
Lehmann, J. (2007). A handful of carbon. *Nature*, 447 (7141): 143-144. doi: 10.1038/447143a.
Leteinturier, B., Laroche, J., Matera, J. & Malaisse, F. (2001). Reclamation of lead/zinc processing wastes at Kabwe, Zambia: a phytogeochemical approach. *South African Journal of Science*, 97 (11-12): 624-627.

Li, C., Ding, S., Yang, L., Wang, Y., Ren, M., Chen, M., Fan, X. & Lichtfouse, E. (2019). Diffusive gradients in thin films: devices, materials and applications. *Environmental chemistry letters*, 17 (2): 801-831. doi: 10.1007/s10311-018-00839-9.

Lofts, S., Simon, B. M., Tipping, E. & Woof, C. (2001). Modelling the solid-solution partitioning of organic matter in European forest soils. *European Journal of Soil Science*, 52 (2): 215-226. doi: 10.1046/j.1365-2389.2001.00367.x.

Luo, X.-S., Yu, S., Zhu, Y.-G. & Li, X.-D. (2012). Trace metal contamination in urban soils of China. *Science of The Total Environment*, 421-422: 17-30. doi: 10.1016/j.scitotenv.2011.04.020.

Mbuki, R. & Mbewe, G. (2017). Phytoremediation of Lead and Zinc Metals Using Sunflower: Sampled from an Abandoned Mine Tailing Dump Site in Kabwe, Zambia. *The International Journal of Multi-Disciplinary Research Pg*: 1-11.

Mia, S., Dijkstra, F. A. & Singh, B. (2017). Chapter One - Long-Term Aging of Biochar: A Molecular Understanding With Agricultural and Environmental Implications. In Sparks, D. L. (ed.) vol. 141 *Advances in Agronomy*, pp. 1-51: Academic Press.

Minestry of mines. (2016). *Environmental and social management framework, Zambia Mining Environment Remediation and Improvement Project*. Ministry Of Mines And Mineral Development Zambia. worldbank.org, SFG2338.

Munera-Echeverri, J. L., Martinsen, V., Strand, L. T., Zivanovic, V., Cornelissen, G. & Mulder, J. (2018). Cation exchange capacity of biochar: An urgent method modification. *Science of the total environment*, 642: 190-197.

Mwandira, W., Nakashima, K., Kawasaki, S., Ito, M., Sato, T., Igarashi, T., Banda, K., Chirwa, M., Nyambe, I., Nakayama, S., et al. (2019a). Efficacy of biocementation of lead mine waste from the Kabwe Mine site evaluated using Pararhodobacter sp. *Environ Sci Pollut Res Int*, 26 (15): 15653-15664. doi: 10.1007/s11356-019-04984-8.

Mwandira, W., Nakashima, K., Kawasaki, S., Ito, M., Sato, T., Igarashi, T., Chirwa, M., Banda, K., Nyambe, I., Nakayama, S., et al. (2019b). Solidification of sand by Pb(II)-tolerant bacteria for capping mine waste to control metallic dust: Case of the abandoned Kabwe Mine, Zambia. *Chemosphere*, 228: 17-25. doi: 10.1016/j.chemosphere.2019.04.107.

Nakayama, S. M. M., Ikenaka, Y., Hamada, K., Muzandu, K., Choongo, K., Teraoka, H., Mizuno, N. & Ishizuka, M. (2011). Metal and metalloid contamination in roadside soil and wild rats around a Pb-Zn mine in Kabwe, Zambia. *Environ Pollut*, 159 (1): 175-181. doi: 10.1016/j.envpol.2010.09.007.

Nelson, D. W. & Sommers, L. E. (1996). Total carbon, organic carbon, and organic matter. *Methods of soil analysis: Part 3 Chemical methods*, 5: 961-1010.

O'Connor, D., Peng, T., Zhang, J., Tsang, D. C. W., Alessi, D. S., Shen, Z., Bolan, N. S. & Hou, D. (2018). Biochar application for the remediation of heavy metal polluted land: A review of in situ field trials. *Science of The Total Environment*, 619-620: 815-826. doi: 10.1016/j.scitotenv.2017.11.132.

Oh, S.-Y. & Yoon, M.-K. (2013). Biochar for treating acid mine drainage. *Environmental engineering science*, 30 (10): 589-593.

Page, N. J. (1964). The sulphide deposit of Nordre Gjetryggen Gruve, Folldal, Norway.

Palansooriya, K. N., Shaheen, S. M., Chen, S. S., Tsang, D. C. W., Hashimoto, Y., Hou, D., Bolan, N. S., Rinklebe, J. & Ok, Y. S. (2020). Soil amendments for immobilization of potentially toxic elements in contaminated soils: A critical review. *Environment International*, 134: 105046. doi: 10.1016/j.envint.2019.105046.

Pandit, N. R., Mulder, J., Hale, S. E., Schmidt, H. P. & Cornelissen, G. (2017). Biochar from "Kon Tiki" flame curtain and other kilns: Effects of nutrient enrichment and kiln type on crop yield and soil chemistry. *PLOS ONE*, 12 (4): e0176378. doi: 10.1371/journal.pone.0176378.

Pribyl, D. W. (2010). A critical review of the conventional SOC to SOM conversion factor. *Geoderma*, 156 (3-4): 75-83.

Puschenreiter, M. (2017). William Davison (Ed.): Diffusive gradients in thin-films for environmental measurements. *Analytical and Bioanalytical Chemistry*, 409 (8): 1973-1974. doi: 10.1007/s00216-016-0178-5.

Rogich, D. G. & Matos, G. R. (2008). *Global Flows of Metals and Minerals*: US Department of the interior, US Geological Survey.

Ruttens, A., Adriaensen, K., Meers, E., De Vocht, A., Geebelen, W., Carleer, R., Mench, M. & Vangronsveld, J. (2010). Long-term sustainability of metal immobilization by soil amendments: Cyclonic ashes versus lime addition. *Environmental Pollution*, 158 (5): 1428-1434. doi: https://doi.org/10.1016/j.envpol.2009.12.037.

Sauvé, S., Hendershot, W. & Allen, H. E. (2000). Solid-solution partitioning of metals in contaminated soils: dependence on pH, total metal burden, and organic matter. *Environmental science & technology*, 34 (7): 1125-1131.

Shamsuddin, J., Jamilah, I. & Ogunwale, J. (1994). Organic carbon determination in acid sulphate soils. *Pertanika*, 17: 197-197.

Silwamba, M., Ito, M., Hiroyoshi, N., Tabelin, C. B., Fukushima, T., Park, I., Jeon, S., Igarashi, T., Sato, T., Nyambe, I., et al. (2020). Detoxification of lead-bearing zinc plant leach residues from Kabwe, Zambia by coupled extraction-cementation method. *Journal of Environmental Chemical Engineering*, 8 (4). doi: ARTN 10419710.1016/j.jece.2020.104197.

Smebye, A., Alling, V., Vogt, R. D., Gadmar, T. C., Mulder, J., Cornelissen, G. & Hale, S. E. (2016). Biochar amendment to soil changes dissolved organic matter content and composition. *Chemosphere*, 142: 100-105.

Sofrá, F. & Boger, D. V. (2002). Environmental rheology for waste minimisation in the minerals industry. *Chemical engineering journal (Lausanne, Switzerland : 1996)*, 86 (3): 319-330. doi: 10.1016/S1385-8947(01)00225-X.

Stumm, W., Morgan, J. J. & Drever, J. I. (1996). Aquatic chemistry. *Journal of Environmental Quality*, 25 (5): 1162.

Saar, R. A. & Weber, J. H. (1980). Lead(II) complexation by fulvic acid: how it differs from fulvic acid complexation of copper(II) and cadmium(II). *Geochimica et Cosmochimica Acta*, 44 (9): 1381-1384. doi: https://doi.org/10.1016/0016-7037(80)90097-6.

Tangviroon, P., Noto, K., Igarashi, T., Kawashima, T., Ito, M., Sato, T., Mufalo, W., Chirwa, M., Nyambe, I. & Nakata, H. (2020). Immobilization of lead and zinc leached from mining residual materials in Kabwe, Zambia: Possibility of Chemical Immobilization by Dolomite, Calcined Dolomite, and Magnesium Oxide. *Minerals*, 10 (9): 763.

Tembo, B. D., Sichilongo, K. & Cernak, J. (2006). Distribution of copper, lead, cadmium and zinc concentrations in soils around Kabwe town in Zambia. *Chemosphere*, 63 (3): 497-501. doi: 10.1016/j.chemosphere.2005.08.002.

Tipping, E. (1994). WHAM - A chemical equilibrium lodel and computer code for waters, sediments and soils incorporating a discrete site/electrostatic model of ion-binding by humic substances. *Computers & geosciences*, 20 (6): 973-1023.

Tipping, E., Rieuwerts, J., Pan, G., Ashmore, M., Lofts, S., Hill, M., Farago, M. & Thornton, I. (2003). The solid–solution partitioning of heavy metals (Cu, Zn, Cd, Pb) in upland soils of England and Wales. *Environmental pollution*, 125 (2): 213-225.

Torgersen, P. (2015). *Biologiske undersøkelser i gruvepåvirka områder, Folla* dirmin.no: Report by COWI for The Directorate of Mining with the Commissioner of Mines at Svalbard.

Tóth, G., Hermann, T., Da Silva, M. & Montanarella, L. (2016). Heavy metals in agricultural soils of the European Union with implications for food safety. *Environment international*, 88: 299-309.

UNICEF. (2020). *The Toxic Truth: Children's exposure to lead pollution undermines a generation of future potential*: Pure Earth.

Willett, I. & Beech, T. A. (1987). Determination of organic carbon in pyritic and acid sulfate soils. *Communications in soil science and plant analysis*, 18 (7): 715-724.

Wills, B. A. & Napier-Munn, T. (2006). *Wills' Mineral Processing Technology: An Introduction to the Practical Aspects of Ore Treatment and Mineral Recovery*. Oxford: Oxford: Elsevier Science & Technology.

Winsley, P. (2007). Biochar and bioenergy production for climate change mitigation. *New Zealand Science Review*, 64 (1): 5-10.

Yabe, J., Nakayama, S. M., Nakata, H., Toyomaki, H., Yohannes, Y. B., Muzandu, K., Kataba, A., Zyambo, G., Hiwatari, M., Narita, D., et al. (2020). Current trends of blood lead levels, distribution patterns and exposure variations among household members in Kabwe, Zambia. *Chemosphere*, 243: 125412. doi: 10.1016/j.chemosphere.2019.125412.

Yang, B., Luo, W., Wang, X., Yu, S., Gan, M., Wang, J., Liu, X. & Qiu, G. (2020). The use of biochar for controlling acid mine drainage through the inhibition of chalcopyrite biodissolution. *The Science of the total environment*, 737: 139485-139485. doi: 10.1016/j.scitotenv.2020.139485.

Yoshii, Y., von Rein, I., Munthali, K., Mwansa, M., Nakata, H., Nakayama, S., Ishizuka, M. & Uchida, Y. (2020). Evaluation of phytoremediation effects of chicken manure, urea and lemongrass on remediating a lead contaminated soil in Kabwe, Zambia. *South African Journal of Plant and Soil*, 37 (5): 351-360.

Zimmerman, A. R. (2010). Abiotic and Microbial Oxidation of Laboratory-Produced Black Carbon (Biochar). *Environmental Science & Technology*, 44 (4): 1295-1301. doi: 10.1021/es903140c.

Appendix

A 1: Correction figure used to give a better estimate for soil organic matter (SOM) in mineral soils with the loss on ignition method. The correction figure of the corresponding clay content of the soil sample is subtracted from the LOI value to account for the weight loss of chemically bound water in clay that evaporates at temperatures exceeding 150°C. Data compiled from (Ekström, 1926).

Soil type	Clay content	Correction figure
Sand and silt	5-9%	1
Light clay	10-24%	2
Medium clay	25-39%	2.5
Stiff clay	40-59%	3.5
Very stiff clay	>59%	4.5

A 2: DGT results calculated with equation 1 and 2 in section 2.4. The samples in the raw dataset (from ICP-analysis) measured under LOD and LOQ are presented as ½ the respective value for each metal. The data presented in the table is based on three replicate samples.

			M (µg)	M (µg)	M (µg)	M (µg)	M (µg)	M (µg)	M (µg)	M (µg)	C_DGT (µg/L)	C_DGT (µg/L)	C_DGT (µg/L)	C_DGT (µg/L)	C_DGT (µg/L)	C_DGT (µg/L)	C_DGT (µg/L)	C_DGT (µg/L)
Sample	Treatment	Deployment (h)	Pb	Pb (SD)	Zn	Zn (SD)	Cu	Cu (SD)	Cd	Cd (SD)	Pb	Pb (SD)	Zn	Zn (SD)	Cu	Cu (SD)	Cd	Cd (SD)
Z1	no BC	6	549.1	63.2	8038.3	497.0	9.6	0.8	10.5	0.5	1094.1	125.9	21163.6	1308.6	24.6	2.1	27.5	1.3
Z1	no BC	48	4257.9	182.4	31038.8	2067.7	65.3	3.4	27.9	3.8	1060.4	45.4	10215.1	680.5	21.0	1.1	9.2	1.3
Z1	BC	6	195.0	24.9	2586.6	68.9	6.7	1.2	3.8	0.3	388.5	49.5	6810.1	181.5	17.3	3.1	10.0	0.8
Z1	BC	48	1110.2	20.7	15917.3	689.2	25.9	1.4	20.3	1.2	276.5	5.1	5238.5	226.8	8.3	0.4	6.7	0.4
Z3	no BC	6	95.9	12.8	640.7	27.6	2.4	0.4	3.5	0.3	191.1	25.4	1686.8	72.6	6.1	0.9	9.2	0.9
Z3	no BC	48	815.8	132.0	4337.5	538.3	5.7	0.8	18.7	1.8	203.2	32.9	1427.5	177.2	1.8	0.2	6.1	0.6
Z3	BC	6	43.0	8.4	214.9	11.9	1.9	0.5	1.5	0.2	85.6	16.7	565.8	31.4	4.8	1.2	4.0	0.5
Z3	BC	48	397.9	30.0	1591.7	182.4	5.3	0.4	8.3	0.6	99.1	7.5	523.9	60.0	1.7	0.1	2.7	0.2
Z5	no BC	6	4.2	2.2	115.8	80.6	1.5	0.9	1.4	0.4	8.4	4.4	304.9	212.2	3.9	2.2	3.7	1.2
Z5	no BC	48	43.4	4.5	660.6	55.1	3.5	0.8	5.5	0.5	10.8	1.1	217.4	18.1	1.1	0.3	1.8	0.2
Z5	BC	6	1.7	0.0	13.1	2.4	0.7	0.0	0.3	0.3	3.3	0.0	34.5	6.4	1.7	0.0	0.7	0.8
Z5	BC	48	21.5	3.6	98.3	15.8	4.5	0.3	1.2	0.1	5.4	0.9	32.3	5.2	1.4	0.1	0.4	0.0
F2	no BC	6	6.8	5.8	108.2	8.4	314.4	55.1	0.6	0.3	13.5	11.6	285.0	22.1	807.5	141.6	1.5	0.9
F2	no BC	48	4.2	2.2	163.2	30.0	1472.4	137.8	0.8	0.1	1.1	0.6	53.7	9.9	472.7	44.3	0.3	0.0
F2	BC	6	1.7	0.0	19.1	2.4	3.3	0.5	0.4	0.3	3.3	0.0	50.3	6.3	8.6	1.4	1.1	0.7
F2	BC	48	2.9	2.2	89.1	49.0	12.7	3.0	0.4	0.2	0.7	0.6	29.3	16.1	4.1	1.0	0.1	0.1
F4	no BC	6	1.7	0.0	14.7	0.7	2507.0	206.8	0.4	0.3	3.3	0.0	38.8	1.8	6439.6	531.1	1.0	0.8
F4	no BC	48	1.7	0.0	39.0	6.1	4616.0	364.7	0.8	0.1	0.4	0.0	12.8	2.0	1482.1	117.1	0.2	0.0
F4	BC	6	1.7	0.0	11.7	1.4	2387.6	119.4	0.5	0.1	3.3	0.0	30.7	3.6	6132.9	306.6	1.3	0.2
F4	BC	48	1.7	0.0	35.8	5.2	6247.6	383.8	0.2	0.2	0.4	0.0	11.8	1.7	2006.0	123.2	0.1	0.1

A 3: Ratio of uptake of the four metals to the DGT estimated as the mean value (n=3) for mass measured at deployment time 48h divided by the mean mass of metals measured at deployment time 6h. If the ratio is 8 (28/6=8), the supply of metals to the DGT is regarded as unlimited as the soil solution sustains a constant concentration in the interface of the DGT device over time. This suggest that the metal replenishment from the geochemically active soil fraction is not kinetically restricted. If the ratio is above 8, the geochemically active metal soil fraction supply more metal to the DGT device than the replenishment initiated by the equilibrium solution around the DGT device . This can be possible due to the high milliequivalent associated with the DGT resin, causing the DGT to be an ultimate sink of geochemically active metals. The "LOD" marks for DGT samples with metal concentrations under the detection limit.

Sample	Treatment	Cd	Cu	Pb	Zn
Z1	no_BC	3	7	8	4
Z1	BC	5	4	6	6
Z3	no_BC	5	2	9	7
Z3	BC	5	3	9	7
Z5	no_BC	4	LOD	LOD	6
Z5	BC	LOD	LOD	LOD	8
F2	no_BC	1	5	LOD	2
F2	BC	1	4	LOD	5
F4	no_BC	2	2	LOD	3
F4	BC	0	3	LOD	3

A 4: Elemental composition of solution from titration batch experiment (used as Input data to WHAM). The displayed values are means (n=3) of ICP-OES/MS analysis of soil solution from batch experiment. Letters a-f indicate level of titration (added HCl for Zambia samples, and KOH for Folldal samples), where a indicates equilibrium solution with 0.01M KCl for each respective sample, and b-f show increasing levels of added titrant at displayed in Table 3. BC= biochar treated sample, nBC= no biochar added. Note the difference in units.

Sample & treatment	pH	DOC	Al	Fe	Cu	As	Cd	Ca	Mg	Mn	Na	Pb	S	Si	Zn
		mg/L	µg/L	µg/L	µg/L	µg/L	µg/L	mg/L	mg/L	mg/L	mg/L	mg/L	mg/L	mg/L	mg/L
Z 1 a BC	6.7	3.6	6.10	5.47	10.20	0.83	8.13	20.33	9.80	0.45	11.00	0.19	35.33	1.53	5.30
Z 1 a nBC	6.3	3.4	7.70	3.90	14.00	0.61	23.00	28.00	9.37	1.37	11.67	0.53	36.00	1.40	14.33
Z 1 b BC	6.3	3.1	7.87	3.93	10.17	0.86	16.00	26.67	11.00	0.83	11.33	0.36	34.33	2.07	11.03
Z 1 b nBC	5.8	3.3	15.33	10.50	18.00	0.71	37.33	34.33	10.33	2.00	12.00	1.00	36.33	2.10	24.00
Z 1 c BC	6.0	2.8	10.37	4.97	10.33	1.20	21.00	30.33	12.33	0.96	11.00	0.46	32.67	2.47	15.00
Z 1 c nBC	5.3	3.2	28.67	19.67	24.00	1.10	53.00	38.00	11.00	2.47	12.00	1.70	34.33	3.30	34.67
Z 1 d BC	5.2	2.7	31.00	7.77	20.00	2.20	51.33	42.33	14.33	2.27	11.00	1.43	31.67	5.07	37.00
Z 1 d nBC	4.6	3.5	104.33	52.33	52.67	1.93	93.00	47.33	12.00	3.53	12.00	3.80	31.67	6.07	55.00
Z 1 e BC	4.9	2.7	42.67	9.23	23.33	2.97	59.33	45.67	15.33	2.43	11.00	1.80	30.33	5.93	42.33
Z 1 e nBC	4.3	3.7	183.33	41.00	78.33	2.30	110.00	50.33	13.00	3.77	12.00	5.73	30.00	6.83	65.33
Z 1 f BC	4.7	2.7	56.33	11.33	30.33	3.33	70.00	49.67	16.00	2.83	11.67	2.23	30.67	6.67	48.00
Z 1 f nBC	4.1	3.9	316.67	30.33	116.67	2.60	130.00	54.00	13.00	4.23	12.00	8.13	29.00	7.37	69.67
Z3 a BC	6.9	6.4	4.40	13.67	6.23	0.69	2.23	46.67	34.33	0.19	23.00	0.07	76.67	2.47	0.42
Z3 a nBC	6.6	6.5	5.03	76.67	7.67	0.50	3.87	56.33	38.33	0.28	23.33	0.08	81.00	2.77	0.83
Z3 b BC	6.1	4.5	6.23	17.33	5.83	0.62	9.00	69.67	46.67	0.51	24.00	0.16	77.33	5.83	2.63
Z3 b nBC	5.7	5.4	12.67	1500.00	10.00	0.44	18.00	82.67	48.67	0.71	24.33	0.34	77.67	7.20	6.23
Z3 c BC	5.7	4.2	10.60	104.67	4.87	0.58	16.33	82.00	50.00	0.76	23.33	0.29	79.00	7.67	5.67
Z3 c nBC	5.4	5.5	25.67	3066.67	9.00	0.43	28.67	93.67	52.33	0.91	24.67	0.63	78.33	9.17	11.00
Z3 d BC	5.5	4.2	15.00	210.00	4.43	0.63	23.67	90.67	53.33	0.88	23.67	0.44	77.00	9.10	8.67
Z3 d nBC	4.9	5.7	44.00	3266.67	7.40	0.58	45.67	103.33	54.33	1.10	24.33	1.13	76.00	11.00	17.33
Z3 e BC	5.0	4.1	29.33	273.33	4.33	0.75	39.00	100.00	57.00	1.17	24.00	0.87	75.67	11.00	14.33
Z3 e nBC	4.6	6.3	83.33	3866.67	7.90	0.98	66.33	116.67	58.00	1.27	25.33	1.90	76.67	12.00	23.33
Z3 f BC	4.6	4.1	54.00	171.00	4.43	0.81	59.33	113.33	61.00	1.37	24.67	1.53	78.00	12.33	21.00
Z3 f nBC	4.3	6.2	213.33	3516.67	9.33	1.08	100.00	126.67	58.67	1.43	24.33	3.80	74.67	14.00	32.00
Z5 a BC	6.7	3.6	6.27	3.97	2.40	0.57	1.20	13.33	6.87	0.16	0.88	0.00	1.20	2.20	0.12
Z5 a nBC	5.9	2.5	6.93	23.27	2.80	0.32	5.43	18.00	6.67	1.07	1.23	0.01	0.90	2.50	0.67
Z5 b BC	6.6	3.0	5.70	4.17	1.93	0.54	1.63	14.67	7.47	0.24	0.91	0.00	1.10	2.50	0.16
Z5 b nBC	5.5	2.2	15.67	990.00	2.27	0.21	9.57	21.33	7.30	1.40	1.30	0.04	0.86	3.00	1.30
Z5 c BC	6.3	2.6	5.77	3.67	1.67	0.52	2.83	17.33	8.30	0.65	0.93	0.01	1.10	2.97	0.31
Z5 c nBC	4.8	1.8	53.33	436.67	1.60	0.20	19.67	25.67	7.93	1.67	1.30	0.12	0.87	3.57	2.27
Z5 d BC	6.1	2.2	6.60	3.63	1.27	0.47	3.50	19.33	9.00	0.74	0.95	0.01	1.10	3.20	0.42
Z5 d nBC	4.4	1.7	153.33	220.00	2.23	0.18	30.67	29.33	8.50	1.93	1.40	0.27	0.84	4.17	3.33
Z5 e BC	5.6	1.8	15.27	14.70	0.99	0.35	8.67	24.00	9.73	1.25	0.94	0.03	1.13	3.90	1.08
Z5 e nBC	4.2	2.0	346.67	400.00	3.73	0.21	40.33	33.33	9.17	2.23	1.40	0.48	0.95	4.93	4.17
Z5 f BC	5.3	1.5	20.33	6.10	0.80	0.32	11.00	26.33	10.33	1.40	0.95	0.05	1.17	4.30	1.40
Z5 f nBC	3.9	2.4	786.67	620.00	6.90	0.22	49.33	36.33	9.73	2.57	1.47	0.92	0.91	5.73	5.13
F2 a BC	4.3	0.3	13.33	5.77	5.10	0.14	0.08	2.00	0.92	0.05	0.09	0.00	6.57	1.13	0.03
F2 a nBC	3.7	0.5	193.33	87.33	63.67	0.15	0.11	0.86	0.25	0.01	0.47	0.01	4.90	0.82	0.03
F2 b BC	5.2	0.2	2.67	1.89	0.17	0.16	0.03	1.57	0.82	0.03	0.12	0.00	8.83	2.47	0.00
F2 b nBC	4.2	0.4	32.00	33.00	17.33	0.15	0.11	0.95	0.26	0.01	0.55	0.00	6.33	1.00	0.03
F2 c BC	5.8	0.3	2.50	0.91	0.04	0.19	0.01	1.37	0.72	0.02	0.14	0.00	9.67	6.07	0.00
F2 c nBC	4.6	0.4	5.20	7.23	3.60	0.16	0.08	0.82	0.24	0.01	0.54	0.01	7.43	1.60	0.01
F2 d BC	6.5	0.4	2.20	0.87	0.04	0.40	0.00	1.50	0.71	0.01	0.14	0.00	11.00	11.67	0.00
F2 d nBC	5.1	0.4	2.47	3.37	0.80	0.34	0.05	0.76	0.23	0.01	0.57	0.00	8.80	4.67	0.01
F2 e BC	6.9	0.7	10.43	13.43	0.12	0.94	0.00	0.80	0.53	0.00	0.17	0.00	11.00	17.67	0.00
F2 e nBC	5.6	0.5	4.33	1.39	0.12	0.88	0.02	0.84	0.23	0.00	0.58	0.00	11.00	8.57	0.00
F2 f BC	7.3	1.2	16.00	22.67	0.95	4.97	0.00	0.39	0.30	0.00	0.20	0.00	11.67	23.33	0.00
F2 f nBC	6.7	0.7	4.67	26.10	0.66	3.00	0.00	0.51	0.17	0.00	0.62	0.00	11.67	16.67	0.00
F4 a BC	3.0	0.7	1933.33	1333.33	710.00	0.06	0.06	3.00	1.87	0.09	0.02	0.01	29.67	1.43	0.03
F4 a nBC	2.9	1.1	1733.33	2366.67	816.67	0.39	0.05	1.63	1.10	0.04	0.23	0.00	28.00	1.17	0.02
F4 b BC	3.5	0.6	1233.33	100.00	446.67	0.10	0.05	3.07	1.87	0.09	0.09	0.00	31.33	1.83	0.02
F4 b nBC	3.4	1.0	1433.33	490.00	666.67	0.23	0.05	1.67	1.10	0.04	0.36	0.00	29.67	1.43	0.02
F4 c BC	4.2	0.5	121.33	11.20	108.00	0.07	0.04	3.00	1.80	0.08	0.17	0.00	32.33	2.30	0.01
F4 c nBC	3.7	1.0	700.00	128.67	436.67	0.12	0.05	1.60	1.03	0.04	0.43	0.00	30.33	1.70	0.02
F4 d BC	4.3	0.6	105.33	20.90	99.67	0.09	0.04	2.80	1.67	0.08	0.22	0.00	35.00	2.57	0.01
F4 d nBC	4.0	0.9	266.67	50.00	260.00	0.08	0.05	1.60	1.07	0.04	0.47	0.00	31.67	2.07	0.02
F4 e BC	4.8	0.5	9.20	8.90	23.67	0.10	0.02	2.43	1.60	0.05	0.29	0.00	36.67	3.30	0.00
F4 e nBC	4.4	0.9	59.33	14.33	112.33	0.07	0.04	1.57	1.03	0.03	0.53	0.00	34.33	2.53	0.01
F4 f BC	5.3	0.7	3.37	8.17	8.47	0.15	0.04	2.27	1.63	0.04	0.33	0.01	40.67	4.57	0.01
F4 f nBC	5.1	0.9	4.47	5.77	21.00	0.15	0.03	1.43	1.00	0.02	0.64	0.00	37.67	3.70	0.00
Instrument			ICP-MS	ICP-MS	ICP-MS	ICP-MS	ICP-MS	ICP-OES	ICP-OES	ICP-OES	ICP-OES	ICP-OES	ICP-OES	ICP-OES	ICP-OES
LOD			0.09	0.28	0.07	0.01	0.00	0.00	0.00	0.00	0.03	0.01	0.01	0.02	0.01
LOQ			0.31	0.92	0.24	0.04	0.00	0.02	0.01	0.00	0.09	0.02	0.05	0.05	0.02
Referance mateerial (1643H)			150	100	22	59	6.4	32	8	0.04	20	0.0115	2.9	2.4	0.078

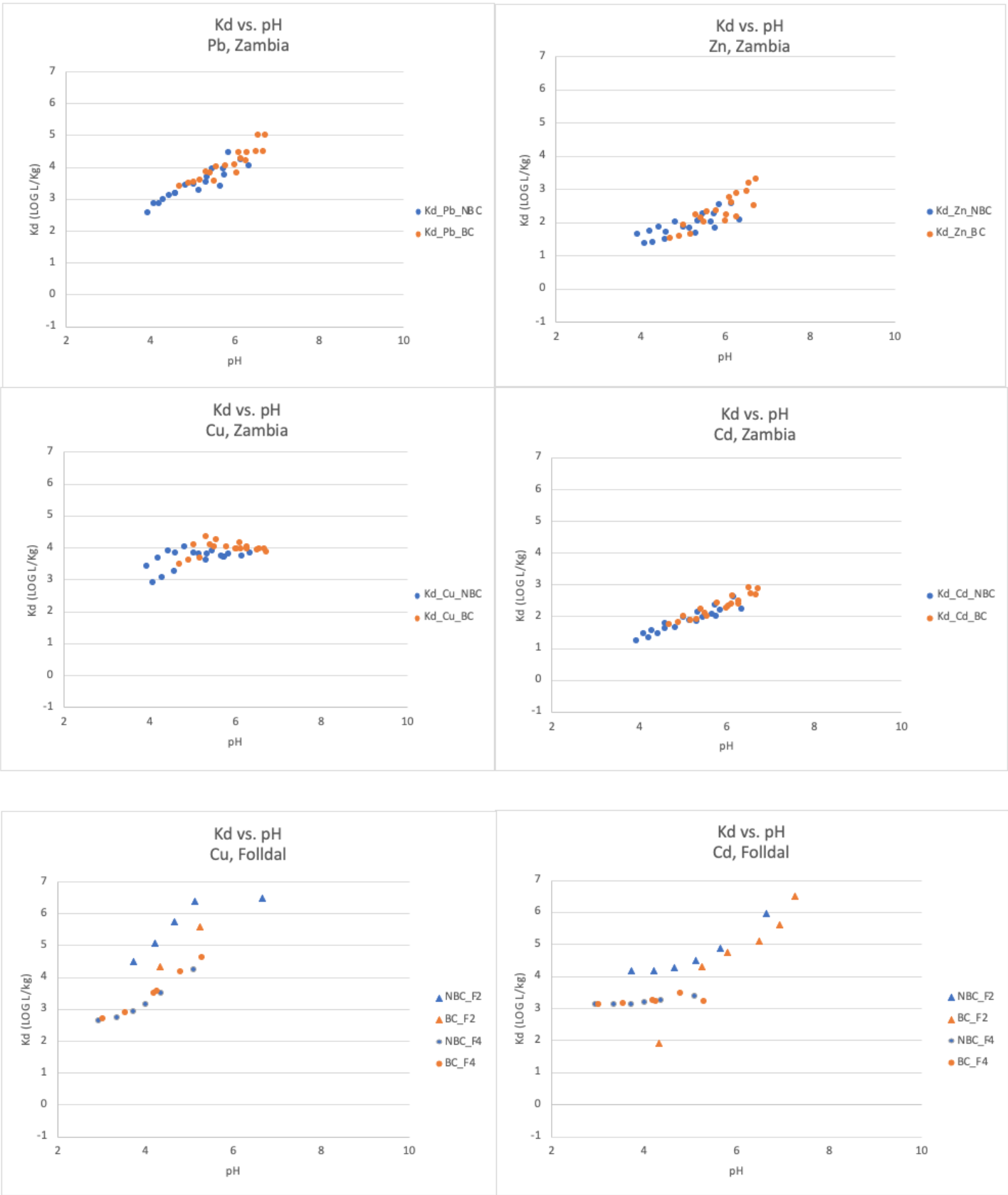

A 5: The background data of the linear relationships presented in Figure 24. The Kd values are based on soil total concentrations and total dissolved concentrations in solution. Presented is the mean values for the titration series, with and without biochar treatment.

Norges miljø- og biovitenskapelige universitet
Noregs miljø- og biovitskapelege universitet
Norwegian University of Life Sciences

Postboks 5003
NO-1432 Ås
Norway